UNIVERSITÀ DEGLI STUDI DI SALERNO

UNIVERSITÀ DEGLI STUDI DI SALERNO

Dipartimento di Farmacia

PhD Program
in **Drug Discovery and Development**
XXXI Cycle — Academic Year 2018/2019

PhD Thesis in

Technologies for the development of health products based on up-cycling of agro-food by-products

Candidate

Tiziana Esposito

Supervisors

Prof. *Teresa Mencherini*

Prof. *Rita Patrizia Aquino*

PhD Program Coordinator: Prof. Dr. *Gianluca Sbardella*

TABLE OF CONTENTS

LIST OF PUBLICATIONS

Papers and Conference Proceedings

Papers

Esposito, T., Celano, R., Pane, C., Piccinelli, A. L., Sansone, F., Picerno, P., Zaccardelli, M., Aquino, R. P. & Mencherini, T. (2019). Chestnut (*Castanea sativa* Miller.) Burs Extracts and Functional Compounds: UHPLC-UV-HRMS Profiling, Antioxidant Activity, and Inhibitory Effects on Phytopathogenic Fungi. Molecules, 24(2), 302.

Esposito, T., Sansone, F., Franceschelli, S., Del Gaudio, P., Picerno, P., Aquino, R. P., & Mencherini, T. (2017). Hazelnut (*Corylus avellana* L.) shells extract: phenolic composition, antioxidant effect and cytotoxic activity on human cancer cell lines. International Journal of Molecular Sciences, 18(2), 392.

Sansone, F., **Esposito, T**., Mencherini, T., Lauro, M. R., Del Gaudio, P., Picerno, P., Pepe, G., & Aquino, R. P. (2018). Particle technology applied to a lactose/NaCMC blend: Production and characterization of a novel and stable spray-dried ingredient. Powder Technology, 329, 304-312.

Sansone, F., **Esposito, T.**, Lauro, M., Picerno, P., Mencherini, T., Gasparri, F., De Santis, S., Chieppa, M., Cirillo, C., & Aquino, R. P. (2018). Application of Spray Drying Particle Engineering to a High-Functionality/Low-Solubility Milk Thistle Extract: Powders Production and Characterization. Molecules, 23(7), 1716.

Aïssaoui, H., Mencherini, T., **Esposito, T**., De Tommasi, N., Gazzerro, P., Benayache, S., Benayache, F., & Mekkiou, R. (2018). *Heliotropium bacciferum* Forssk. (Boraginaceae) extracts: chemical constituents, antioxidant activity and cytotoxic effect in human cancer *in vivo* cell lines. Natural Product Research, 1-6.

Piccinelli, A. L., Pagano, I., **Esposito, T**., Mencherini, T., Porta, A., Petrone, A. M., Gazzerro, P., Picerno, P., Sansone, F., Rastrelli, L., & Aquino, R. P. (2016). HRMS

profile of a hazelnut skin proanthocyanidin-rich fraction with antioxidant and anti-*Candida albicans* activities. Journal of Agricultural and Food Chemistry, 64(3), 585-595.

Esposito, T., Mencherini, T., Lembo, S., Gazzerro, P., Sansone, F., Chiuccariello, G., Picerno, P., & Aquino R. P. Ingrediente fitoattivo da scarti di castagna (*Castanea sativa*): formulazione di una emulsione cosmetica, valutazione della stabilità *in vitro* e della tollerabilità cutanea. Natural 1, 52-57, Marzo 2018.

Sansone, F., Mencherini, T., Picerno, P., **Esposito, T**. & Aquino, R. P., Microincapsulazione di un estratto di *Lannea Microcarpa* ad attività antiossidante. Natural 1, 42-48, Marzo 2017.

Esposito, T., Mencherini, T., Sansone, F., Piccinelli, A. L., Gazzerro, P., & Aquino, R. P., Formulazione e caratterizzazione di un'emulsione cosmetica a base di un estratto di mela annurca ad attività antiossidante. Natural 1, 60-64, Giugno 2016.

Esposito, T., Mencherini, T., Sansone, F., Porta, A., Campiglia, P., Aquino, R. P., Sviluppo formulativo di emulsioni cosmetiche idratati ed elasticizzanti: valutazione della stabilità *in vitro* e dell'efficacia funzionale *in vivo*. Natural 1, 38-46, Marzo 2016.

Conference Proceedings

Esposito, T., Sansone, F., Mencherini, T., & Aquino, R. P. Up-ciclying of hazelnut by product in a new functional spray dried powder. Innovation in local drug delivery school for doctorate in pharmaceutical technology. Lake Como School of Advanced Studies, September 25-28, 2018.

Esposito, T., Sansone, F., Vilela, C., Silva, N. H. C. S, Almeida, A., Piccinelli, A. L., Aquino, R. P., Freire, C. S.R., & Mencherini, T. Roasted Hazelnut (*Corylus avellana* L.) Skins: from a by-product to an active ingredient for food packaging

films. 113° Congresso della Società Botanica Italiana, Fisciano (SA), 12-15 settembre, 2018.

Mansour, A., Mencherini, T., Celano, R., **Esposito, T**., Sansone, F., Aquino, R. P., Rastrelli, L., & Picerno, P. A new cineol derivative, polyphenols and norterpenoids from Saharan myrtle tea (*Myrtus nivellei*): isolation, structure determination, and antioxidant activity. World Congress and Expo on Scientific Federation on Traditional & Alternative Medicine. Valencia, Spain, June 19-21, 2017.

Mencherini, T., **Esposito, T**., Piccinelli, A. L., Franceschelli, S., Porta, A., Sansone, F., Picerno, P., & Aquino, R. P. Chemopreventive and Anti-*Candida albicans* Extracts and Polyphenols from The Hazelnut (*Corylus avellana* L.) Industry By-Products. World Congress and Expo on Scientific Federation on Traditional & Alternative Medicine. Valencia, Spain, June 19-21, 2017.

Kerbab, K., Benayache, S., **Esposito, T.**, Celano, R., Rastrelli, L., Picerno, P., Aquino, R. P., Sansone, F., & Mencherini, T. *Halimium halimifolium* functional drink (tea): chemical characterization and microencapsulation in a new nutraceutical dosage form. Fourth International Congress on Cocoa Coffee and Tea. Turin, Italy, June 25-28, 2017.

Esposito, T., Pane, C., Sansone, F., Picerno, P., Zaccardelli, M., Aquino, R.P., & Mencherini, T. Chemical characterization of chestnut (*Castanea sativa*) bur extracts with activity against phytopathogenic fungi. SIF, XV Congress of the Italian Society of Phytochemistry jointly with 1St international Congress on Edible, Medicinal and aromatic plant (ICEMAP 2017). Pisa, Italy, June 28- 30, 2017.

Bechlem, H., **Esposito, T**., Sansone, F., Petrone, A. M., Porta, A., Mencherini, T., Benayache, S., De Tommasi, N. *Mentha pulegium* extract: chemical composition, antioxidant and anti-*candida albicans* activities. SIF, XV Congress of the Italian Society of Phytochemistry jointly with 1St International Congress on Edible, Medicinal and aromatic plant (ICEMAP 2017). Pisa, Italy, 28- 30 June, 2017.

Esposito, T., Pane, C., Sansone, F., Picerno, P., Zaccardelli, M., Aquino, R. P., Mencherini, T., Antifungal extracts from Chestnut (*Castanea sativa*) by-products: characterization and *in vitro* activity against phytopathogenic fungi. SCI, XXVI Congresso Nazionale della Società Chimica Italiana. Paestum (Sa), Italy, 10-14 settembre, 2017.

Mansour A., Mencherini T., Celano R., **Esposito T.,** Sansone F., Aquino R. P., Rastrelli L., Campone L., Picerno, P. Phytochemical investigation and antioxidant activity of *Myrtus nivellei* teas. P. XXVI SILAE & IX COCOCRO. Cartagena Colombia, September 25 - 29, 2017.

Esposito, T., Sansone, F., Mencherini, T., & Aquino, R.P. Hazelnut by-product: from waste to a novel spray dried ingredient. Advanced School in Nanomedicine, Pula (CA), Sardinia, Italy, 25-28 September, 2017.

Sansone, F., Mencherini, T., **Esposito, T.,** Picerno, P., Lauro, M. R., Aquino, R. P. Bitter orange juice spray dried microparticles as a functional ingredient for yogurt. 21st International Symposium on Microencapsulation. Faro, Portugal, September 27-29, 2017.

Esposito, T., Pane, C., Sansone, F., Picerno, P., Zaccardelli, M., Aquino, R. P., Mencherini, T. Polyphenol-rich extracts from chestnut (*Castanea sativa*) bur with activity against phytopathogenic fungi. 3rd International Conference on Natural Products Utilization: From Plants to Pharmacy Shelf. ICNPU-2017, Bansko, Bulgaria, 18-21 October, 2017.

AIM AND OUTLINE OF THE PhD PROJECT

A large volume of waste and by-products is produced during production, harvesting, and industrial processing of agro-foods, such as vegetables and fruits. For many years, they have been considered undervalued and neglected substrates. The removal of residues from production lines has a negative impact on industry economy, and the disposal in landfill generates harmful effects on the environment and public health (Dreyer et al., 2019). In recent years, scientific research has shown greater interest in the recovery of their functional and nutritional components, improving them from waste to bioactive resources for health or food products (Ran et al., 2018; Galanakis, 2013; Galanakis, 2012; Schieber et al., 2001).

The exploitation of wastes and by-products as safe ingredients for pharmaceutical, food and nutraceutical purposes, or active additives for packaging films, requires a complex process of recovery, chemical quali-quantitative characterization, biological investigation, and technological transformation of bioactive derivatives (Sansone et al., 2019).

The main drawbacks for an efficient re-use of vegetable residue derivatives are their occurrence as sticky materials, with penetrating smell and unpleasant taste, critical water solubility, and dramatic stability behaviour over time. The constituents release and degradation/oxidation process taking place during the storage period can reduce the bioactive molecules content and, consequently, the nutritional and biological value (Rawson et al., 2011; Bustos et al., 2018). Moreover, the low solubility in biological fluids could also limit their bioavailability, as well as the therapeutic effect, after oral administration (Sansone et al.; 2014 a; Sansone et al., 2014 b). Various technological approaches can be used to transform plant extracts into new dried materials overcoming critical stability and solubility problems. The microencapsulation in wall/coating polymer or the embedding in polymeric matrix reduces the moisture/water content and acts as a physical barrier to oxygen and

small molecules inhibiting chemical and enzymatic degradations, masks unpleasant taste and odour of the substances, isolates incompatible compounds and controls the release of the bioactive compound at a desired target (Nesterenko et al., 2013; Jyothi et al., 2010; Augustin et al., 2013). Some "mild" encapsulation physical techniques such spray drying, spray chilling/cooling, co-crystallization, extrusion or fluidized bed coating, production of lipid particle such as liposomes, seem to be suitable to process the most thermolabile plant materials (Martín et al., 2010; Jyothi et al., 2010; Augustin and Hemar, 2009).

What is proposed in the present project particle engineering, involving production of micro- or nano- particles, is to convert extracts from wastes and by-products in a particulate long-lasting stable material (Munin and Edwards-Lévy, 2011).

Another emerging opportunity to up-cycling agro-food wastes and by-products is the production of extracts with proven antioxidant and antimicrobial properties, which would be utilized in making edible films aimed at active packaging. The incorporation of functional extracts into the film-forming matrix allows the improvement of the film characteristics, subsequently avoiding oxidation and microbial spoilage of foodstuffs (Mellinas, et al., 2016; Cazon et al., 2017; Hanani et al., 2019).

In this context, the aim of the present PhD project was to design and develop new bioactive polymeric particle systems and edible films containing extracts obtained from agro-food wastes and by-products, with the purpose to contribute to the zero waste society and country.

In particular, the PhD program involved:

- Selection of wastes/by-products from Campania agro-industries (hazelnut shells and skins from Hazelnuts South Italy Manufacturing S.r.l., Baiano, Avellino, and chestnut spiny burs from Società Cooperativa Agricola Castagne di Montella, Montella, AV);

- Production, chemical and biological characterization of the extracts from selected wastes/by-products: I) hazelnut shells (HSE), II) hazelnut skins (RHS-H) and III) chestnut spiny burs (CSB-H) polar extracts;
- Design, development, technological and biological characterization of new polymeric microparticles systems loaded with HSE;
- Design, development and characterization of active edible films loaded with RHS-H and CSB-H, and evaluation of their functional efficacy.

The first part of the project focuses on the study of Hazelnut shells, the by-product of the industrial cracking phase of edible kernel. A polar extract (HSE) was produced by-exhaustive maceration, and the chemical investigation, by a combined use of chromatographic (Sephadex LH-20, RP-HPLC-DAD, HPLC-HRMS) and spectroscopic techniques (NMR), led to isolation and characterization of different classes of phenolic compounds. HSE total phenol content, antiradical activity, and inhibitory effect against human melanoma (primary and metastatic, A375, and SK-Mel-28, respectively) and cervical cancer (HeLa) cell lines, and HaCaT (immortalized human keratinocytes), a non-malignant epithelial skin line, were investigated (results Section A part I).

Despite the fact that HSE showed a high polyphenol content and demonstrated significant biological activities, it appeared in crystalline form and insoluble in water, issues that reduce both its functional effectiveness and stability over time, preventing a potential industrial application. With the aim to overcome this problems, new microparticulate powders loaded with the functional raw HSE extract were produced by spray drying.

Spray drying is a mild, one-step technology, largely employed by food industries, to transform a starting solution/suspension/emulsion into a micro- nanoparticulate powder. In the last decades the research group in Pharmaceutical Technology of the University of Salerno has acquired competence to apply the technique to

thermolabile plant extracts and natural compounds producing new stable products with high value.

Recently, the technology has been applied to extracts obtained from vegetable waste and by-products (Ozkan et al., 2019). The selection of polymers and coating carriers is crucial in stabilizing the extracts via spray drying, since the microparticles obtained are less permeable to oxygen and moisture, they preserve their biological activity, and allow an adequate release of bioactives into the cellular environment and biological fluids.

Pre-formulation studies allowed to select the appropriate multipolymeric matrix composed of coating polymers and loading carriers (proline, medium viscosity hydroxyethyl cellulose, and pectin). The influence of instrumental and operating (temperature, air and fluid flow, pressure, nozzle diameter, liquid feed viscosity and pH) process conditions on yield and encapsulation efficiency was evaluated. The produced engineered particles were characterized in terms of active HSE loading (HPLC-DAD), particles dimension (Laser Light Scattering), morphology (SEM and FM), thermal behavior (DSC), water dissolution release (USP II), preservation of bioactivity (DPPH test, MTT assay), and stability under harsh storage conditions (ICH-Guide Lines). The developed technological method seems to be suitable to transform HSE raw material in a stable powder to be enclosed in a topical or oral dosage form as active ingredient (results Section A part II).

During the PhD project, Chestnut Spiny Burs (CSB) were selected as interesting agro-waste, produced during the harvesting phase of chestnut fruit. Researches in literature report the occurrence of glucose esters with gallic acid (-mono, -di, and -trigalloylglucose), ellagitannins (vescalagin/castalagin), phenolic acids (gallic, ellagic, protocatechuic, cholorgenic acid), flavonoids (apigenin, quercetin, and quercetin 3-O-β-glucoside) in chestnut burs (Braga et al., 2015; Pinto et al., 2017;

Li et al., 2015). Nevertheless, CSB results a poorly explored solid waste and very limited data are available on its chemical characterization.

Phytopathogenic fungi are damaging for fruit and vegetable productive chain, causing both in field and post-harvest yield losses and food decay also finding out serious risks for consumers, because of dangerous secondary metabolites production like mycotoxins (De Corato, 2019; Mansour et al., 2017). A limited number of authorized synthetic fungicides acts in their management. Their widespread use involves developing resistant strains and raises environmental and human health concerns because of persistent chemical residues (Esposito et al., 2017). To overcome these major drawbacks, an attractive alternative or a complementary mean to synthetic antimicrobial is getting natural derivatives from plants or agro-industrial residues, having a non-toxic and biodegradable profile (Chen et al., 2019; Yang and Zhang, 2019).

Therefore, in the present project, the potential of CSB as source of phenolic compounds with antioxidant and antimicrobial activity was investigated.

The complete polyphenol profile and the chemical markers content was determined by a UHPLC-PDA-HRMS method. The major compounds were isolated and characterized by NMR techniques. The *in vitro* scavenging activity against the radicals $DPPH^{\bullet}$ and $ABTS^{+}$ was verified. CSB extracts and marker compounds were also evaluated as inhibitive effect on mycelial growth and spore germination of *Alternaria alternata*, *Fusarium solani*, and *Botrytis cinerea* (results Section B part I).

In a previous work (Piccinelli et al., 2016), a methanol extract from Roasted Hazelnut Skins, obtained by exhaustive maceration, was studied. The extract (RHS-M) showed a high content of proanthocyanidins, a good antioxidant and antifungal activity against *Candida albicans*. Based on the research group acquired know-how, Hazelnut skins were the last selected by-product. During the PhD project, a

hydro-alcoholic extract (RHS-H) was produced, using the Pressurized Liquid Extraction Technique (PLE). PLE is an innovative "*green"* extraction technique, which uses GRAS solvents, such as ethanol and water, and allows to obtain high extraction yields, in the shortest time and with a lower amount of organic solvents (Ameer et al., 2017; Dai and Mumper, 2017). The RHS-H extract was compared with the previously studied RHS-M in terms of extraction yield, total polyphenol content, and scavenging activity against free radicals (results Section B Part I).

The final goal of the present PhD project, achieved during a research period at CICECO, Chemistry Department (Aveiro University), was to design and develop antioxidant and antimicrobial food packaging films by incorporating the hydroalcoholic extract obtained from RHS (RHS-H) and CSB (CSB-H) into Pullulan (PL) matrix. Among the film-forming polysaccharides, PL is a non-toxic exopolysaccharide obtained from the fermentation of the fungus *Aureobasidium pullulans*. It is a water soluble polymer with impressive film-forming ability and originating transparent, tasteless, odourless films (Tabasum et al., 2018). The effect of extracts on the film mechanical properties, thickness, infrared spectroscopy characteristics (FTIR-ATR), optical properties (UV-Vis transmittance), and biological activity was studied (results Section B Part II). The developed CSB-H and RHS-H films are shown to be an interesting tool to extend foodstuffs shelf-life, being able to protect from the influence of external environmental and biotic factors (oxidative processes and microorganism spoilage).

INTRODUCTION

1.1. Wastes and by-products: production and management

In the last years, the accelerated development of the countries, with the global population expansion, and the ineffective management strategies, has caused a rapid increase in production and accumulation of waste and by-products into the agro-food sector (Mirabella et al., 2014; Giampieri et al., 2018; Song et al., 2015). The European Union (EU) (Commission Council Directive 2008/98/CE) defines the waste as a material which the holder discards, or indented, or is required to discard. Otherwise, a by-product is the production residue available for other applications without any further processing than normal industrial practice (Santana-Meridas et al., 2012). Wastes and by-products occur during each stage of the food value chain: from agricultural production, industrial manufacturing and processing, storage and transport phase, up to retail and household consumption (**Figure 1**) (Kumar et al., 2017; Plazzotta et al., 2017).

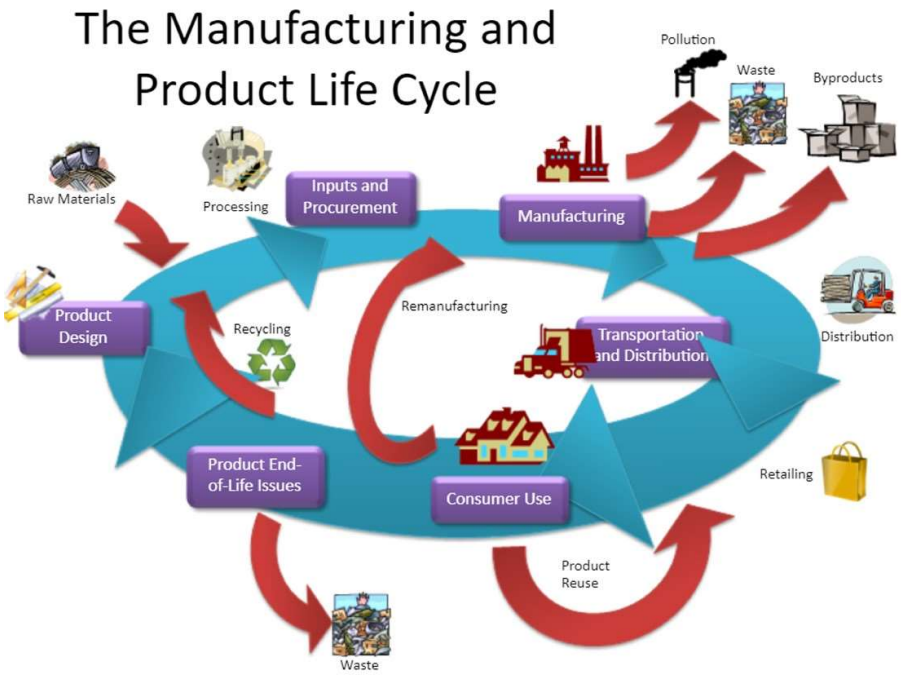

Figure 1. Product life cycle (www.epa.gov//rcc)

Based on the raw material origin, wastes and by-products are classified into two main groups: plant- and animal-derived wastes. Among plant derived there are:

- Agricultural residues: crop residues (formed during production, harvesting and processing in farms); agro-industrial residues, produced in postharvest phase (such as peels, shells, skins, seeds, stems, leaves, waste waters and unusable pulp) (Pfaltzgraff et al., 2013; Lozano and Lozano, 2018);
- Forestry by-product: from harvesting of forest and forestry plantations (branches, leaves and needles);
- Agro-industrial by-products: arose during manufacturing and industrial processes;
- Food waste, derived from food and drink manufacturing;
- Woody industry by-product: derived from woody, pulp and paper industries (Sánchez et al., 2019).

Vegetable-derived waste represents the larger portion (63%) of the whole food supply chain and represent a major source of carbohydrates, lipids, proteins, minerals, and other phytochemicals (Pfaltzgraff, et al., 2013; Jin et al., 2018). Food manufacturing industry contributes about 39% in producing wastes and by-products (**Figure 2**); 40-50% are the global loss and waste from fruit and vegetables, as reported by Food and Agricultural Organization (Sansone et al., 2019).

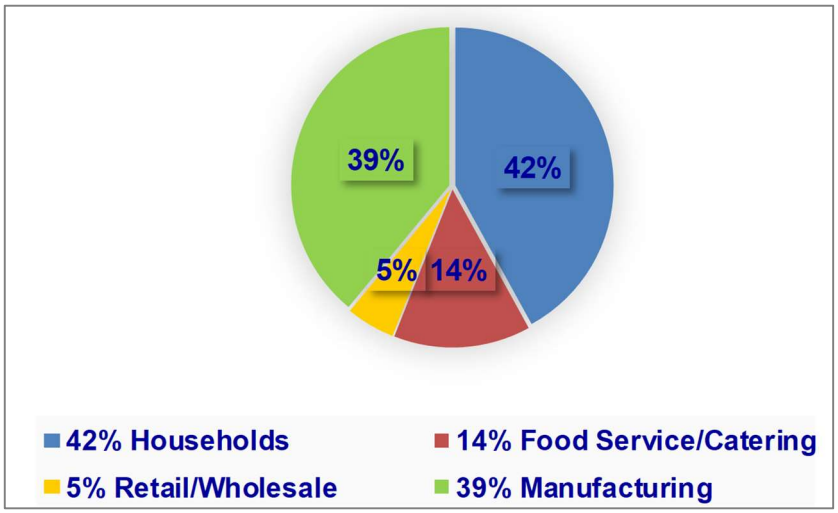

Figure 2. Percentage breakdown of EU27 food waste (European Commission, 2010)

In Europe, the production of agro-food wastes is estimated at 250 million tonnes/year and in Italy most of these wastes arose from cereal (11 million tonnes/year), grapevine (2-3 million tonnes/year), and olives (1.2 million tonnes/year) processing industry.

For many years, by-products and wastes have been undervalued and neglected substrates (Galanakis, 2013). The disposal in landfill resulted expensive for industry, and is harmful for environmental and human health (Song et al., 2015). Usually, waste and by-products are constituted by high percentage of moisture (74-90%), organic components, and active enzymes. This make them unstable materials, causing a rapid growth of pathogenic microorganisms, auto-oxidation and degradation process. Their anaerobic decomposition cause methane production, a gas 25 times more powerful than carbon dioxide. However, the presence of suspended solids (SS) in high amount with high Biochemical (BOD) and Chemical Oxygen Demand (COD) affects both the recovery strategies and treatments costs. All these negative aspects contribute not only to the global pollution but also are

responsible to: - reduce natural resources available, - reduce fertility in fields, and - lose of biodiversity (Song et al., 2015; Pfaltzgraff et al., 2013). For these reasons, in the last years, several strategies were employed in response to growing society demands of sustainability. The challenge for food industry has been the valorisation of wastes and by-products, by the transformation in a renewable, low cost material with high value, becoming an important resource (Kowalska et al., 2017). In the European contest, the waste framework directive (Directive 2008/98/EC) introduced a new approach in managing waste and by-product to sustain their reuse and valorisation (Demirbas, 2011; Ravindran and Jaiswal, 2016). The directive is based on "waste hierarchy" (**Figure 3**), and it includes, in descending order of priority, the waste prevention, reuse, recycling, recovery, and disposal in order to contribute to the zero waste society and country. The aim is to generate the smallest quantity of waste, extracting the maximum benefits from the product, in order to decrease the environmental impact and to preserve the resources (Plazzotta et al., 2017; Ravindran and Jaiswal, 2016).

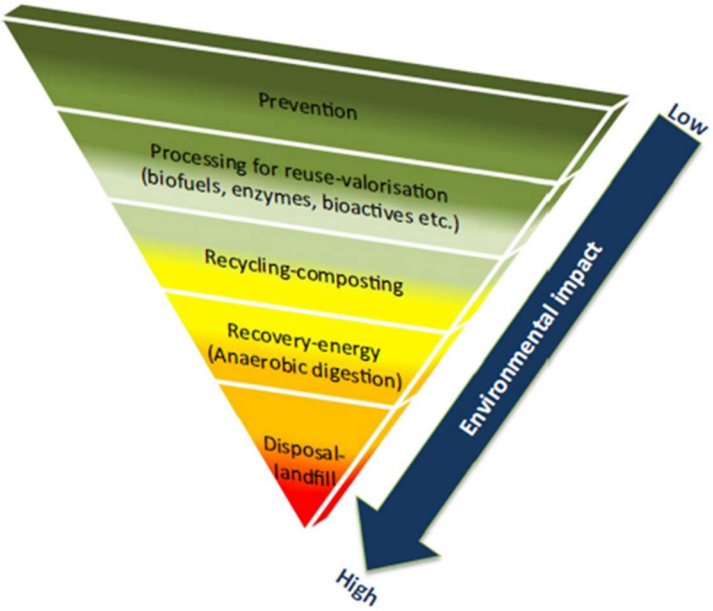

Figure 3. Hierarchy for waste processing (Ravindran and Jaiswal, 2016)

Specifically, the different goals are placed following a hierarchy according to the environmental impact that they determine. The most sustainable solutions are: prevention, processing for reuse-valorisation (redistribution for human consumption, animal feed, extraction of compounds for industrial use i.e. recovery of polymers and bioactive compounds to obtain high value products such as cosmetics, nutraceuticals, functional products), composting, and energy recovery (anaerobic digestion) (**Figure 4**) (Ravindran and Jaiswal, 2016).

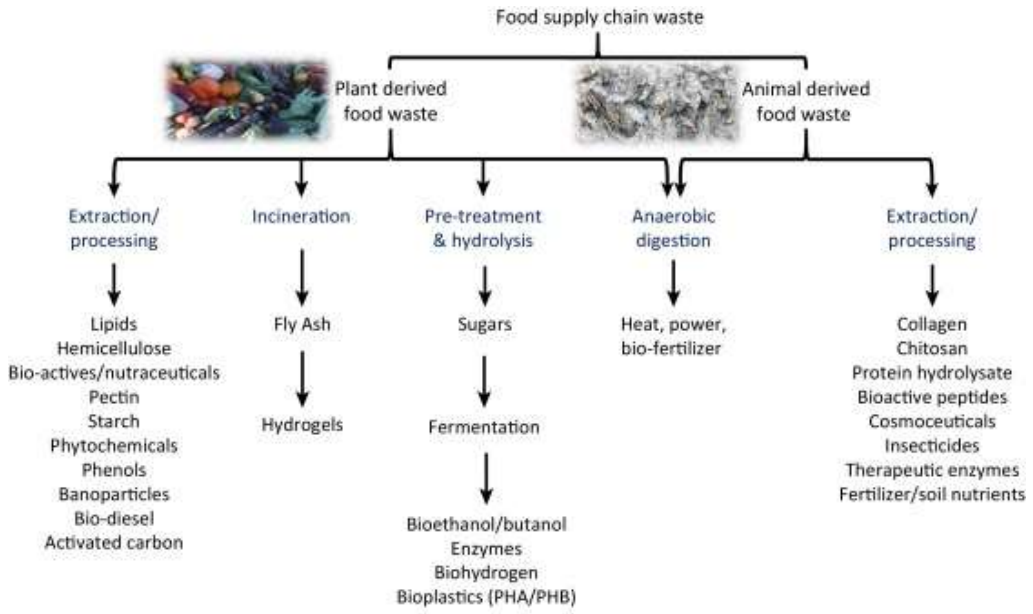

Figure 4. Flow diagram of reutilization of wastes (Ravindran and Jaiswal, 2016)

1.2. From wastes and by-products to high-value ingredients

Wastes and by-products of agro-food manufacturing chains contain a high amount of add-value molecules, such as polysaccharides, proteins, vitamins, fats, flavour compounds, and phytochemicals. The recovery of bioactive components with health-promoting benefits suggests the exploitation of vegetable residues as functional ingredients in developing nutraceuticals, functional or novel foods, active food packaging, and pharmaceutical products. Polyphenols, as glycosides or aglycones, combined with organic acids, or present as polymerized molecules with high molecular weight, such as tannins, are one the main class of phytochemicals identified in waste and by-products (Kammerer et al., 2014). Polyphenols possess considerable therapeutic interest for their antioxidant, anti-inflammatory, and antimicrobial activities, useful for treatment of cardiovascular diseases, cancer,

ageing, neurodegenerative pathologies, and diabetes (**Figure 5**) (Castro-Muñoz et al., 2016).

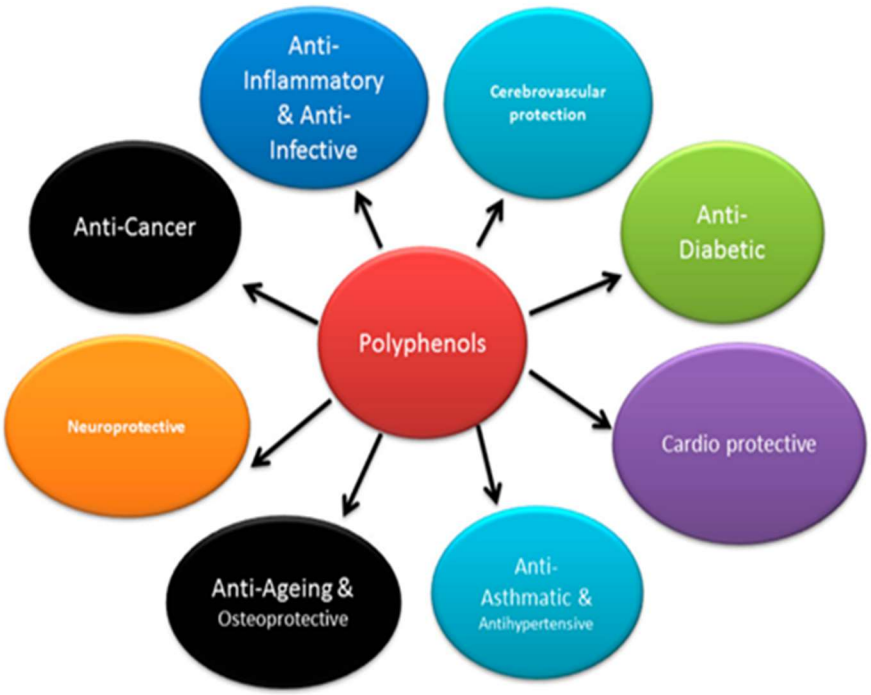

Figure 5. Principal biological properties of polyphenols (Ganesan and Xu, 2017)

The antioxidant mechanism of action of polyphenols is widely investigated *in vitro* and *in vivo*. They act scavenging the free radicals, inhibiting the lipid oxidation, chelating transition metals, activating transcription factors and enzymes (Ganesan and Xu, 2017; Li et al., 2014). The antiproliferative effect, the antiestrogenic activity, the changes in cellular signalling, support the antitumor and chemopreventive activity of polyphenol-rich plant extracts (Negi, et al., 2018; Niedzwiecki et al., 2016; Li et al., 2014). Moreover, polyphenols decrease the onset of bacterial, fungal, and viral human pathologies by the involvement in reduction of host ligands adhesion, inhibition of biofilm formation, neutralization of

microbial toxins (Daglia, 2012; Li et al., 2014). Furthermore, for their antimicrobial and antioxidant efficacy, polyphenols appear a natural and eco-friendly alternative to synthetic preservatives in cosmetic or food products in which chemical degradation and microbiological spoilage are the principal causes of quality loss (Piccinelli et al., 2016; Li et al., 2014; Sansone et al., 2019).

Anyway, a complex process of extraction, analytical and biological characterization is necessary to develop bioactive ingredients for health purposes from agro-food residues. The first step is the selection of the extraction technique. The vegetable residue can be used fresh, frozen or dried, and usually its particle size is reduced by milling, grinding, and homogenization (Sansone et al., 2019; Dai and Mumper, 2010). Conventional solid-liquid extraction and non-conventional methods (pressurized fluid extraction, supercritical fluid extraction, ultrasound-, microwave-, and enzyme-assisted extraction, pulsed electric field extraction) are applied to get back bioactive molecules (**Figure 6**). The selection of procedure and process parameters (time, temperature, solvent polarity, pH, matrix/solvent ratio) depend on the target of bioactive molecules to recover and the type of vegetable matrix, and they influence on both the process yield, and economic and environmental impact (Dai and Mumper, 2010; Kumar et al., 2017).

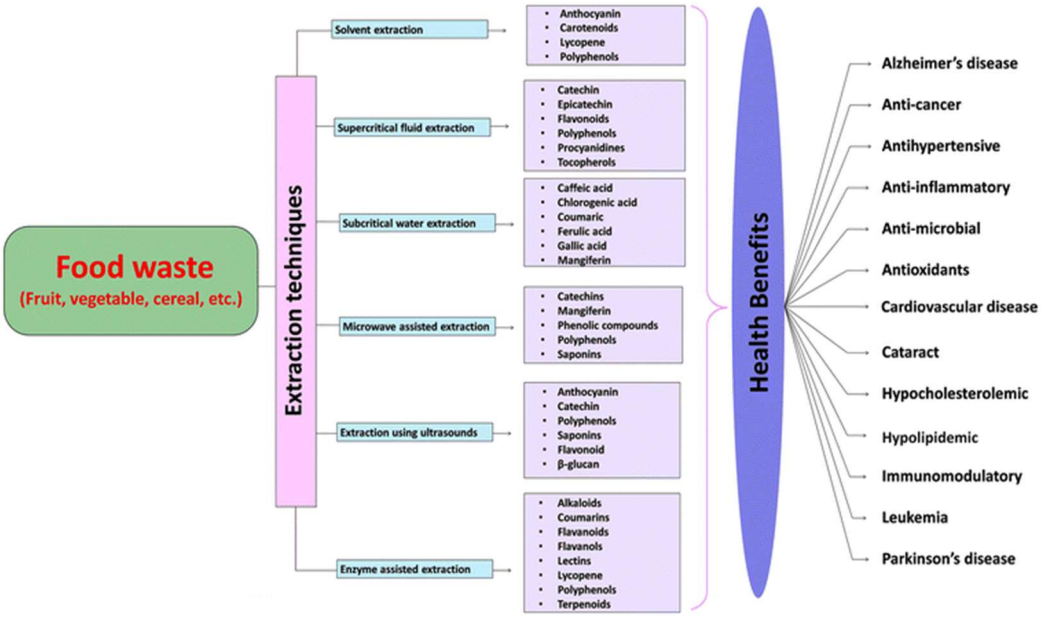

Figure 6. Extraction of bioactive compounds from food wastes by different techniques and their health benefits (Kumar et al., 2017)

The obtained extracts are complex mixtures of bioactive molecules, and the combined use of analytical techniques, such as High-Performance Liquid Chromatography (HPLC) coupled to Nuclear Magnetic Resonance (NMR) or Mass Spectrometry (MS) analysis, led to isolation and chemical identification of pure compounds and functional markers of extracts, improving the quality control of process and product.

1.3. Technological approaches to transform extracts from wastes and by-products into high value ingredients

Despite their high functionality, the plant extracts occurring as sticky materials with penetrating smell and unpleasant taste also having a poor solubility in water and in aqueous biological fluids (Sansone et al., 2019; Shishir and Chen, 2017). These

critical characteristics could limit their use as therapeutic agent, because negatively affecting the absorption process and bioavailability, also involving practical difficulties for an industrial use. In addition, constituents release and degradation/oxidation process taking place during the storage period may reduce the active ingredient content and, consequently, the nutritional and biological value (Tolve et al., 2016; Wang et al., 2009; Shu et al., 2006). A convenient way to improve the quality of a plant extract increasing handling, shelf-life, and bioavailability is to transform it into a stable dry powder form. Various technological approaches can be used to transform plant extracts into new dried materials overcoming critical stability and solubility problems. In the present project particle engineering, involving production of micro- or nano- particles, is proposed to convert extracts from wastes and by-products in a particulate long-lasting stable material (Munin and Edwards-Lévy, 2011), obtaining a final product which may be easy stored (improved stability) and handled (increased technological performance) to be enclosed in various functional dosage forms (Shishir and Chen, 2017; Sansone et al., 2013).

Particle engineering involves several technological aspects from the embedding polymer matrix, encapsulation efficiency, solid state, morphology and solubility modification, as well as size reduction of the raw waste material (Đorđević et al., 2015). Therefore, a multidisciplinary research is necessary to design and develop new particulate systems which may be innovative dietary supplements on its own or original, stable and bioavailable extra-functional ingredients in foods or food packaging. The micro-nano-encapsulation techniques can be applied to plant derivatives to transform them into particulate powder forms by using appropriate coating polymers brushing up shelf-life, organoleptic characteristics, also enhancing the water solubility (Shishir and Chen, 2017; Laine et al., 2008; Tuyen et al., 2010; Ersus and Yurdagel, 2007). From a food biomedical, pharmaceutical

and cosmetic technology perspective, the microencapsulation in wall/coating polymer or the embedding in polymeric matrix reduces the moisture/water content, and acts as a physical barrier to oxygen and small molecules inhibiting chemical and enzymatic degradations. Moreover, the process masks unpleasant taste and odour of the substances, isolates incompatible compounds, and controls the release of the bioactive compound at the target site (Nesterenko et al., 2013; Jyothi et al., 2010; Augustin, et al., 2013). Some encapsulation physical techniques, such as spray drying, spray chilling/cooling, co-crystallization, extrusion or fluidized bed coating, and production of lipid particle, such as liposomes, seem to be suitable to process plant materials. These techniques are defined as "mild" because they are able to process the most thermolabile plant matrices avoiding degradations of functional components (Martín et al., 2010; Jyothi et al., 2010; Augustin and Hemar, 2009). It is possible to produce biocompatible, biodegradable and non-toxic particles using food-grade coating/embedding polymers (pectins, alginates, cellulose derivatives, chitosans, fibers). Their application is also attractive because they have shown excellent potential as carrier materials in controlled release dosage forms and are inexpensive and readily available (Kulkarni, et al., 2012; Beneke et al., 2009). In relation to both encapsulation technique and polymer matrix used it is possible to produce a final product with enhanced technical characteristics in a form suitable for the final administration (mainly oral or topical ones). To verify the efficiency of applied encapsulation method, some critical features of the produced engineered particles (morphology, dimensional distribution, solid state, water dissolution rate) as well as the stability under harsh storage conditions of final formulation need to be investigated.

1.3.1. Spray drying technique

Spray drying is a transformation of feed from a fluid state into a dried particulate form by spraying the feed into a hot drying medium. It is a "one-step" process widely used in cosmetic, pharmaceutical and food industries, to transform a starting solution/suspension/emulsion into a powder form. The first one is the atomization of the liquid stream by an appropriate device. In particular, the term atomization refers to the formation of a powder or liquid suspension in a gas leading to very large surface areas of particle droplets. The drying material never reaches the inlet temperature of drying gas, so, the atomization phase makes the spray drying process not only a drying method for drying heat sensitive substances, but also, a method of drying allowing for the formation of particles with the desired physico-chemical and morphological properties (Shishir and Chen, 2017; Singh and Van den Mooter, 2016). The main components of a spray dryer are (**Figure 7**):

- heating system
- atomizer or nozzle
- drying chamber
- cyclone
- dry particles collector

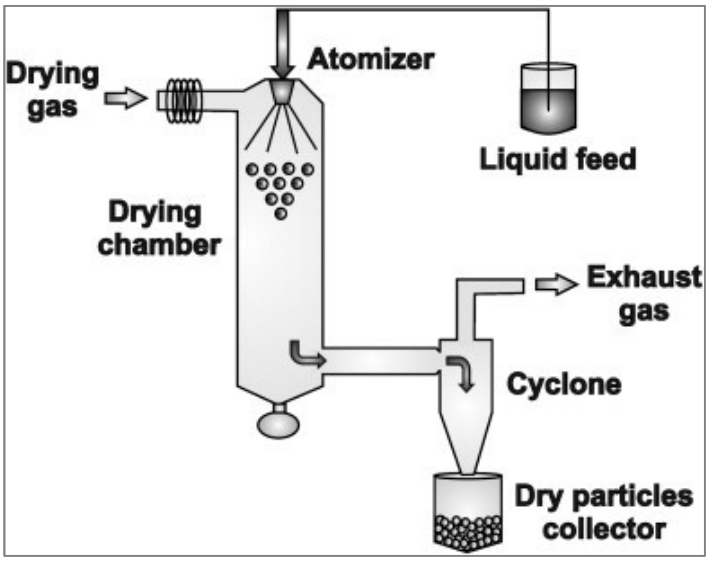

Figure 7. Diagram of the equipment and process of conventional spray-drying (Sosnik and Seremeta, 2015)

The liquid feed solution is pumped by a peristaltic pump through the atomizer or nozzle into the drying chamber (**Figure 8**), where it comes into contact with the heated air which evaporates the solvent; then the solution is practically sprayed through the nozzle into the spray chamber where it comes in contact with the hot air. The dry particles are forced by a cyclone into a glass collector at the end of the device, while dry gas are removed from the drying chamber.

Each process phase, as well as the conditions under which it is conducted, has a huge effect on the drying process efficacy and the final product properties. To obtain a well-dried powder some parameters can be modified: the increase of inlet temperature, can proportionally increases solvent evaporation rate; the increase air inlet flow, at constant temperature, increases the solvent evaporation; the decrease of the inlet solution flow lowers the amount of solvent which must be vaporized in the unit of time. Moreover, to obtain large particles it is possible to increase flow

rate of the liquid feed, and use large nozzle diameter and high formulation concentration. At the contrary, smaller particles can be obtained from low surface tension, high atomization pressure and small nozzle diameter (Sansone et al., 2011; Sosnik and Seremeta, 2015).

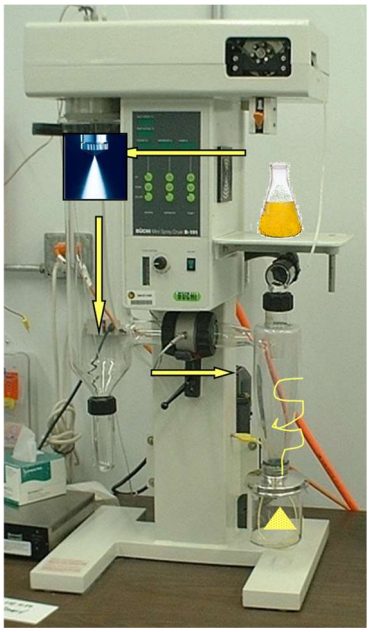

Figure 8. Spray drying process

Spray drying has become popular in pharmaceutical field due to the ability to dry the most thermolabile fluid extracts without risking the decomposition of their components (Sollohub and Cal, 2010; Gimbun et al., 2018; Moreno et al., 2016;). The spray drying of fluid extracts results in a product with better properties compared to other drying methods, since spray-drying produces homogeneous powders. This process is also suitable to promote the formation amorphous material starting from materials with a high crystallinity degree (Tontul and Topuz 2017; Đorđević et al., 2015; Sansone et al., 2019).

1.3.1.1. Spray Drying of plant extracts designed for tableting or encapsulation

In recent years, there has been an increasing use of spray drying technique in several sectors, from pharmaceutical to food and cosmetics. Plant dry extracts are commonly obtained by spray drying technique (Tontul and Topuz 2017; Sansone et al., 2019), but the process could negatively affect the flowability of resultant powder. The main cause is the small size of its particles, which is common with spray dried powders. Otherwise, a free-flowing powder is very important in formulating tablets or capsules. The mechanisms require the ability to separate small doses of powder from the bulk. The homogeneity of the doses depends on the rheological properties of the powder and its flowability (Sollohub and Cal, 2010). The rheological properties depend on the physico-chemical properties of the powder and can only change by modification of these physico-chemical properties. Flowability, on the other hand, is dependent on the type of surface upon which the pouring of the powder takes place. The smaller the dry extract's particles, the greater number of problems related to powder pouring. The composition of plant extracts is another cause of difficulties during the spray drying process. Extracts contain many ingredients that demonstrate high viscosity under spray drying conditions (e.g., low molecular-weight sugars and organic acids), which results in an increased tendency to leave undried material deposits on the chamber walls (Iyer, et al., 2013; Cal and Sollohub, 2010). This, in turn, disrupts the chamber's hydrodynamics and hinders the complete drying of the product.

1.3.1.2. Carrier substances to enhance the spray-drying process

Plant extracts are therefore usually spray dried together with carrier substances intended to facilitate the drying process. Because some of the problems encountered in spray drying plant extracts result from the surface properties of the powder

particles, encapsulation by co-spray drying might be helpful (Murugesan and Orsat, 2012).

The next goal for the technique of co-spray drying of active extracts with excipients is to increase the extract's aqueous solubility. This issue is of importance because plant extracts have generally low solubility in water. Increasing the aqueous solubility of an extract can help in the development of new therapeutic methods. Moreover, approximately the totality of raw plant extracts cause problems during their formulation process, and fail to became marketed products due to issues related to their high lipophilicity (e.g., low aqueous solubility, low/unrepeatable bioavailability, difficulties in administration) (Gallo, et al., 2013). The most frequently used method for increasing the aqueous solubility of an active substance is to reduce its particle size, thus increasing the surface area in contact with the solvent. Spray drying is a way to produce/create particles with reduced size and to control particle size and morphology if the material is dried from a solution. In addition, it allows for control of the particle's properties. Aqueous solubility of a co-spray-dried material is related distinctly to process parameters like inlet temperature, concentration in feed, and flow rate, which have the most influence on the particle characteristics responsible for solubility (particle size and crystallinity rate) (Sansone et al., 2019; Tontul and Topuz, 2017).

However, this technique also has some limitations especially related to the classes of polymers and solvents that can be used and, therefore, to the final composition and viscosity of the feed matrices to be submitted to the process. The selection of the solvent, suitable for the spray drying microencapsulation technique, must be carried out on the basis of the following criteria:

•low boiling point of the solvent: to facilitate its evaporation. In this way, the spray can be carried out at lower temperatures, resulting in less thermal stress and lower thermal degradation of the active;

• good solubility of the active and polymer in the feed liquid in order to reduce the amount of solvent required;
• low viscosity of the feed solution: to improve atomization and facilitate solvent evaporation. In fact, a high viscosity of the matrix would not allow a sufficient atomization and an adequate evaporation of the solvent (Singh and Van de Mooter, 2016).

Therefore, in order to obtain the best microencapsulation results, it becomes essential to select the solvent system, the coating polymer, the loading carriers and the emulsifying/stabilizing agent of the aqueous/organic system, the relative concentrations in the feed liquid and the ratios in which the polymer is used with respect to the extract. It is generally necessary to start from a homogeneous liquid feed (solution, suspension or emulsion), in which active ingredients and polymers are able to interact upon solvent evaporation (Sansone et al., 2011; Sansone et al., 2018 a).

The polymers used in microencapsulation can be classified according to their origin as: natural or synthetic; moreover, they can be biodegradable or non-biodegradable. There are different types of polymers used in the preparation of microparticles:

• proteins (collagen albumin, gelatin, casein);
• polysaccharides (starch, cellulose and its derivatives, alginates, chitosan, pectins, gums) (Yang et al., 2015);
• polyesters (PLA, PGA, PLGA, poly- and goat lactones);
• polyacrylates (acrylates, methacrylates, copolymers, methacrylates);
• polyanhydrides;
• lipid materials (glycerides, waxes) (Singh and Van den Mooter, 2016).

Great attention has been paid to polysaccharides, such as pectins and cellulose derivatives because they result easily available, non-toxic, biocompatible, biodegradable, and easily modified (Yang et al., 2015; Singh and Van den Mooter,

2016). Amino acids are also employed to reduce hygroscopicity of spray dried powder because are able to improve flowability, confer an anti-caking effects and maintaining the particle shape and the integrity against the moisture stress (Hyung et al., 2008). Some amino acids, including arginine (Arg), phenylalanine (Phe), and leucine (Leu) are often used as effective dispersibility enhancers able to effectively load active ingredients (Prota et al., 2011; Chang et al., 2014).

1.4. Edible films

Foods are manly organic raw materials and are subject to deterioration due to a progressive alteration of their chemical, physical, organoleptic, microbiological and structural characteristics.

Currently the most used material in food packaging is plastic (Horodytska et al., 2018). In fact, it has been estimated the production of about 300 million tons of plastic materials, of which 39.6% is represented by packaging industry (Pineros-Hernandez et al., 2017). Most of these plastic packages are used once and then discarded, which greatly contributes to the total waste stream (about 20% of the total world volume) (Tencati et al., 2016). Plastic polymers possess several interesting properties suitable for food packaging production such as transparency, softness, heat sealing ability, good resistance to weight, excellent waterproof efficacy (Wróblewska-Krepsztul et al., 2018). Furthermore, they are characterized by mechanical properties such as tensile and tear strength, and constitute a good barrier to oxygen. However, these plastic materials are not totally recyclable or biodegradable (their degradation requires more than 100 years), so their use causes negative effects on the environment (Wróblewska-Krepsztul et al., 2018). Moreover, over 99% of plastic materials derived from petroleum, an exhaustive fossil resource, contributing to depletion of fossil resource, to environmental

pollution and to high energy consumption during the manufacturing process (Gómez-Guillén et al., 2009).

For this reason, in recent years, food industries have a great interest in development of biodegradable and natural polymers, such as proteins, polysaccharides, and biodegradable lipids, as eco-friendly alternative to plastic polymers for the production of films useful as packaging to preserve fruits, vegetables, and processed foods extending their shelf-life (Mir et al., 2018; Wróblewska-Krepsztul et al., 2018; Salarbashi et al., 2019).

1.4.1. Main edible film components

The application of edible films for food products is closely related to their cost, availability, functionality, as well as mechanical (flexibility, tension) and optical (brightness and opacity) properties, barrier effect against gas permeation, resistance to water and micro-organisms, and sensory acceptability by consumers.

In particular, these properties depend by the film components (chemical-physical properties of selected polymers), the conditions in which the film are produced (type of solvent, pH, concentration of components, and temperature), and type and concentration of additives (plasticizers, cross-linking agents, antimicrobials, antioxidants or emulsifiers) (Ganiari et al., 2017; Salgado et al., 2015) (**Figure 9**).

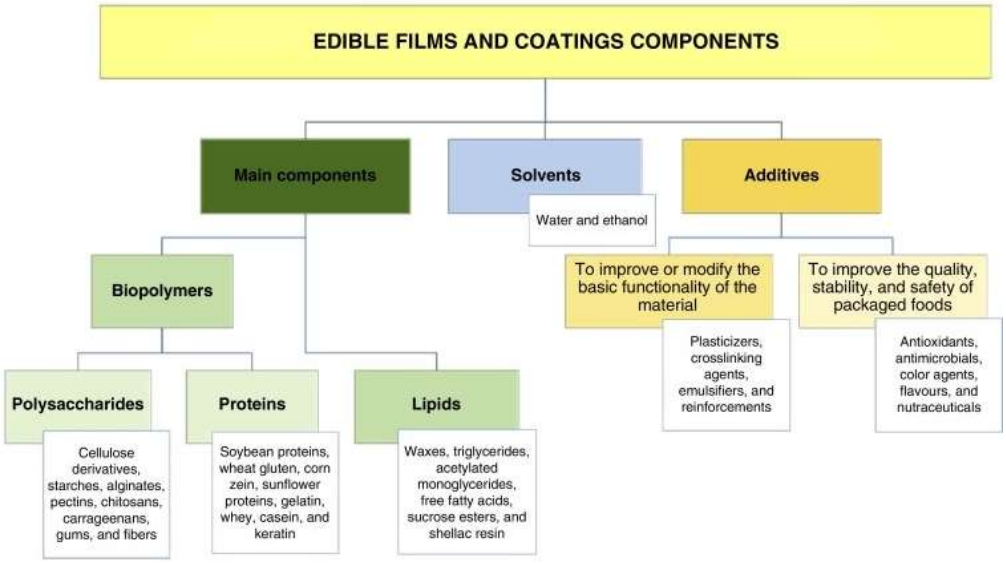

Figure 9. Principal constituents of edible films (Salgado et al., 2015)

Edible and biodegradable films must meet a number of specific functional requirements; they must constitute a barrier against humidity, gas and solutes, must possess suitable mechanical and rheological characteristics and non-toxicity. The materials used for production of edible films have to possess several characteristics (**Figure 10**):

•"barrier" property against the permeation of gases and vapours (carbon dioxide, oxygen, nitrogen, water vapour) between the external environment and the inside of the packaging, avoiding its deterioration;

• absence of migration from the package to the food of harmful chemical compounds for consumer's health (inks, solvents, plasticizer, additives, etc.);

•optical properties (transparency, colour, brightness) stable in different storage conditions (at different temperature and humidity conditions);

• good mechanical properties that allow their easy to process with traditional technologies;

• easy disposal, recycling or reuse (Salgado et al., 2015; Han, 2014).

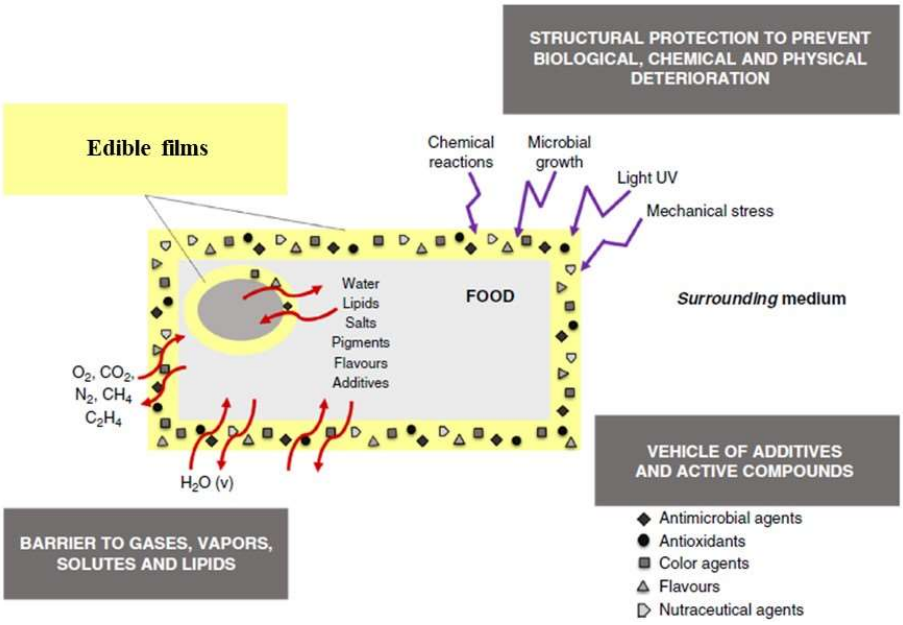

Figure 10. Main functions of edible films edible films (Salgado et al., 2015)

1.4.1.1. Polymers

Biopolymers are the main materials used for the realization of edible film and can be employed alone or in combination. Their chemical-physical characteristics affect the film properties. They are produced only by renewable ingredients and can be consumed with the food product.

On the basis of their origin and production, biopolymers can be classified as (**Figure 11)**:

- polymers extracted from natural material (mainly plants): polysaccharide (such as starch and cellulose) and proteins (for examples casein and gluten);
- polymers generated by chemical synthesis using biological and renewable monomers such as polylactic acid;

- polymers produced by micro-organisms or bacteria genetically modified, such as Pullulan.

Natural polymers can be also classified according to their components into: hydrocolloids, lipids and composites (Hassan et al., 2018; Jiménez, et al., 2018; Srinivasa and Tharanathan 2007; Santacruz et al., 2015).

Hydrocolloids are polysaccharides, such as starch alginate, carrageenan, carboxymethylcellulose, gum arabic, chitosan, pectin, and xanthan gum, usually used by food industry as stabilizers, thickening and gelling agents (Cazon et al., 2017).

Edible films made with starch, an odourless, tasteless and colourless polymer, are semi-permeable to carbon dioxide, have good barrier properties to oxygen, reducing microbial proliferation on food. Films based on alginate result strong but not very resistant to water, due to its hydrophilic nature. Among cellulose derivatives, only hydroxypropyl cellulose (HPC), hydroxypropylmethylcellulose (HPMC), carboxymethylcellulose (CMC) or methylcellulose (MC), are employed in edible films production. The resulted films show a moderate strength, and appear resistant to oils and fats, flexible, transparent, tasteless, colourless, tasteless, water-soluble and possess moderate oxygen barriers. However, films derived from cellulose have poor water vapour barrier effect and reduced mechanical properties (Mellinas et al., 2016; Shit and Shah, 2014). Chitosan is one of the natural polymers widely used in the realization of edible films, as it is biodegradable, chemically inert, biocompatible. It allows to design films with a good permeability to oxygen and carbon dioxide, as well as excellent mechanical and antimicrobial properties against bacteria, fungi and molds, without the use of additional additives (Mellinas et al., 2016; Mujtaba et al., 2018; Shit and Shah, 2014). Several studies report the use of proteins, such as gluten, collagen or gelatine, in the composition of edible films, showing good mechanical properties and barrier ability against oxygen, but not

towards humidity. Furthermore, substances such as gluten, cause allergies and intolerances (Hassan et al, 2018). Lipids such as acetylated monoglycerides, natural wax and surfactants can be used in the production of edible films. Paraffin, wax and beeswax are the most used lipid substances. They are employed as hydrophobic substances, and therefore able to block the moisture passage. However, the films produced are more fragile with low mechanical strength and consequently must be associated with other film-forming agents, such as proteins or cellulose derivatives (Hassan et al, 2018; Shit and Shah, 2014).

Combining the use of proteins and carbohydrates, proteins and lipids, carbohydrates and lipids or synthetic and natural polymers are obtained composite films. They are generally used to combine the properties of the individual polymers, in order to improve the efficiency of the obtained film in terms of mechanical properties and barrier effect towards water, oxygen and carbon dioxide (Ganesan et al., 2018; Shit and Shah, 2014).

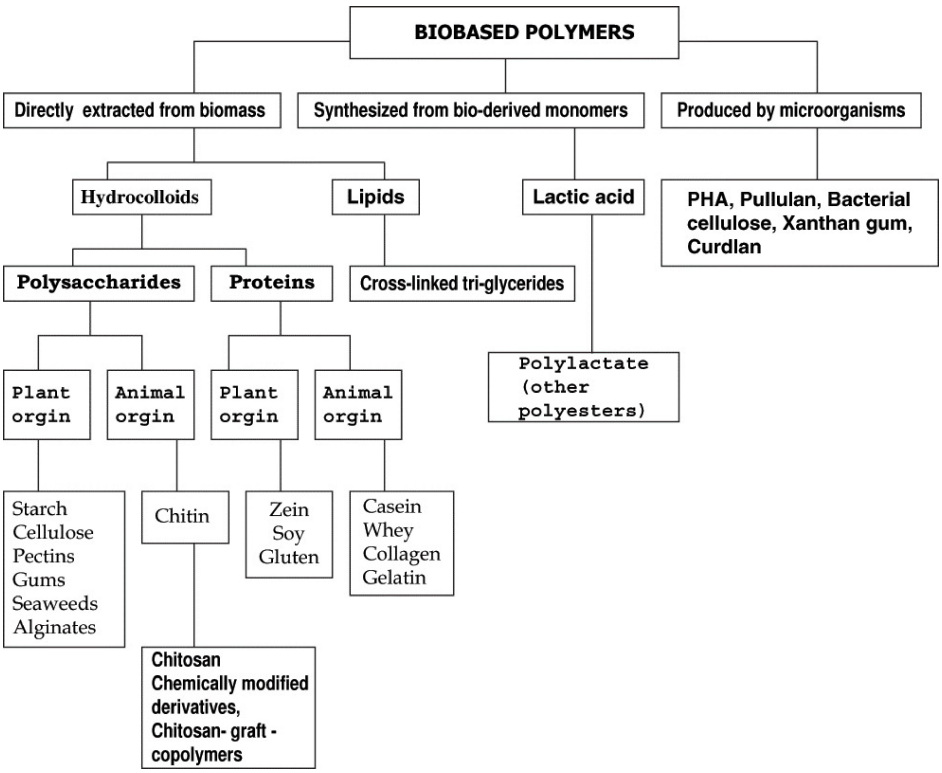

Figure 11. Diagram of polymers based on origin and production method (Srinivasa and Tharanathan, 2007)

1.4.1.2. Plasticizers

Plasticizers are low molecular weight molecules, non-volatile, able to reduce films fragility or increase polymers thermoplasticity. In fact, they interfere with polymer-polymer interactions to break the hydrogen bonds and break down the high intermolecular forces, thus make the resulting film soft and flexible (Han, 2014; Suderman et al., 2018). Plasticizers that can be used in edible films are: low molecular weight sugars (sucrose), polyols (glycerol, sorbitol, propylene glycol), lactic acid (non-volatile, odourless and classified as GRAS by the FDA, excellent preservative agent), acetic acid (used as a food additive with the acidity regulator

function) (Han, 2014). Their presence not only decrease film brittleness and stiffness but reduce also their permeability to water vapour and gases (Suderman et al., 2018).

1.4.1.3. Active additives

Among the major causes of food spoilage there are microorganisms and oxidations of some components, such as vitamins and lipids. To prevent lipid oxidation and microrganisms growth, the new packaging strategies, promote the addition of bioactive ingredients (such as essential oils and plant extracts), with proven antioxidant and antimicrobial properties in order to improve foods quality and prolong their shelf life. Edible films are promising systems to be used as active ingredient carriers, resulting more effective of antimicrobial and antioxidant additives dispersed directly in food. In fact, the film network is able to gradually release bioactive compounds from the film to the surface of products (Vilela et al., 2018; Hassan et al., 2018). The use of natural additives responds to the growing need of consumers, which require less use of synthetic substances in food (Ganiari, et al., 2017; Benbettaïeb et al., 2018; Bouarab et al., 2018). Several works report as the addition of extracts, rich in phenolic compounds, improves the scavenging ability of films by singlet oxygen deactivation, peroxide enzyme inhibition, transition metal chelation, enzymatic detoxification of reactive oxygen species, and their stabilization through the radical transfer of hydrogen (Benbettaïeb et al., 2018).

1.4.2. General characteristics of edible films

It is known that the presence of water can increase numerous reactions including browning, lipid oxidation, and vitamin degradation, but also promote microbial

growth and cause changes in structure. These events are all associated with the quality and shelf-life of the food.

Protein and polysaccharide films provide a good barrier against oxygen and oils, but poor against water. To improve this property edible films are developed by combining polysaccharides or proteins with lipids (Han, 2014). The barrier properties of edible films are mainly related to the physical and chemical nature of the polymers from which they are made, but also depend on the nature of the plasticizer used. Also the passage of oxygen from the environment to the food is at the base of the deterioration of many components (lipids, vitamins, colouring), of microbial growth and of sensory and nutritional changes. Many protein-based films provide an excellent barrier against oxygen. Adding plasticizers to the composition usually results in an increase in oxygen permeability due to an enhanced free volume in the film network (Han, 2014).

The mechanical properties of an edible film reflect its durability and its ability to increase the structural integrity and mechanical properties of the food product. The edible films must generally be resistant to breaking and abrasion, and flexible, in order to adapt to possible deformations without breaking (Han, 2014).

Two sets of forces are involved in the films; cohesion between the polymeric molecules of the film-forming materials, and adhesion between the film and the substrate. The degree of cohesion affects film properties such as strength, flexibility and permeability. Strong cohesion reduces gas barrier and solute properties and increases porosity. Cohesion depends on the chemical structure of the biopolymer, on the manufacturing procedure (temperature, pressure, type of solvent and dilution, application technique, solvent evaporation technique, etc.), the presence of plasticizers and cross-linking additives and the final thickness of the films. Film cohesion is favoured by high-chain polymers.

1.4.3. Production techniques

The techniques for the production of edible films have been developed to form films directly on the surface of food, as separating or self-supporting elements.

An edible film is essentially a three-dimensional gel polymeric network. Regardless of the film making process, for wet casting or dry casting, the film-forming materials should give rise to a gel structure which includes all the incorporated film-forming agents, therefore, plasticizers, other additives and, in the case of wet casting, the solvent. Biopolymers are usually gelatinized to obtain the film-forming solution. Sometimes a drying step is needed to remove excess solvent from the gel structure (Mellinas et al., 2016).

In the film forming protocol, the first important step is the production of a homogeneous solution, suspension or emulsion, mixing all components by low-speed stirring (Mellinas et al., 2016).

Another important step is degassing and defoaming, in order to remove air microbubbles, which, if left suspended, tend to remain entrapped within the dried film, acting as structural defects that cause fractures or brittle area in edible films.

The dry process does not use a liquid solvent such as water or alcohol, but the film-forming materials are heated to increase the temperature above the melting point and to obtain their melting. In this case it is essential to know thermoplastic properties of polymers and materials employed to study the film production process.

At the contrary, the wet process uses solvents for the dispersion of film components; then a drying step is performed. The selection of solvent in this process is a very important factor; since the film produced must be edible and biodegradable, only water and ethanol can be used as solvents, because recognised as safe (Blanco-Pascual and Gómez-Estaca, 2016, Monrad, et al., 2010; Manchanda, et al., 2018).

In order to obtain a film with a homogeneous structure, all ingredients, such as biopolymers and plasticizers, including active agents must be perfectly dissolved in the solvent; if necessary emulsifiers can be added to avoid phase separation. There are several ways to produce edible films: Dipping, Spraying and Casting.
The Dipping technique is used to obtain films useful for food characterized by an irregular surface, but requiring a uniform coating.
The Spraying method is adopted to obtain a thinner and more uniform film compared to that obtained by immersion; usually this technique is used to cover only one side of the food with the film (Gore, et al., 2016).

1.4.3.1. Casting technique

Casting is a technique used for preparation films with active thermolabile compounds (natural extracts) because low temperatures are required to remove the solvents. The solvent-casting protocol consists of casting the polymer solution onto a substrate and then evaporating the solvent without implementing further mechanical or thermal stress. After drying, film is formed and is removed from the substrate (**Figure 12**). The casting technique is the oldest technology used in plastic films manufacturing. Nowadays, the solvent cast technology is becoming increasingly attractive for the production of edible films with extremely high quality, uniform thickness distribution, maximum optical purity. The process parameters (temperature, relative humidity and rate of drying) influence the mechanical, barrier, and thermal properties of resulting edible films (Espitia et al., 2014; Umaraw and Verma, 2017). The film-forming mechanism during solvent casting is complex, involving conformational change of the polymer, as well as solvent-polymer and polymer–polymer interactions that continue to evolve as the solvent evaporates under different drying conditions. It is a technique widely used also on an industrial scale (Siemann, 2005; Dominguez et al., 2018).

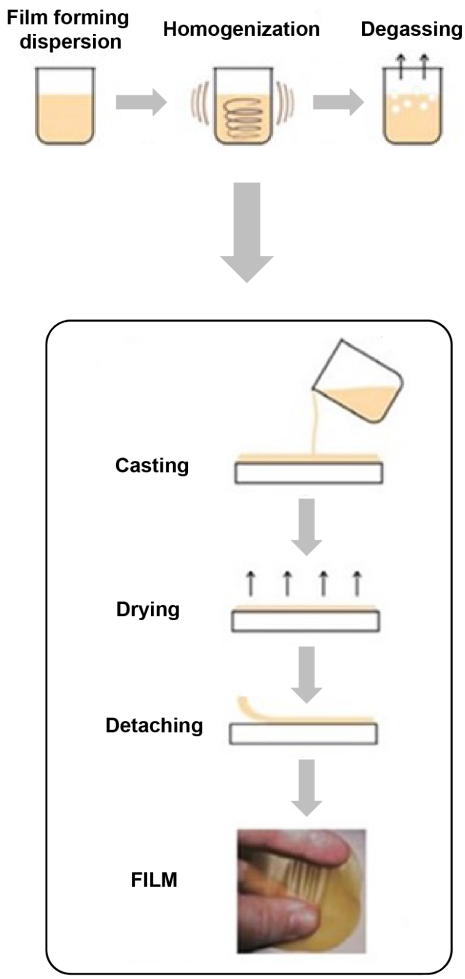

Figure 12. Production of films by casting technique (Otoni et al., 2017)

RESULTS AND DISCUSSION
SECTION A

HAZELNUT (*Corylus avellana* L.) SHELLS: FROM WASTE TO A NOVEL SPRAY DRIED INGREDIENT

Scientific background and research aim

Hazelnut (*Corylus avellana* L., Betulaceae family) is one of the most cultivated and marketed nut in the world. Italy is the second largest hazelnut-producing area (about 105.000 t (tonnes)/year), behind Turkey (about 600.000 t/year) (FAOstat Agriculture data, 2014). About 10% of the world crop is sold as in-shell product consumed fresh or roasted, and the remaining 90% as shelled kernels and used as an ingredient in food (bakery, candy, and chocolate) processing industries (Ciarmiello et al., 2014). During the kernel harvesting and industrial processing, a large amount of waste and by-products, including green leafy covers, hard shells, and skins, are produced.

Figure 13. Hazelnut shells

Unfortunately, disposing these biodegradable wastes represents a serious environmental and economic problem for the hazelnut-industry (Piccinelli et al., 2016). The hard shells, obtained after cracking the kernel, representing about the 50% of the total nut weight, account for a majority of these by-products, and are actually used for burning as a heat source, for mulching, and furfural production in the dye manufacture (Stévigny et al., 2007).

However, some researchers have reported the antioxidant efficacy of hazelnut kernel and shell extracts because of the presence of a high total phenol compounds

content (Contini et al., 2007; Delgado et al., 2010; Shahidi et al., 2007). As well-known, polyphenols display a wide spectrum of biological properties useful for preventing and treating age-related diseases, cardiovascular problems, inflammation, and microbial pathologies (Li et al., 2014). However, natural antioxidants show potential chemopreventive efficacy against several human cancer cell lines (Di Domenico et al., 2012; You and Park, 2010; Lo et al., 2010).
For these reasons, the recovery of bioactive compounds with healthy effects from the hazelnut residues is an interesting strategy to upgrade this low cost material. The first section (Section A Part I) of this work, reports the study on the chemical composition of a polar extract from hazelnut shells (HSE), and the *in vitro* free radical scavenging activity of HSE and pure compounds. Moreover, the antiproliferative and pro-apoptotic activities of HSE and its components against a panel of human cancer cell lines, such as primary and metastatic melanoma (A375 and SK-Mel-28, respectively) and cervical cancer (HeLa) cells, were evaluated. Finally, the activation of caspase-3 through the cleavage of its substrate, PARP-1, in the HSE-induced apoptotic process, was investigated. Despite the complex process of production, and chemical and biological characterization, HSE appears sticky, brown coloured, with penetrating smell, critical water solubility, and potential chemical-physical instability, involving practical difficulties for an industrial use. Therefore, as described in the second part of this section (Section A Part II), HSE was converted into a long-lasting stable and handled microparticulated powder by spray-drying technology. An accurate selection of carrier and coating polymers and process parameters led to design a multipolymeric matrix. The influence of instrumental and operating parameters on yield and encapsulation efficiency was evaluated. The produced microparticulate powders were characterized for solid state (particles dimensions, morphology, amorphous or crystalline form), and water dissolution rate.

The optimized formulation was subjected to accelerated stability test under harsh storage conditions (ICH -International Conference on Harmonization). Finally, the functional stability of HSE-loaded particle system was investigated.

PART I

Chemical composition, antioxidant and cytotoxic activity of Hazelnut Shells polar extract

Based on the article: Hazelnut (*Corylus avellana* L.) Shells Extract: Phenolic Composition, Antioxidant Effect and Cytotoxic Activity on Human Cancer Cell Lines. T. Esposito, F. Sansone, S. Franceschelli, P. Del Gaudio, P. Picerno, R. P. Aquino and T. Mencherini, International Journal of Molecular Sciences, 2017, 18, 392.

A.I.1. Extract preparation, chemical composition, and quantitative analysis

In order to investigate the chemical profile and biological activities of hazelnut shells, a methanol extract (HSE) from powdered and defatted (using *n*-exane and chloroform) shells was prepared by exhaustive maceration at room temperature (3 times x 24 h). A portion (1.5 g) of HSE was subjected to molecular exclusion chromatography (Sephadex LH-20), and the six main collected fractions were purified by RP-HPLC chromatography with Refractive Index Detector to give twelve main compounds (**1-12**). The structures of the isolated compounds (**Figure 14**) were elucidated by their NMR and MS data in comparison with those being in literature. The compounds were identified as: four dihydro[b]benzofuran-type neolignans (**1**–**4**), lawsonicin (**1**) (Mencherini et al., 2011), cedrusin (**2**) (Kim et al., 2005), balanophonin (**3**) (Haruna et al., 1982), and ficusal (**4**) (Li et al., 2000); seven phenolic derivatives, dihydroconiferyl alcohol (**5**) (Huang et al., 2014), veratric acid (**6**) (Crestini et al., 2006), vanillic acid (**7**) (Mencherini et al., 2011), gallic acid (**8**), methyl gallate (**9**) (Picerno et al., 2011), C-veratroylglycol (**11**) (Li et al., 2010), and β-hydroxypropiovanillone (**12**) (Karonen et al., 2004); and a cyclic diarylheptanoid, carpinontriol B (**10**) (Lee et al., 2002). Compounds **1**–**6** and **9**–**12** have never been identified in hazelnut**,** while vanillic and gallic acids (**7**–**8**) were revealed in hazelnut kernel and shells by Ciemniewska-Zytkiewicz et al., 2015. As example, in the Supplemetary Material (**Section S 1**) the structural characterization of the compound **1** has been reported.

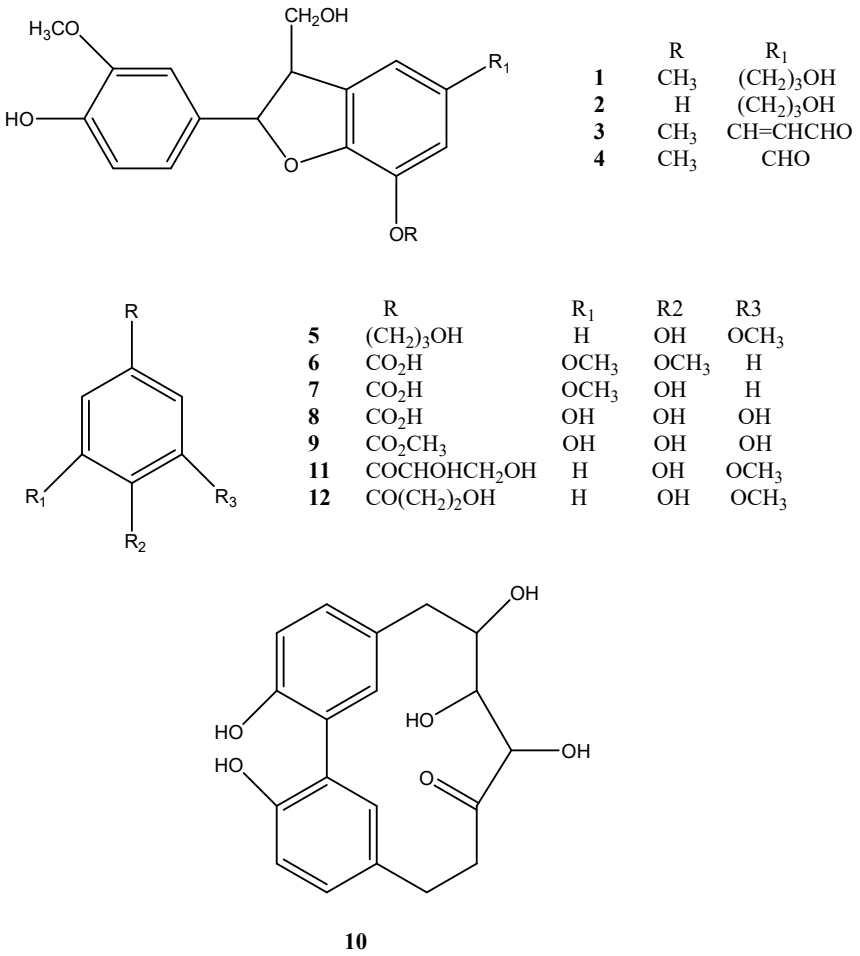

	R	R_1
1	CH_3	$(CH_2)_3OH$
2	H	$(CH_2)_3OH$
3	CH_3	CH=CHCHO
4	CH_3	CHO

	R	R_1	R2	R3
5	$(CH_2)_3OH$	H	OH	OCH_3
6	CO_2H	OCH_3	OCH_3	H
7	CO_2H	OCH_3	OH	H
8	CO_2H	OH	OH	OH
9	CO_2CH_3	OH	OH	OH
11	$COCHOHCH_2OH$	H	OH	OCH_3
12	$CO(CH_2)_2OH$	H	OH	OCH_3

10

Figure 14. Structure of compounds (**1-12**) isolated from hazelnut shells extract (HSE)

To perform the quality control of HSE, the marker compounds were identified and their quantitative analysis was carried out by HPLC-DAD, using calibration curves of isolated compounds. The HPLC fingerprint was reported in **Figure 15**. Lawsonicin (**1**), cedrusin (**2**), and C-veratroylglycol (**11**) were the major components of HSE corresponding to 1.98, 1.79, and 2.93 %, w/w of dry extract, respectively. The other isolated compounds (**3**, **4**-**10**, and **12**) were present as minor constituents.

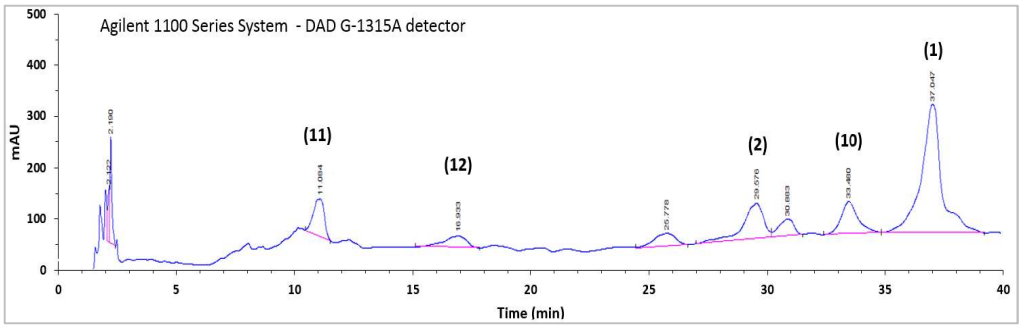

Figure 15. HPLC-DAD fingerprint (230 nm) of hazelnut shells extract (HSE). The peak numbers in this figure correspond to compounds in **Figure 14**.

A.I.2. Free Radical Scavenging Activity

Phenolic compounds are generally recognized to possess a strong antioxidant activity due to redox properties, which can play an important role in neutralizing free radicals, quenching singlet and triplet oxygen, or decomposing peroxides (Kerbab et al., 2015). Since HSE contain a high amount of polyphenols, the free-radical scavenging activity of the extract was verified by DPPH test. The DPPH$^{\bullet}$ is a stable free radical, widely recognized as a rapid and easy tool to estimate the free radical-scavenging activity of different types of plant extracts (aqueous and organic) and pure compounds (lipophilic and hydrophilic) (Kedare and Sigh, 2011). The antioxidant samples, acting as electron or hydrogen donors, convert the DPPH$^{\bullet}$ to a stable non-radical form, with a visible change of solution colour, that is proportional to the scavenging effectiveness of the samples (Slatnar et al., 2015). As showed in **Table 1**, HSE possessed a significant and concentration-dependent free radical scavenging (EC_{50} = 31.71 µg/mL) which may be correlated to its high polyphenol content, evaluated by Folin-Ciocalteu method, and expressed as gallic acid equivalents (193.83 mg GAE/g of the extract). Moreover, in order to identify the compounds responsible for the HSE activity, the free-radical scavenging

activity of all isolated compounds was also verified. Gallic acid (**8**) and methyl gallate (**9**), water-soluble polyphenols, resulted very effective in quenching free-radicals, exhibiting an EC_{50} of 1.20 and 1.95 µg/mL, respectively, 10-fold higher than α-tocopherol (EC_{50} = 10.10 µg/mL) used as positive control (**Table 1**). Compounds **1-3**, **6-7** and **9-12** were less active than the previous phenol compounds with EC_{50} values ranging from 42.73 to 89.22 µg/mL (**Table 1**). Finally, compounds **4** and **5** showed a weak free-radical scavenging effect *in vitro*, resulted about 10-fold less active than α –tocopherol (**Table 1**). The strong antioxidant effect of phenolic acids such as compounds **8** and **9** is due to three free hydroxyl groups at position 3, 4 and 5 on the aromatic ring (Rice Evans et al., 1996). The lack of hydroxyl group followed by the O-methylation of one or both o-hydroxyl groups on the aromatic ring reduced drastically the activity as observed for veratric (**7**) and vanillic (**6**) acid (**Table 1**), respectively. Additionally, in the series of di-ortho phenolic derivatives, compound **12** was more active than compounds **11** and **5** (**Table 1**). Probably, the existence of the hydroxyl group (**11**) or the substitution of the carbonyl group with a methylene group (**5**) in the side chain may cause the reduction of the antioxidant activity. Considering the structures of neolignans **1**-**4**, the free-radical scavenging activity was as follows **2**>**3**>**1**>**4**, suggesting that the antioxidant effect could be related to 3-phenylpropan-1-ol unit and free hydroxyl group at position C-3' (Huang et al., 2013). On the other hand, it has been observed that the blocking of OH at C-3' (Lawsonicin, **1**), the loss of side chain (Ficusal, **4**) or the presence of a carbonyl group on the side chain (Balanophonin, **3**) reduced the antioxidant activity. In conclusion, the additive and synergistic effect of phenols present in HSE, could be ascribed as responsible of the significant free radical scavenging activity of the hazelnut shells extract, and they exert a better antiradical effect in combination each other than as individual compound (Dai and Mumper, 2010).

Table 1. Total Phenol Content and free-radical scavenging activity of HSE and compounds **1-12**

Extract and compounds	Phenol content (mg/g extract)[a]	EC_{50}[c] (μg/mL)[c]
HSE	193.83 ± 3.60[b]	31.71 ± 1.42[b]
1		74.31 ± 3.80
2		42.73 ± 2.52
3		59.21 ± 2.96
4		160.00 ± 4.50
5		118.70 ± 3.51
6		55.41 ± 1.20
7		58.61 ± 3.52
8		1.20 ± 0.22
9		1.95 ± 0.81
10		78.23 ± 2.10
11		89.22 ± 3.23
12		54.61 ± 2.82
α-tocopherol[d]		10.10 ± 1.31

[a]Gallic acid equivalent; [b]Mean ± SD of three determinations by the Folin-Ciocalteu method; [c]EC_{50} ± standard deviation (data from three experiments in triplicate); [d]Positive control of the DPPH assay.

A.I.3. Cytotoxic Activity of HSE and Isolated Compounds

The cytotoxic activities of gallic acid and neolignans with a dihydro[*b*]benzofuran against several cancer cell lines have been reported in literature (Lo et al., 2010; Mencherini et al., 2011; Huang et al., 2013; Chung et al., 2011). Therefore, the antiproliferative activity of HSE, rich in this kind of compounds, was evaluated against human melanoma (primary A375, metastatic SK-Mel-28), and cervical cancer (HeLa) cell lines, by MTT assay. The conventional chemotherapy, surgery, radiation, alone or in combination, used for treating of melanoma and cervical

cancer, are rather unsatisfactory (Di Domenico et al., 2012; Lo et al., 2010). Therefore, in the last years, the use of plant extracts as novel foods or active additives in functional foods, dietary supplements and natural remedies has attracted considerable interest. HSE exhibited a significant ($p < 0.05$) and concentration-dependent inhibitory effect on the tumor cell lines growth (**Table 2**). To localize the activity within HSE, the cytotoxic effect of all isolated compounds (with exception of **9** because of its very small amount) was tested in the same conditions. The results showed that balanophonin (**3**), and gallic acid (**8**) were cytotoxic on all three cell lines with IC_{50} values ranging from 142.01 to 200.02 μM (**Table 2**). Instead, the neolignan cedrusin (**2**) was found active in A375 and HeLa cells (IC_{50} = 130.00 and 141.02 μM, respectively) for the first time. On the contrary, other neolignans (lawsonicin **1**, and ficusal **4**), phenol derivatives (dihydroconiferyl alcohol **5**, veratric acid **6**, vanillic acid **7**, C-veratroylglycol **11**, and β-hydroxypropiovanillone **12**), and cyclic diarylheptanoid (carpinontriol B **10**) were not cytotoxic up to 1000 μM (**Table 2**). Our results, highlighted as the effect of HSE on cancer cell growth is due to a synergy of action of its major (cedrusin) and minor chemical components (balanophonin, and gallic acid).

Table 2. Effect of HSE and its compounds on human cancer cell lines

	Cell line		
Extract or compound	A375[a] (IC_{50})[b]	SK-Mel-28 [a] (IC_{50})[b]	HeLa [a] (IC_{50})[b]
HSE	584.00 ± 9.01[c]	459.02 ± 8.36	526.01 ± 8.90
1	NA[d]	NA	NA
2	130.00 ± 4.22	N.A	141.02 ± 3.84
3	142.01 ± 3.63	150.05 ± 4.10	143.04 ± 4.41
4	NA	NA	NA
5	NA	NA	NA
6	NA	NA	NA
7	NA	NA	NA
8	170.02 ± 3.21	150.02 ± 4.02	200.02 ± 3.33
10	NA	NA	NA
11	NA	NA	NA
12	NA	NA	NA

[a]A375 and SK-Mel-28, melanoma cells; HeLa, cervical cancer cells; [b]IC_{50}, required concentration of extract or pure compound to inhibit cell proliferation by 50% expressed as µg/mL for extract and µM for compounds; [c]IC_{50} ± standard deviation (data from three experiments in triplicate); [d]Not active (IC_{50}>1000 µM)

Despite apoptosis induction in cancer cells has been recognized as a possible property of gallic acid as a chemotherapeutic agent (Lo et al., 2010; You and Park, 2010; Liu et al., 2014), there is no available study showing the mechanism of cedrusin and balanophonin in human cancer cell death. Thus, the potential apoptotic effect of HSE and its cytotoxic compounds (**2-3**, and **8**) was investigated on A375, SK-Mel-28 and HeLa cell lines. The presence of hypodiploid nuclei in the cells, after incubating with the extract (100-500 µg/mL) or compounds (each 100-500 µM) for 24 h, was evaluated by flow-cytometric analysis (Mencherini et al., 2011). **Figure 16** showed that HSE induced apoptosis in all treated cells increasing in a dose-dependent manner the percentage of hypodiploid nuclei. Notably, this effect

was significant ($p<0.05$) up to 250 µg/mL and was more potent in A375 cells with respect to SK-Mel-28, and HeLa cells. A pro-apoptotic effect was also exhibited by compounds **2**, **3** and **8** (data not shown).

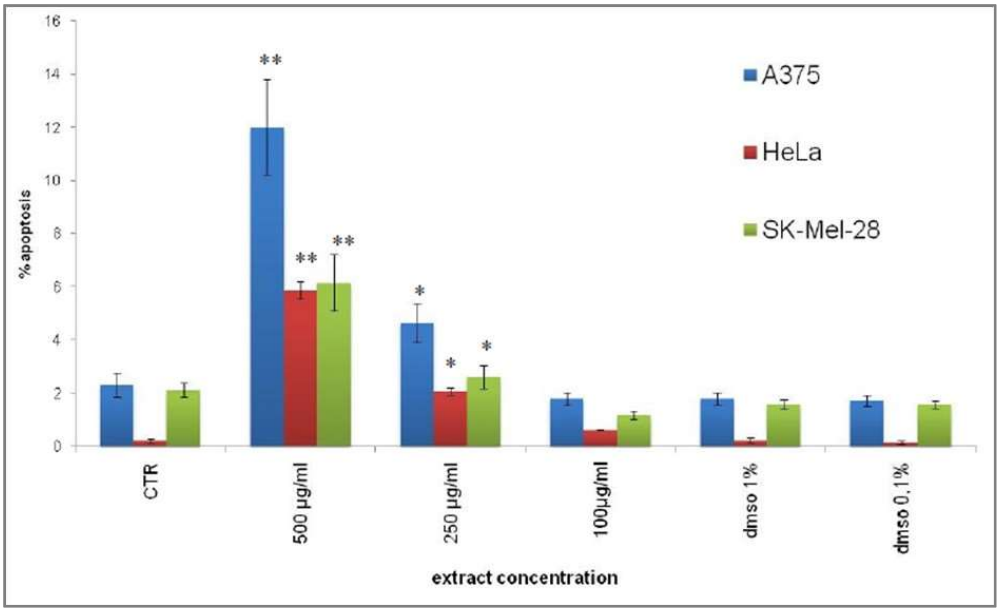

Figure 16. Effects of HSE on apoptosis of A375, SK-Mel-28 and HeLa cells. Analysis of percentage of nuclei in apoptosis was performed with propidium iodide staining. Cancer cells were incubated with different concentrations of HSE (100-500 µg/mL) for 24 hrs. Cells were then collected, and the percentage of hypodiploid nuclei was analysed by flow cytometry (*$p < 0.05$, **$p < 0.01$ vs control cells).

The activation of caspases, a family of cysteinyl-aspartate proteases, usually present as inactive zymogen forms, is one of the most common signalling cascade involved in apoptosis. During the execution phase of apoptosis, caspases cleave several proteins that are necessary for the cell function and survival and among them, PARP-1 (poly(ADP-ribose) polymerase-1), a nuclear enzyme involved in DNA repair, DNA replication, modulation of chromatin structure and apoptosis (Talanian et al., 2000). In response to genotoxic stress PARP-1 is cleaved by caspase-3 and 7

into a ~25 kDa N-terminal fragment containing the DNA binding domain (DBD) and a ~85kDa C-terminal fragment that retains basal enzymatic activity PARP-1 recognizes DNA strand interruptions and can complex with RNA and negatively regulate transcription. Through these processes, PARP-1 cleavage may help cells to commit to the apoptotic pathway. Thus, PARP-1 plays a central role in apoptosis determining the cell fate (Chaiatanya et al., 2010; Diamantopoulos et al., 2014). So, the expressed levels of caspase-3 and cleaved PARP-1 by Western blotting analysis were evaluated, in order to investigate the mechanism of both HSE and compounds-induced apoptosis in A375, SK-Mel-28 and HeLa cancer cells. The results indicated that HSE and compounds **3** and **8** induced activation of caspase-3 after 24-48 h of treatment and PARP-1 cleavage (**Figure 17**) in Hela and SKMel-28 cell lines, but not in A375 cells. The mechanism through which the HSE and compounds induce apoptosis in A375 cell line deserve to be further investigated.

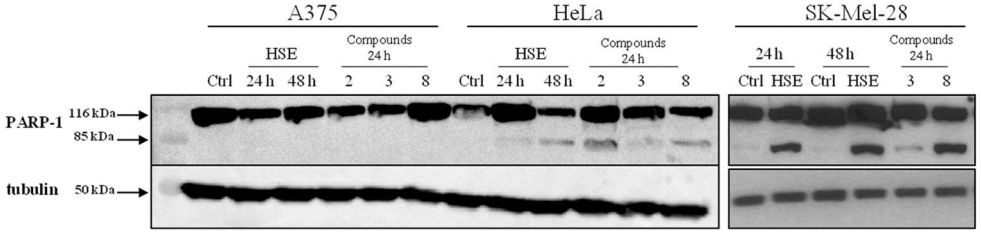

Figure 17. PARP-1 expression in A375, HeLa and SK-Mel-28 cell lines after 24 and 48 hrs of treatment. HSE and compounds induce PARP-1 cleavage in HeLa and SK-Mel 28, but not in A375 cell lines.

PART II

New polymeric microparticles systems loaded with the polar extract (HSE) from hazelnut shells

A.II.1. Formulation studies and production of preliminary microparticulate systems

The polar extract (HSE), as reported in the previous paragraphs, showed a significant scavenging activity *in vitro* against the radical DPPH and an inhibitory effect on human melanoma and cervical cell lines, inducing apoptosis by caspase-3 activation (Esposito et al., 2017). A particle engineering approach, involving the production of microparticles by spray drying, is proposed to convert the functional extract in a water soluble and long-lasting stable material in powder form (Munin and Edwards-Lévy, 2011; Sansone et al., 2014 a; Sansone et al., 2014 b). After a comprehensive formulation study, the appropriate polymeric matrix, as coating polymers and loading carriers, able to transform HSE in a microparticulate powder form by spray drying technique, was selected. In particular, a combination of L-proline (P) as loading carrier and hydroxyethylcellulose (HEC) as coating polymer was used.

Amino acids, including arginine (Arg), phenylalanine (Phe), and leucine (Leu) are often used in microencapsulation process as effective dispersibility enhancers able to load active ingredients (Prota et al., 2011; Chang et al., 2014).

P is an abundant amino acid in foods of animal origin (milk, meat, salmon) and vegetable (wheat, barley, corn) and also present in high concentrations in many drinks, such as wine, grapes juice and beer (Liu et al., 2017).

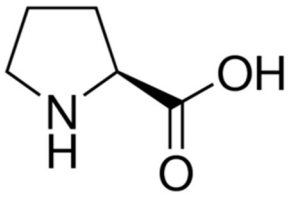

Figure 18. Structure of L-proline

P possess the highest solubility in water and alcohol among amino acids (Hyung et al., 2008) and it has been proven to be essential for the production of collagen and healthy joints, tendons and skin (Hyung et al., 2008). Due to its ring structure, P stabilize the α-helix conformation and increases its synthesis in human fibroblast cells (Ponrasu et al., 2013). P has important roles in multiple biological processes such as cellular bioenergetics, cell growth, oxidative and osmotic stress response, protein folding and stability, and redox signalling. It is used by the organisms, through the catabolic proliferative way, as a source of carbon, azote and energy. The exhaustion of proline dehydrogenase dependent on FAD (PRODH) and sodium glutamate semi aldehyde dehydrogenase (GSALDH), responsible for the conversion of P into glutamate, in man causes hyperprolinemia, associated with mental disorders, such as schizophrenia (Liu et al., 2017). Some research reported the role of P in osmotic and oxidative stress protection, protein chaperoning, cell signalling, programmed cell death, and it is involved in extracellular matrix (ECM) integrity (ECM degradation plays a critical role in the formation of tumours and metastasis) (Natarajan et al., 2012; Roomi et al., 2008). In particular, P metabolism affects cell survival and death outcomes by influencing the intracellular redox environment during oxidative and nutritional stress conditions. Moreover, proline oxidative catabolism induces apoptosis through the mitochondrial (intrinsic) pathway (Natarajan et al., 2012; Roomi et al., 2008; Krishnan et al., 2008). Furthermore, P acts as an antioxidant by upregulation and stabilization of antioxidant enzymes, scavenging of ROS, metal chelation, equilibrium of intracellular redox homeostasis and improvement of cellular resistance to hydrogen peroxide (Leal, et al., 2019).

HEC (hydroxyethylcellulose) is also a polymer derived from cellulose, with average molar mass of about 120 000 Da. It is a non-ionic, water-soluble, biocompatible and non-toxic polymer, with good film-forming properties.

Moreover, its high water solubility and stability in the pH range of 3.0 ∼11.0 makes easy the combination with saline solutions also in presence of metal ions (Liu et al., 2006 a; Benyounes et al., 2018).

The viscosity is a limiting parameter to process a liquid feed by spray drying (Sansone et al., 2013). Thus, a series of pilot experiments were conducted to determine the HEC concentration giving the viscosity of the liquid feed compatible with the spray drying process. Results are reported in **Table 3**.

Table 3. Results of HEC viscosity in water at different concentrations

HEC CONCENTRATION % (w/v)	VISCOSITY a t 30'' (mPa.s)	Instrumental reliability value (valid range 18 – 100)
0.10	68.31	79.51
0.30	81.42	94.44
0.50	81.80	95.71
1.00	92.53	22.00

[a] viscometer Visco Basic Plus, Fungilab S.A. (L1, 100 rpm)

Preliminary satisfactory results in term of matrix processability were obtained with an aqueous liquid feed with a concentration of 0.1% w/v HEC and 5% w/v P in a 98:2 P:HEC ratio (HEP-1) (**Table 4**). This matrix amount was able to load 0.25% of raw HSE (HEP-HSE) (**Table 5**). The liquid feeds were spray dried under the following experimental conditions: Inlet/outlet temperatures = 125/85 °C, Ø Nozzle = 0.7 mm, Drying air flow = 500- 600L/h, Air pressure = 6 bar, Aspirator= 100%, Spray flow = feed 3mL/min. All the results are reported in **Table 4** and **5**. The production yield of the micro-powder (HEP-HSE) was not so satisfactory (38.9%) (**Table 5**).

A.II.2. Optimization of polymeric matrix and production of microparticulate systems

In order to optimize the produced microparticulate system in term of process yield, encapsulation efficacy, morphology, particle size, and water dissolution profile, high methoxylated pectin from citrus (PEC) and sodium carboxymethylcellulose (NaCMC) were selected as additional coating polymers and separately included in the polymeric matrix.

PEC is a structural component of the cell wall present in all higher plants and commercially available. It is a heterogeneous polysaccharide made up by linear (1→4)-linked-α-D-galacturonic acid residues partially interrupted by (1→2)-linked side chain consisting of L-rhamnose and some other neutral sugar residues.

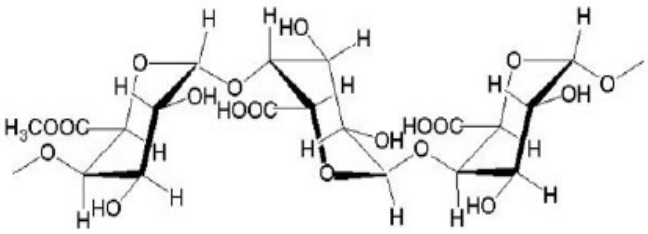

Figure 19. Representative structure of Pectin

Pectins can be classified according to their degree of esterification, expressed as a percentage of carboxyl groups, in low methoxyl pectin (DE < 50%) and high methoxyl pectin (DE> 50%) (Zainudin et al., 2018). In particular, high methoxyl pectin (DE> 50%) is able to gel, forming a particularly stable polymeric network, both at low acid pH (pH ≈ 5) and in the presence of sugars, without the need for divalent ions as occurs for pectins with a low degree of esterification or alginates. Moreover, the high methoxyl pectin is characterized by a low hygroscopicity; an

important property to improve the products stability during storage. Furthermore, PEC is widely used as a gelling agent, stabilizer and thickener in foods and their viscosity depends on the molecular weight, pH, ionic strength and arrangement of the carboxyl groups (Sansone et al., 2011; Brejnholt, 2009).

PEC, with high degree of esterification (76%), used during the present PhD project, was obtained as by-product from a local citrus transforming.

The sodium carboxymethylcellulose (NaCMC) is reported in the "GRAS list" (Generally Recognized As Safe) and it is considered safe for food use by the SFC (Committee for Food Security) and JECFA (Joint Committee of FAO/WHO Expert Committee on Food Additives) (Sansone et al., 2018 b).

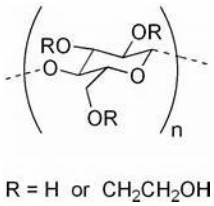

Figure 20. Structures cellulose derivatives

It is a polymer derived from cellulose with very versatile solubility and technology characteristics. In fact, it is soluble both in cold and in hot water, stable in pH ranges between 5 and 10 and has a good compatibility with alcohol (it can be added in the dispersions up to 40% w /v). It has film-forming properties useful in the spray drying particle formation phase and binder properties during formulation phases with possible compression or granulation. After the dispersion in water, the solution shows a pseudo-plastic behaviour, with variable viscosity, depending on the concentration used. Moreover, it is a good stabilizer for emulsions and film-forming agent. It is not compatible with cationic agents, compatible with anionic and non-ionic substances. As stabilizer in emulsions it is generally used at concentrations between 0.2 and 1%, while for the preparation of aqueous gels, it is used in a

concentration range between 1 and 3%. In addition, as food additive it is identified as "E466", and has long been used as in food preparations based on cream, fish, meat and fruit, desserts, ice creams and creams (Sansone et al., 2013). NaCMC is used in colloidal delivery system for sensitive ingredients (De Cicco et al., 2014; Sansone et al., 2013).

The addition of NaCMC (HEP-NaCMC-27) (**Table 4**) as coating polymer did not result suitable for the particle formation. The presumable chemical interaction between NaCMC and P (Boopathy and Kamasamy, 2015) led to complexes formation resulting in sticky powder without particles formation. Otherwise, the use of PEC in formulation gave better results. More than 40 pilot experiments were carried out to found the optimum HEC:P ratio, select a coating co-polymer, and optimize the feed preparation method. Moreover, in order to improve the solubility of HSE raw material, lecithin (L) and ethanol were used in the feed suspension. L is a food emulsifier employed to stabilize the organic water/solvent system. L, in spite of its natural origin and its dietetic and health functions, is considered a food additive and is identified as E322. It is used in food products, because contain high phospholipids amount. Moreover, it is involved in liposomes and micelles formation. L is also an emulsifier, manly used in formulation in a range between 3 and 5%; while concentrations lower than 3% are used to stabilize homogeneous suspensions (Bettiol and Cecchi, 2013).

L and ethanol are EFSA authorized ingredients and they are GRAS (Chatzidaki et al., 2015). The experiments led to select HEP-46 as the best formulation. Satisfying process efficiency (yield and loading) and well formed microparticles were obtained using 0.5% w/v of PEC in a liquid feed with 0.2% w/v HEC, 5% w/v P and 0.2% L in a 85.0:3.4:8.2:3.4 P:HEC:PEC:L ratio (HEP-46) (**Table 4**). For the matrix preparation a Hot-Cold-Hot method (H-C-H) was used. Spray drying conditions: Inlet/outlet temperatures = 125/85°C, Ø Nozzle = 0.7 mm, Drying air

flow = 600 L/h, Air pressure = 6.5 bar, Aspirator = 100%, Spray flow feed = 3.8 mL/min, obtaining the formulation HEP-HSE-46 (**Table 4-5**).

Table 4. Composition and characteristics of HEP blanck powders

Sample	P g/100mL	HEC g/100mL	PEC g/100mL	L g/100mL	NaCMC g/100mL	Preparation method[a]	Yield[b] %
HEP-1	5.00	0.10	-	-	-	H-C	35.80 ± 5.40
HEP-NaCMC-27	2.50	0.10	-	-	0.20	H-C	48.10 ± 2.10
HEP-46	5.00	0.20	0.50	0.20	-	H-C-H	50.00 ± 2.02

[a] H-C = Hot/cold; H-C-H = Hot/cold/Hot method
[b]Average of triplicate analyses ± standard deviation
P, L-proline; HEC, hydroxyethylcellulose medium viscosity; PEC, pectin; L, lecithin; NaCMC, sodium carboxymethylcellulose

A.II.3. Characterization of the produced microparticles

A.II.3.1. Yield and loading efficiency

Composition and main characteristics of the optimized powder (HEP-HSE-46) were compared to HEP-HSE and unprocessed extract (HSE) (**Table 5**). The production yields of HEP-46 (blank), and HEP-HSE-46 were highest (50% and 43%, respectively) then the first formulations HEP-1 and HEP-HSE (35% and 39%, respectively). However, the process yield of loaded particles (HEP-HSE-46) did not exceed 50% probably for the low amount of material sprayed (100 mL) and the loss of the smallest and lightest particles with the exhaust of the spray dryer. The Actual Active Content (AAC) of both unprocessed and processed extract (AAC-HSE) was determined by HPLC method (previously reported for quantitative analysis of HSE), to verify the percentage of lawsonicin, the most representative neolignan (3.16% w/w) of HSE and thus chosen as chemical marker. These values led to calculate the effectively loaded extract (Actual Extract Content, AEC-HSE). AEC-HEP-HSE-46 resulted very close to the amount of extract used to prepare the liquid

feed (Theoretical Extract Content, TEC-HSE). Consequently, the loading efficiency (LE) value, calculated as the ratio of AEC to TEC, was very satisfying (95.12%, **Table 5**) in comparison to HEP-HSE (92.1%).

Table 5. Composition and characteristics of HEP-HSE ans HEP-HSE-46 powders prepareted in comparision to the corresponding unprocessed extract

Sample	P g/100mL	HEC g/100mL	PEC g/100mL	Extract g/100mL	Yield[f] %	TEC [a] %	TAC [b] %	AEC [c] %	AAC [d] %	Ee[e] %	d_{50} µm (span)[g]
HSE raw	-	-	-	-	-	-	-	-	3.16 ± 1.5[f]	-	-
HEC	-	-	-	-	-	-	-	-	-	-	277.22 (1.60)
P	-	-	-	-	-	-	-	-	-	-	250.10 (1.71)
PEC	-	-	-	-	-	-	-	-	-	-	50.53 (1.32)
HEP-HSE	5.00	0.10	-	0.25	39.81 ± 9.40	4.67	3.13	4.30	3.11 ± 0.91[f]	92.10	18.41 (1.60)
HEP-HSE-46	5.00	0.20	0.50	0.25	43.0 ± 3.00	4.10	2.20	3.90	2.10 ± 0.93[f]	95.00	3.00 (1.20)

[a] Theoretical extract content: amount of extract in the feed/ total feed components *100
[b] Theoretical active content: AAC unprocessed extract * amount of extract in the feed/total feed components
[c] Actual extract content: AAC-HEP-$_{HSE/HSE46}$/AAC unprocessed extract * 100
[d] Actual Active content: content of lawsonicin calculated by HPLC-DAD
[e] Encapsulation efficiency: AEC/TEC* 100
[f] Average of triplicate analyses ± standard deviation
[g] Span value calculated as (d_{90}- d_{10}) /d_{50}

A.II.3.2. Dimensional and morphology analysis

Laser Light scattering (LLs) analysis was carried out to investigate the particle size distribution. As reported in **Table 5**, HEP-HSE and HEP-HSE-46 microparticles had narrow size distribution (d_{50} 18.41 and 3.0 μm) with respect to L-proline, (P, d_{50} 250.10 μm), hydroxyethylcellulose (HEC, d_{50} 277.22 μm) and pectin (PEC, d_{50} 52.53 μm) as raw materials (**Table 5**). The lowest mean diameter (3.02 μm) was observed for HEP-HSE-46 (**Table 5**). This behavior is due to the right physical interaction between matrix components leading to the rearrangement of P crystals in spherical agglomerates during the spray drying process (Sansone et al., 2013). The use of organic solvent and lecithin solution to better expose the extract to the aqueous polymeric feed seems to positively affect the interaction of extract with the matrix components, resulting in a reduced dimensional distribution of the obtained particles.

The morphological characterizations of the produced powders were conducted by microscopy analysis (FM and SEM), and the micrographs of obtained lots were compared to HSE and P raw materials. The unprocessed extract appears as a material in a cluster crystalline state with irregular shape and surface (**Figure 21 a**), and differences between HEP-HSE and HEP-HSE-46 (loaded microparticles) have been detected.

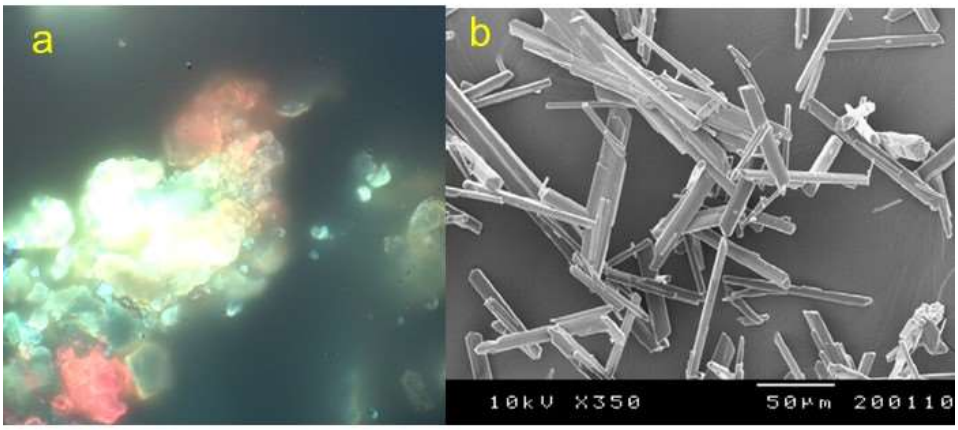

Figure 21. FM image (**a**) of HSE raw material and SEM micrographs (**b**) of L-proline (reported by Hyung et al., 2008): crystalline clusters with difference fluorescence (**a**) due to the different nature of bioactive compounds

Normally, the morphology of P shows a needle crystalline form (Hyung et al., 2008; **Figure 21b**). After the spray drying process, P did not lose its crystalline state, but it is involved in a spherical agglomeration process due to a physical interaction with HEC (HEP-1) (**Figures 22a** and **b**) and in HEP-HSE-46 (**Figures 22 c** and **d**). In HEP-1 (**Figures 22 a** and **b**) some particles have fractures and clusters on the surface indicating that a coating with HEC-alone was not able to completely form the particles. In HEP-HSE-46, the presence of PEC in combination with HEC and lecithin leads to well-formed particles free of fractures; the presence of agglomeration is probably due to the small size of particles (**Figures 22 c** and **d**).

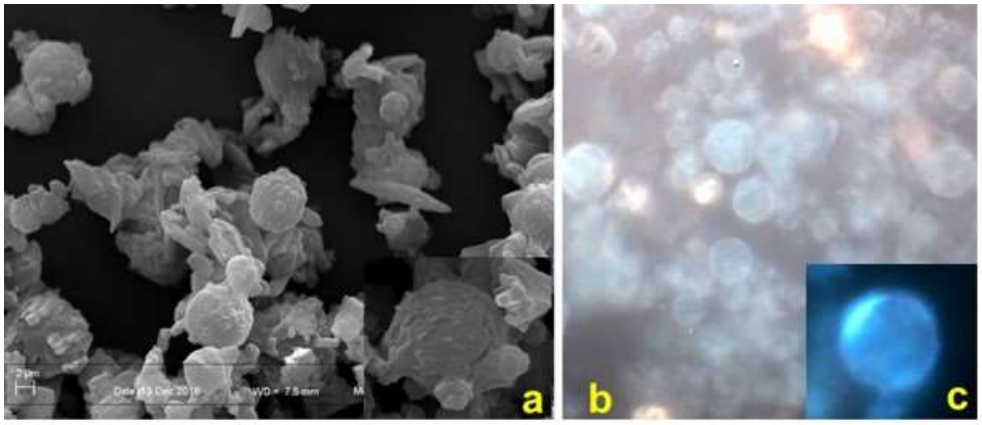

Figure 22. SEM micrographs of HEP-1(**a** and **b**) and HEP-46 (**c**) blank microparticles

In HEP-HSE, the extract negatively affected the agglomeration process of P during microparticles formation probably competing with the coating cellulose polymer (**Figure 23 a**). The powder showed a single cluster zone without a clear microparticles formation (**Figure 23 a**). FM image showed a not completely loading of the extract that did not interact with the matrix (**Figure 23 b** and **c**).

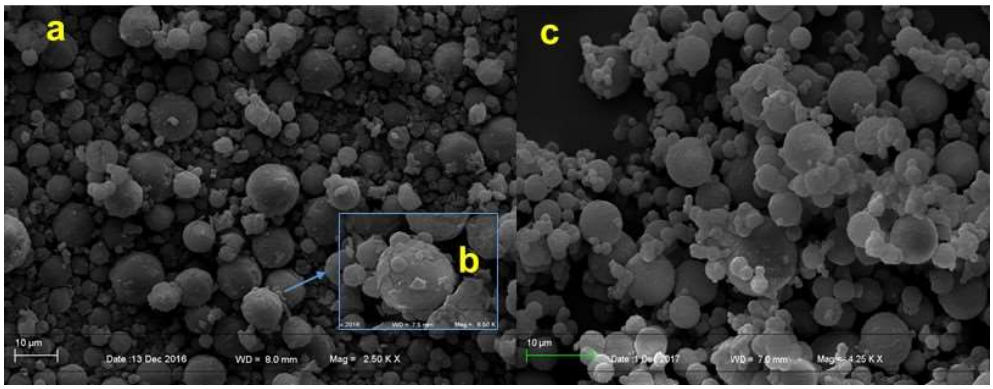

Figure 23. HEP-HSE SEM micrographs (**a**) and FM images (**b** and **c**)

On the contrary, in HEP-HSE-46 (**Figure 24 a** and **b**) spherical, well-formed and completely coated microparticles have been obtained during the spray drying

process. Furthermore, the extract is homogeneously distributed and better encapsulated within the microparticles. (**Figure 24 b** and **c**).

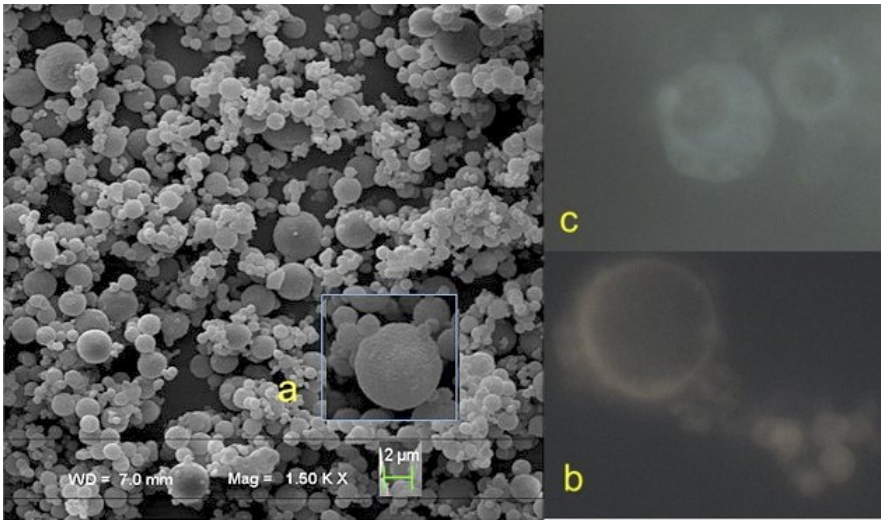

Figures 24. HEP-HSE-46 SEM micrographs (**a**) and FM images (**b** and **c**)

A.II.3.3. Thermal analyses

In order to provide information on solid state and extract-polymer interactions as well as on physical stability of materials after the technological process, differential scanning calorimetric technique was used (Boopathy and Kamasamy, 2015). Comparing DSC thermal profiles of HEP-46 and HEP-1 (blanks, **Figures 25, b** and **c**), it is possible to observe an anticipation of P crystals agglomerate melting peak, shifted by 8 Celsius degrees in HEP-HSE-46 (221.45°C) with respect to HEP-1 (228.81°C), accompanied by a reduction of enthalpy (-68.11 mJ for HEP-46 and -287.68 mJ for HEP-1), indicating a reduction in crystallinity. In all thermograms, it is possible to observe a thermal event around 290°C, due to the product final degradation. This event possesses a lower intensity for HEP-HSE 46 (**Figure 25 b**) with respect to HEP-HSE (**Figure 25 d**) indicating that the extract was completely

encapsulated in the matrix. Moreover, it is also detectable a reduction of the free water content (visible in the thermograms in the 50-100°C range temperature) for both HEP-46 (blank) and HEP-HSE-46 (loaded) with respect to HEP-1 and HEP-HSE, which could positively affect the stability of formulations. The thermal analysis of the optimized formulation HEP-HSE-46 confirmed that extract well interacts with matrix in solid state formation, confirming the reduction in crystallinity previously obtained only for blank samples (unloaded microparticles).

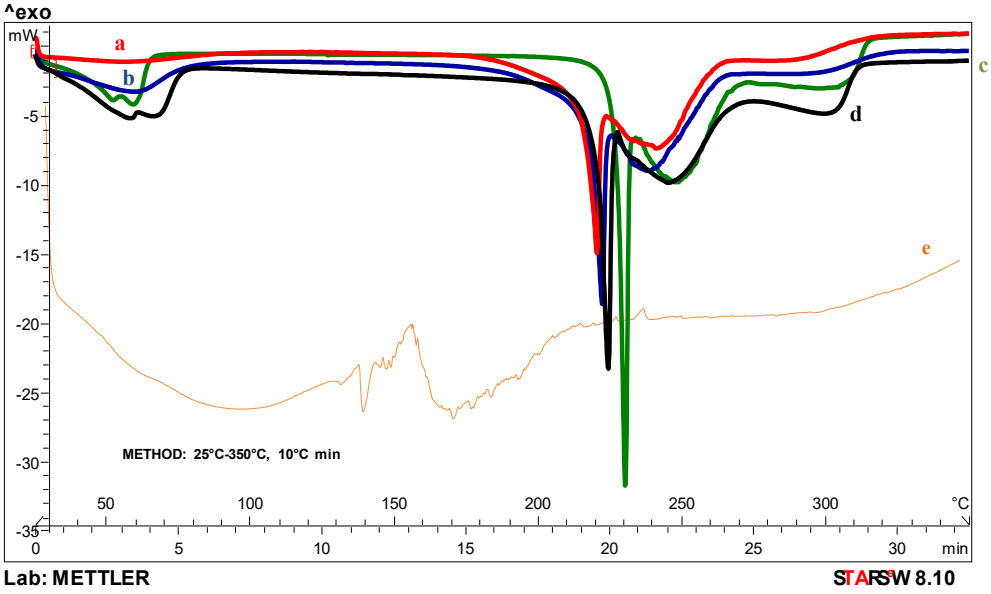

Figure 25. Differential scanning calorimetry (DSC) of HEP-HSE-46 (**a**), HEP-46 (**b**), HEP-1 (**c**), HEP-HSE (**d**) and compared to unprocessed extract (HSE, **e**).

A.II 3.4. In vitro dissolution/release tests

Dissolution studies of both HEP-HSE-46 and HEP-HSE were performed using USP II Apparatus, compared with the unprocessed HSE and the resulting dissolution/release profiles in distilled water are reported in **Figure 26**. AAC value

was calculated by-HPLC method (as reported in paragraph A.III.1.7) to identify the quantity of lawsonicin released. The standard curve was analysed using the linear correlation between concentration and peak area integration (regression equation y = 9579.9 x-19.612, r = 0.9999, at five concentration levels in the range of 0.01-0.00125 mg/mL). The dissolution/release profile of HEP-HSE and HEP-HSE-46 microparticles showed a drastic improvement of HSE release with respect to the raw material. In 15 min, 88.5 % and 91.2% of release/dissolution of the extract was obtained from HEP-HSE-46 and HEP-HSE, respectively. In the same time only 33.12% of the unprocessed extract (HSE) was dissolved. The behavior of HEP-HSE-46 and HEP-HSE could be explained by an increase of the microparticles-water interaction due to both the smallest dimensions (d_{50} 3.02 and 18.41 μm) and spherical state of the powders, enhancing the total surface exposed to the dissolution medium and, consequently, promoting the dissolution (Boopathy and Kamasamy, 2015). The improved HSE/matrix interaction, combined with the use of lecithin and further dimensional reduction, promotes the release of HSE from HEP-HSE-46 compared to HEP-HSE, to achieve 100% dissolution in 30 minutes. The very low standard deviation obtained confirms the homogeneity of the formulation also in terms of loading and distribution of the extract in the matrix. The increase of solubility in aqueous media is of great importance because this characteristic can enhance the functionality of the engineered encapsulated formulation (Sansone et al., 2018 a).

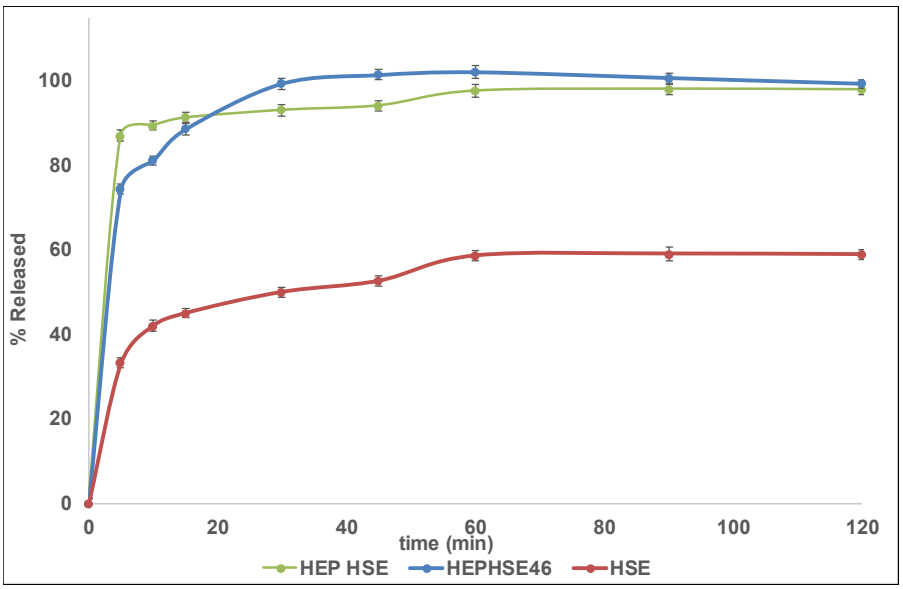

Figure 26. Dissolution/release profile of HEP-HSE and HEP-HSE-46 microparticles compared with HSE (unprocessed extract)

A.II.4. Stability studies of HEP-HSE-46

Based on the results obtained, HEP-HSE-46 proved to be the best formulation in terms of process yield, encapsulation efficiency, thermal profile and with improved release of the functional compounds from the extract in water. The extract, as previously demonstrate, contains a high polyphenols content. The polyphenols possess several biological activities, such as antioxidant, antimicrobial, anti-inflammatory, anti-cancer, with beneficial effects on human health (Esposito et al., 2017). However, they are dramatically unstable, because they undergo to oxidation and degradation processes, which take place especially during the storage period. This causes a reduction of active compounds, and consequently, a lower nutritional and biological value (Sansone et al., 2019). In order to evaluate the shelf-life and the effect of the spray drying process on the stability of HSE under storage

conditions, accelerated stability test was performed according to the ICH guidelines (International Conference Harmonization), under harsh storage condition, for 6 months, at 40°C and 75% Relative Humidity (RH%). Microscopy and DSC analyses were used to evaluate changes in structure and possible degradations. Before further characterizations, HEP-HSE-46 have been stored for 48h in a hermetically sealed desiccator (25°C), in order to evaporate the residual process humidity content. **Figure 27** show the results obtained for HEP-HSE-46 after storage period of 1 month with respect to HEP-HSE-46 at t_0 (48h in desiccator). The results displayed the presence of a small percentage of free water, absorbed during the spray drying process, after 48h in desiccator. The peak was already visible after 1 month (**Figure 27**). Analysing the thermal profile (**Figure 27**), the presence of water did not cause degradation events or the formation of chemical interactions, but affected the morphology of particles (**Figure 28 a** and **b)**.

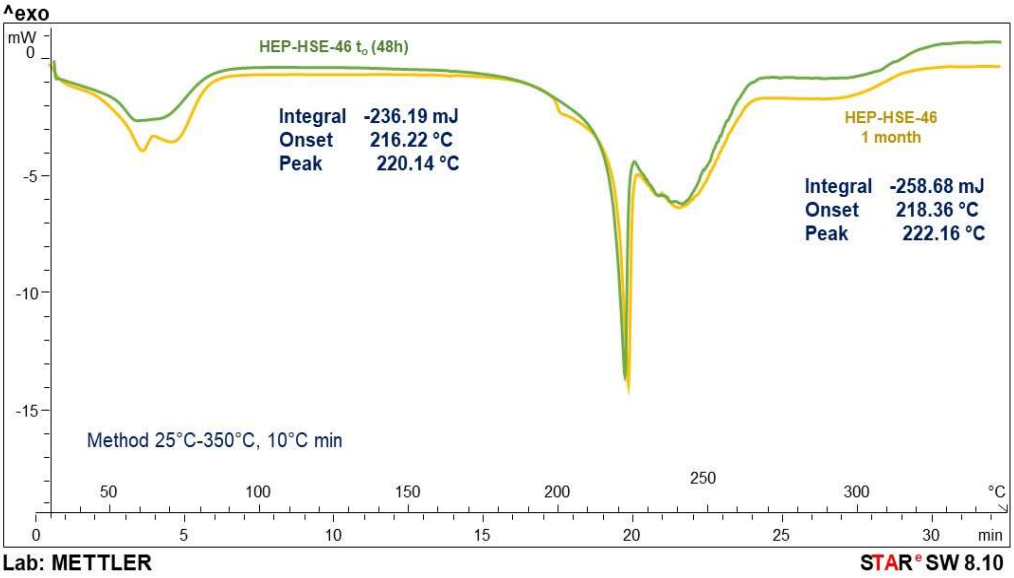

Figure 27. Differential scanning calorimetry (DSC) thermograms of HEP-HSE46 at t_0 (green profile), and after 1 month (yellow line)

In fact, the SEM images reported high degree of aggregates, and the particles showed an irregular shape and surface with predominant crystalline aspect (**Figure 28 b**), although no breakings are visible in the structures.

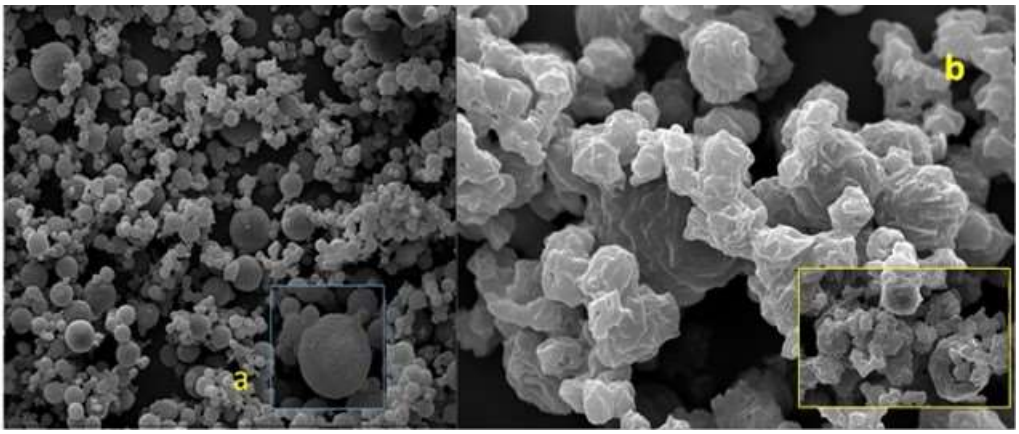

Figure 28. Scanning electron microscopy (SEM) images of (**a**) HEP-HSE-46 at t_0 and (**b**) HEP-HSE-46 after 1 month

The physical instability was probably due to the residual process humidity content of powder. Thus, the storage period of HEP-HSE-46 in desiccator was extended to 72 h, and the accelerated stability assay was repeated, in the same condition. The results obtained exhibited a clear reduction of the free water (**Figure 29**), and the morphology of the particles resulted unaltered, also after 6 months (**Figures 30 a** and **b**).

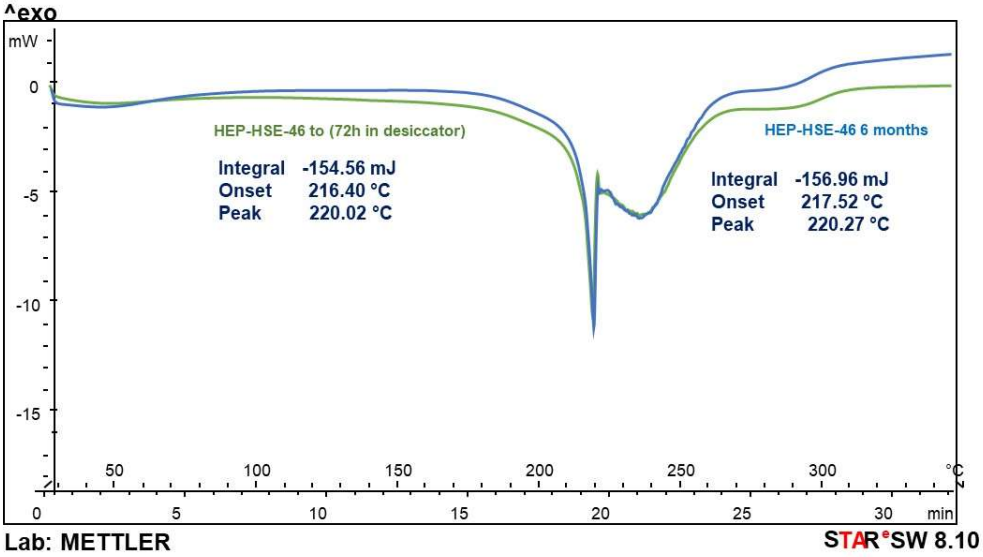

Figure 29. Differential scanning calorimetry (DSC) thermograms of HEP-HSE-46 at t_0 (green profile), and after 6 months (blue line)

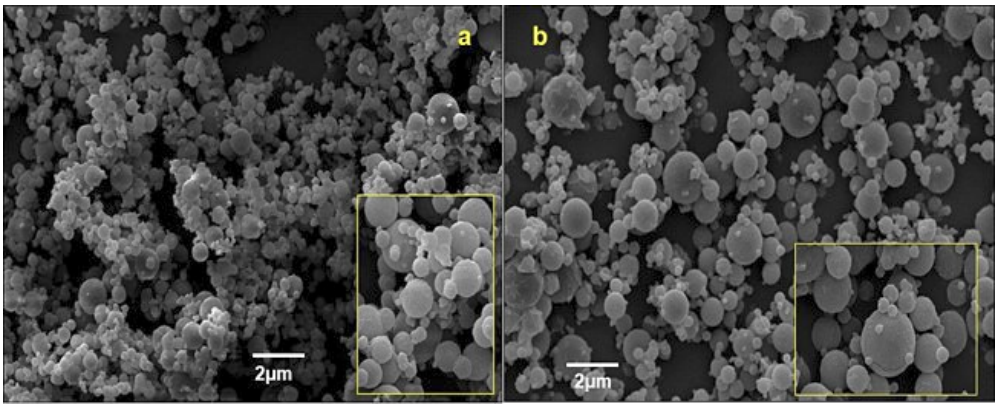

Figure 30. Scanning electron microscopy (SEM) images of (**a**) HEP-HSE-46 at t_0 and (**b**) HEP-HSE-46 after 6 months

The lawsonicin content, the major compound of HSE, and the free radical scavenging activity were verified, both after the spray drying process (after 72 h in the desiccator) and after 6 months under the storage condition and compared with

the unprocessed extract (HSE). The results, summarized in **Table 6**, showed that HEP-HSE-46 did not exhibit a significant reduction of the lawsonicin content (lower than 1%) after the transformation process and 6 months of storage. On the contrary, HSE proved a significant ($p < 0.05$) lower active content. Moreover, the antiradical activity was evaluated by the DPPH test, to verify that the formulation process and the storage period have not altered the free radical scavenging activity of HSE (Sansone et al., 2011). As reported in **Table 6**, the effect remained unaltered after spray drying process (EC_{50} 33.20 ± 0.61 µg/mL) and until 6 months of harsh storage condition (EC_{50} 32.80 ±1.01 µg/mL). On the contrary, at the same conditions, HSE raw extracts proved a significant ($p<0.05$) reduction of EC_{50} values from 33.42 ± 1.40 µg/mL to 40.04±2.11 µg/mL

Table 6. Actual Active Content (%) and free-radical scavenging activity of extract before (HSE unprocessed extract) and after microencapsulation process (HEP-HSE-46 microparticles)

	0	6 months	0	6 months
Materials	AAC% [ab]		DPPH test EC_{50} [acd]	
HSE Unprocessed extract	3.16 ± 0.80	1.15 ± 0.40*	33.42 ± 1.40	40.04 ± 2.11*
HEP-HSE-46	2.10 ± 0.40	2.00 ± 0.60	33.20 ± 0.61	32.80 ±1.01
α-tocopherol [e]			10.12 ± 1.32	9.14 ± 1.20

[a]One-way analysis of variance (ANOVA) followed by and Tukey HSD test; means ± SD, *P <0.05
[b]Actual Active content (AAC): content of lawsonicin calculated by HPLC-DAD
[c]EC_{50} ±standard deviation (data from three experiments in triplicate)
[d] In unit of µg of HSE or HEP-HSE-46/mL
[e]Positive control of the DPPH test

The results demonstrated that the optimized matrix and process parameters allowed to protect the antiradical efficacy of HSE, obtaining a long lasting, stable microparticulate system.

A.II.5. Functional activity of HEP-HSE-46

As demonstrated previously, HSE possesses not only a significant scavenging activity *in vitro* against the radical DPPH, but also an inhibitory effect on human melanoma and cervical cancer cell lines. In order to investigate if the spray-drying process affect HSE functional properties, the inhibitory effect of the optimized batch (HEP-HSE-46) on the growth of human normal (HaCaT) and cancer (A375, SK-Mel-28 and Hela) cell lines was evaluated. The results of MTT test (**Table 7**) showed that the inhibitory effect of HEP-HSE-46 remained unchanged (for SK-Mel-28) or resulted improved (for A375 and HeLa), proving as spray drying process did not affect HSE efficacy. On the contrary, the produced amorphous microsystems were able to improve the wettability of HSE and the release of HSE active components in water cellular environmental (Sansone et al., 2018 a). Moreover, the occurrence of Proline in the multi-polymeric HEP-HSE-46 matrix well affect the cytotoxic properties of HSE raw extract. An adequate supply of amino acids, such as proline, allows an adequate formation and a structural stability of the extracellular matrix (ECM). The microenvironment of ECM plays an important role in several phenomena occurring within the cell. Alterations in its structure, determined by changes in the molecular composition, can destroy the microenvironment homeostasis, causing the formation of tumors and metastases (Gallagher et al., 2005; Roomi et al., 2008; Kardos et al., 2015). In particular, the proline metabolism, generated by the proline oxidase (PRODH), seems to be able to catalyse the generation of Reactive Oxygen Species (ROS), usually produced in high levels in cancer cells (Prasad et al., 2017), and to induce apoptosis in several tumor cell lines (Roomi et al., 2008). Moreover, PRODH helps to maintain the ATP levels of the cell during oxidative and nutritional stress conditions, because changes in the intracellular redox environment are responsible of cell survival and death (Natarajan et al., 2012; Roomi, et al., 2008; Liu et al., 2006 b). Finally, HEP-HSE-

46 did not exhibit any cytotoxic effect (up to 15 mg/mL) on normal skin cell line (HaCaT) used in the assay, supporting its safety use. The results suggest that the developed spray drying method is suitable to transform HSE raw material in a water-soluble, easy handling and functional powder that can be used as in topical or oral dosage forms. Furthermore, the obtained formulation appears as a good candidate for further *in vivo* studies, in order to support its potential use as adjuvant in the treatment or prevention of cancer forms.

Table 7. MTT assay of raw extract (HSE) and optimized batch (HEP-HSE-46)

Cell lines[a]	**IC_{50} HSE Unprocessed extract µg/mL**[b]	**IC_{50} HEP-HSE-46 mg/mL**[c]
HaCaT	500.00 ± 7.31[d]	>15[d]
SK-Mel-28	459.00 ± 8.31[d]	10.55 ± 3.01
A375	584.00 ± 9.02[d]	4.55 ±1.24 [d]
HeLa	526.01 ± 8.92 [d]	8.07 ± 2.15 [d]

[a]A375 and SK-Mel-28, melanoma cells; HeLa, cervical cancer cells; HaCaT immortalized human keratinocytes; [b] IC_{50}, required concentration of extract to inhibit cell proliferation by 50%; [c] IC_{50}, concentration of HEP-HSE46 required to inhibit cell proliferation by 50% expressed as mg/mL; in this case the result is depending on the Actual Extract Content (AEC, 3.9% in HEP-HSE-46); [d]IC_{50} ± standard deviation (data from three experiments in triplicate).

A.II.6. Conclusion

Several studies have demonstrated that extracts, rich in polyphenols, possess different biological activities, such as antioxidant and cancer preventing properties. In fact, polyphenol have been found to reduce cell proliferation or inducing apoptosis in culture of human cancer cell lines, through the de-regulation of signalling pathway involved in cancer development (Di Domenico et al., 2012; Lo et al., 2010). Today, there is an increasing interest in the use of nutraceuticals, based on plant extracts or food wastes and by-products, as potential chemopreventive agents, to be used in combination with chemotherapeutics, as a new strategy in cancer control (Zlotogorski et al., 2013; Aparicio-Fernaändez et al., 2006; Mehta et al., 2010). Results obtained during the present PhD project showed as a polar extract (HSE), from a by-product of the hazelnut industrial processing, may be a health-promoting ingredient with powerful antioxidant and promising chemopreventive properties, potentially expandable in nutraceuticals and dietary supplements, or as novel food (Esposito et al., 2017). However, HSE is in crystalline form, sticky, not soluble in water and unstable for a potential industrial use. With the aim to overcome stability and bioavailability problems, new microparticulate powders loaded with the antioxidant and chemopreventive raw HSE extract were produced by spray drying. The tandem polymeric matrix based on L-proline as loading carrier, hydroxyethylcellulose and pectin as additional coating co-polymers led to satisfactory formulation (HEP-HSE-46) with good technological properties, improved water solubility, unchanged free radical scavenging activity and chemopreventive effects against human cancer cells (A375, SK-Mel-28 and HeLa), stable up to six months in accelerated stability condition. In conclusion, spray drying method seems to be the right approach to transform HSE raw material in a stable powder useful as functional and stable ingredient in the manufacturing of a new health product.

MATERIALS AND METHODS
OF
SECTION A

A.III.1.1. Chemicals

Analytical grade *n*-hexane, chloroform ($CHCl_3$) and methanol (MeOH) used for extraction and isolation procedures were purchased from Sigma-Aldrich (Milan, Lombardia, Italy). Methanol deuterated (CD_3OD), Folin-Ciocalteu phenol reagent, 1,1-diphenyl-2-picrylhydrazyl radical (DPPH), α-tocopherol, HPLC-grade methanol (MeOH), ethanol (ETOH) and L-proline were obtained from Sigma-Aldrich (Milan, Lombardia, Italy). Medium viscosity hydroxyethyl cellulose (HEC, Natrosol MR), sodium carboxymethylcellulose (NaCMC, E466) and lecithin (L, E322) were supplied by ACEF Spa. (Fiorenzuola D'Arda, PC, Italy). Pectin (PEC 09/051, 76% degree of esterification) was recovered from the citrus peel obtained during processing of Agrumi Gel s.n.c. company (Barcellona Pozzo di Gotto, Messina, Italy). HPLC-grade water (18 mΩ) was prepared by a Milli-Q_{50} purification system (Millipore Corp., Bedford, MA). Water and MeOH employed for the electrospray ionization ESI-MS analysis were of HPLC super gradient quality (Romil Ltd., Cambridge, U.K.).

A.III.1.2. General chromatographic and Spectroscopic Procedures

A Bruker DRX-600 NMR spectrometer, operating at 599.19 MHz for ^1H and 150.858 MHz for ^{13}C, using the TopSpin 3.2 software package, was used for NMR experiments in CD_3OD. Chemical shifts are expressed in δ (parts per million) referring to the solvent peaks δ_H 3.31 and δ_C 49.05 for CD_3OD, with coupling constants, *J*, in Hertz. ^1H-^1H DQF-COSY, ^1H-^{13}C HSQC, and HMBC experiments were obtained using conventional pulse sequences (Kerbab et al., 2015). ESIMS was performed on a Finnigan LC-Q Deca instrument (Thermoquest, San Jose, CA, USA), equipped with Xcalibur software. Chromatography was performed over Sephadex LH-20 (Pharmacia, Uppsala, Sweden). Thin-layer chromatography

(TLC) analysis was performed with Macherey−Nagel precoated silica gel 60 F_{254} plates (Delchimica, Naples, Italy), and the spray reagent cerium sulfate (saturated solution in dilute H_2SO_4) and UV (254 and 366 nm) were used for the spot visualization. Preparative HPLC separations were performed with a Waters 590 series pumping system equipped with a Waters R401 refractive index detector and a Rheodyne injector (100 µL loop), using µ-Bondapak C_{18} (300 x 7.8 mm i.d., 10 µm, Waters) or Luna C_8 (250 × 10.0 mm i.d., 10 µm, Phenomenex, Torrance CA) columns. Quantitative HPLC analysis was carried out on an Agilent 1100 series system equipped with a Model G-1312 pump, a Rheodyne Model G-1322A loop (20 µL), and a DAD G-1315A detector. Peaks area was calculated with an Agilent Integrator.

A.III.1.3. Hazelnut Shell Material and Extract Preparation

Hazelnuts South Italy Manufacturing S.r.l., in Baiano (Avellino, Italy), a local company, has provided Hazelnut shells. The shells were ground in a Mortar Grinder (mod. RM 100, Retsch, Bergamo, Italy) for 15 min. The obtained powder (1000 gr) was defatted with *n*-hexane and chloroform, and then extracted at room temperature with methanol (3 x 24 h) to give 20.8 g of residue (HSE). The extraction yield, gravimetrically determined (balance Denver Instruments-PK-201, max 2400 g d = 0.1 g; +15/30°C), and expressed as the weight percentage of the dry matter compared to the total amount of the started powder, was 2.08 %, w/w.

A.III.1.4. Isolation Procedure of Compounds 1-12

A portion of HSE (1.50 g) was fractionated over a Sephadex LH-20 column (1 m × 5 cm) using MeOH as eluent (flow rate 0.5 mL/min). Fractions (8 mL each) were collected, analysed by TLC (Si-gel, n-BuOH–AcOH–H2O (60:15:25), $CHCl_3$–

MeOH–H_2O (7:3:0.3) and combined to six major fractions (**I-VI**) based on TLC pattern. All fractions were further purified by RP-HPLC. Fractions **I**, **III** and **V-VI** were purified on a C_8 column (flow rate 2.0 mL/min) with the elution solvent MeOH/H_2O 4:6 v/v. Fraction **I** (545.0 mg) yielded compounds **5** (6.3 mg, t_R = 15 min), and **2** (33.4 mg, t_R = 26 min) while fraction **III** (99.0 mg) afforded compounds **6** (9.2 mg, t_R = 20 min), and **7** (1.3 mg, t_R = 32 min). Fraction **V** (38.8 mg) consisted of compounds **8** (1.8 mg, t_R = 8 min), and **9** (0.2 mg, t_R = 14 min). Fraction **VI** (105.2 mg) gave compound **10** (2.8 mg, t_R = 42 min). Fraction **II** (114.8 mg) was separated on a C_8 column (flow rate 1.5 mL/min) using as solvent system MeOH/H_2O 4:6 v/v to afford compounds **11** (5.4 mg, t_R = 8 min), **12** (3.2 mg, t_R = 14 min), **2** (2.3 mg, t_R = 24 min), and **1** (2.5 mg, t_R = 54 min). Finally, fraction **IV** (53.8 mg) was purified using MeOH/H_2O 5:5 v/v on a C_{18} column (flow rate 2.0 ml/min) to obtain compounds **4** (1.7 mg, t_R = 14 min), and **3** (2.0 mg, t_R = 19 min).

A.III.1.5. Spectroscopic Data

Lawsonicin (**1**). NMR and optical rotation data were consistent with those previously reported (Mencherini et al., 2011). ESI-MS (positive mode), *m*/*z* 361.4 $[M + H]^+$.

Cedrusin (**2**). NMR and optical rotation data were consistent with previously reported (Kim et al., 2005). ESI-MS (positive mode), *m*/*z* 347.3 $[M + H]^+$.

Balanophonin (**3**). NMR data were consisted with previously reported (Haruna et al., 1982). ESI-MS (positive mode), *m*/*z* 357.3 $[M + H]^+$.

Ficusal (**4**). NMR and optical rotation data were consistent with those previously reported (Li et al., 2000). ESI-MS (positive mode), *m*/*z* 331.1 $[M + H]^+$.

Dihydroconyferyl alcohol (**5**). NMR data were consistent with previously reported (Huang et al., 2014). ESI-MS (positive mode), *m*/*z* 183.2 $[M + H]^+$.

Veratric acid (**6**). NMR data were consistent with previously reported (Crestini et al., 2006). ESI-MS (negative mode), *m*/*z* 181.1 $[M - H]^-$.

Vanillic acid (**7**). NMR data were consisted with previously reported (Mencherini et al., 2011). ESI-MS (negative mode), *m*/*z* 167.1 $[M - H]^-$.

Gallic acid (**8**), and *Methyl gallate* (**9**) NMR data were consistent with those previously reported (Picerno et al., 2011). ESI-MS (negative mode), *m*/*z* 169.1 $[M - H]^-$ and 183.1 $[M - H]^-$, respectively.

Carpinontriol B (**10**). NMR and optical rotation data were consistent with those previously reported (Lee et al 2002). ESI-MS (positive mode), *m*/*z* 344.1 $[M + H]^+$.

C-Veratroylglycol (**11**). NMR data were consistent with those previously reported (Li and Seram, 2010). ESI-MS (positive mode), *m*/*z* 213.3 $[M + H]^+$.

β-Hydroxypropiovanillone (**12**). NMR data were consistent with those previously reported (Karonen et al., 2004). ESI-MS (positive mode), *m*/*z* 197.0 $[M + H]^+$.

A.III.1.6. Quantitative Determination of Total Phenol Content

HSE was analyzed for its total phenolic content according to the Folin-Ciocalteu colorimetric method (Esposito et al., 2017). A 1:10 dilution of the sample was prepared with H_2O (500µL) to which 500 µL of Folin Cicalteau reagent was added; after 3 minutes 500 µL of a 10% sodium bicarbonate solution was added. The absorbance of the samples was read after 1 hour, at 723 nm. Total phenols were expressed as Gallic acid equivalents (mg/g extract, means ± standard deviation of three determinations).

A.III.1.7. Quantitative HPLC Analysis of HSE

Quantitative HPLC was conducted using a Nucleodur 100-5 C_{18} column (150 x 4.6 mm, 5 µm, Machery-Nagel). The solvents were H_2O (solvent A) and MeOH

(solvent B). The elution gradient used was as follows: 0→3 min, 5% B; 3→7 min, 5→30% B; 7→7 min, 30% B; 17→35 min, 30→50% B. Analysis was carried out in triplicate, at a flow rate of 0.8 mL/min with a DAD detector set at 230 nm. Lawsonicin (**1**), c-veratroylglycol (**11**), and cedrusin (**2**) (isolated from HSE and characterized by NMR, and MS data) were used to prepare standard solutions at three concentration levels in the range 0.25-1.00 mg/mL for compounds **1** and **11**, and 0.25-2.00 mg/mL for **2**. The standard curves were analyzed using the linear least-squares regression equation derived from the peak area (regression equation y = 30885.7x-1704.1, r = 0,9989 for **1**; y = 16.723,0 x-1348,2, r = 0,9997 for **2**; y = 8761.8x + 104.0, r = 1.0000 for **11**, where *y* is the peak area and *x* the concentration). The peaks associated with compounds **1**, **2**, and **11** were identified by retention times, and confirmed by co-injections of HSE with isolated compounds. HSE was dissolved in MeOH, and analyzed under the same chromatographic conditions.

A.III.1.8. Bleaching of the free-radical 1,1-Diphenyl-2-picrylhydrazyl (DPPH Test)

The antiradical activities of HSE and compounds **1-12** were determined using the stable 1,1-diphenyl-2-picrylhydrazyl radical (DPPH), according to our procedures previously reported (Piccinelli et al., 2016). Briefly 1.5 mL of DPPH solution (25 mg/mL in methanol, prepared daily) was added to 0.375 mL of various concentrations of each sample under investigation in MeOH solution (ranged from 12 to 100 µg/mL). The mixtures were kept in the dark for 10 min at room temperature and the decrease in absorbance was measured at 517 nm against a blank consisting of an equal volume of methanol. α-tocopherol was used as positive control. The DPPH concentration in the reaction medium was calculated from a calibration curve (range = 5-36 µg/mL) analyzed by linear regression (y = 0.0228x-0.0350, R^2 = 0.9999), and EC_{50} (mean effective scavenging concentration) was

determined as the concentration (in micrograms per milliliter) of sample necessary to decrease the initial DPPH concentration by 50%. All tests were performed in triplicate. A lower EC_{50} value indicates stronger antioxidant activity.

A.III.1.9. Cell Cultures

Human malignant melanoma (A375), and SK-Mel-28, human cervical cancer (HeLa), and HaCaT (immortalized human normal keratinocytes), and supplements for cell cultures were obtained from Gibco Life Technology Corp. (ThermoFischer Scientific, Milan, Italy). HaCaT, A375 and HeLa cell lines were grown at 37 °C in Dulbecco's modified Eagle's medium containing High glucose supplemented with 10% fetal calf serum, and 100 units/mL each of penicillin and streptomycin, and 2 mmol/L glutamine. Human melanoma (SK-Mel-28) cell line was grown at 37 °C in minimum essential medium (MEM) supplemented with 10% fetal calf serum and 100 units/mL each of penicillin and streptomycin. At the onset of each experiment, cells were placed in fresh medium and then cultured in the presence of different concentrations of HSE or its constituents.

A.III.1.10. Cell Viability Assay

MTT (3-[4,5-dimetiltiazol-2,5-diphenyl-2H-tetrazolium bromide]) assay was used in order to assess the cells viability and to compare the effect of potentially cytotoxic substances with a control condition. Such molecule has a characteristic yellow colour and is reduced by mitochondrial enzyme succinate dehydrogenase to a formazan salt, which precipitates as in blue/purple crystals. This is a colorimetric assay, in which the amount of formazan produced is measured spectrophotometrically and it is proportional to the number of viable cells. To perform the assay, the cells were grown in 96-well plates, in numbers of 7000 per

well and after 24 h were treated with increasing concentrations of HSE from 10 µg/mL to 1 mg/mL, and with pure compounds from 10 nM to 500 µM, in triplicate for a given time (24 and 48 h). The stock solution of the extract and compounds was prepared in DMSO, and the final tested concentrations were prepared by diluting in the culture medium immediately before use. On the contrary, the optimized formulations, HEP-46 and HEP-HSE-46 was dissolved directly in the culture medium to obtain the used concentration of 15 mg/mL. At the end of treatment, the plates were centrifuged at 1200 rpm for 5 minutes, the medium was aspirated and added 100 µL of 1 mg/mL MTT to each well and the plates were kept at 37° C for the time necessary to the formation of salt formazan (1-3 hours depending on cell type). The solution was then removed from each well, and the formazan crystal within the cells were dissolved with 100 µL of DMSO. Absorption at 550 nm for each well was assessed by a Multiskan Spectrum Thermo Electron Corporation Reader. IC_{50} values were calculated from cell viability dose-response curves and defined as the concentration resulting in 50% inhibition of cell survival compared to untreated cells.

A.III.1.11. Flow Cytometry Analysis

Apoptosis was analyzed by propidium iodide incorporation in permeabilized cells and flow cytometry. Cells (5×10^4) were cultured in 24-wells plates. After 24 h, HSE or compounds were added at different doses, and cells were re-cultured for different times (24, 48 h). For apoptosis analysis, permeabilized cells were labelled with propidium iodide (PI) by incubation at 4°C for 30 min with a solution containing 0.1% sodium citrate, 0.1% Triton X-100 and 50 mg/ml PI (Sigma-Aldrich, St. Louis, MO). The cells were subsequently analyzed by flow cytometry by a FACSCalibur flow cytometer (Becton Dickinson, North Ryde, NSW, Australia). Each determination was repeated three times.

A.III.1.12. Western Blotting Analysis

Cell extracts were lysed in modified RIPA buffer (Tris-HCl pH 7.4 10 mM, NaCl 150 mM, EDTA 1 mM, NP40 1% Na-deoxycholic 0.1%, PMSF 1 mM, protease inhibitor cocktail). Equal amounts of proteins were separated by 10-12% SDS-PAGE and blotted on ECl Hybond nitro-cellulose membranes (GE Healthcare). Filters were blocked in PBS containing 10% non-fat dry milk and 0.1% Tween-20 and incubated overnight with optimal dilutions of PARP-1 (F-2) antibody (sc-8007 Santa Cruz Biotech) for detection of full-length and the C-terminal cleavage product (95 kD) of PARP-1. Anti-mouse IgG HRP conjugated were used as secondary antibody, bands were visualized by autoradiography of ECL reaction (Pierce). Anti α-tubulin antibody were used as control for equal amounts of proteins loaded on the gel.

A.III.2.1. Liquid feeds preparation and spray drying condition

The liquid feeds were spray-dried using a Büchi B-191 Mini Spray Dryer (Büchi Laboratoriums-Technik, Flawil, Switzerland) and two different preparation methods were employed to prepare the HEP-HSE and HEP-HSE-46 batches. A Hot-cold (H-C) method was used to produce HEP-HSE. In 100 mL of water was added 0.1% w/v HEC, heated to 75 °C, and 5% w/v P, added at room temperature, in a 98: 2 P: HEC ratio (total amount 5.10 g). The matrix was added to 0.25% of HSE, sonicate 30' and left under stirring until the spray drying process. The liquid feeds were spray dried under the following experimental conditions: Inlet/Outlet temperatures = 125/85 °C, Ø Nozzle = 0.7 mm, Spray flow feed = rate 3mL/min, Drying air flow = 500-600 L/h, Air pressure = 6 bar, Aspirator = 100%. The better formulation (HEP-HSE-46) was obtained by using a Hot-Cold-Hot (H-C-H) method. The liquid feed was produced using 0.2% w/v HEC, 5% w/v P and 0.2%

L in at 85.0: 3.4: 8.2: 3.4 P: HEC: PEC: L ratio (total amount 6.15 g). Pec was added in 80 mL of water, at 75 °C; at room temperature P was included and finally, at 50 °C, HEC was dissolved, leaving under stirring overnight. Separately, 0.25% w/w of HSE was dissolved adding 20 mL of ethanol and 20 mL of a 1% w/v lecithin solution and by homogenization with an Ultra-Turrax T-25 (IKA ULTRA-TURRAX T25 digital) at 10000 rpm for 5 min. The suspension containing the extract was slowly poured into the feed under continuous magnetic stirring. The suspension, gently stirring, was pumped under the following optimized process parameters: Inlet/Outlet temperatures = 125/85 °C, Ø Nozzle = 0.7 mm, Drying air flow = 600 L/h, Spray flow feed rate = 3.8 mL/min, Air pressure = 6.5 bar, Aspirator = 100%. As references, extract-free powders (blanks: HEP-1 and HEP-46) were produced using the same experimental conditions. Each preparation was produced in triplicate. HEP-1 and HEP-HSE were stored for 48h in the desiccator, while HEP-46 and HEP-HSE-46 for 72h, both at room temperature, before characterization.

The viscosity measurements of liquid feeds were carried out, before spray drying, by a Visco Basic plus viscometer (FungiLab s.a., Barcelona, Spain) at 25°C, with a spindle L1, at 100 rpm, each 30 seconds after the rotation speed started. The results were expressed as centiPoise (cP) and the accuracy of the measurement was expressed in terms of error %.

A.III.2.2. Powders characterization

A.III.2.2.1 Yield and loading efficiency

Production yield was determined gravimetrically (balance Crystal 100 CAL – Gibertini Novate, Milanese, Italy, max 110 g d = 0.1 mg; +15 °C/30°C) and was

expressed as the weight percentage of the final product compared to the total amount of the materials present in the liquid feed.

The Theoretical Extract Content (TEC) was calculated as the percentage of HSE content compared to the initial total amount of all feed components before spray-drying.

According to Esposito et al 2017, Actual Active Content (AAC) of the unprocessed extract HSE and of spray-dried microparticles (HEP-HSE and HEP-HSE-46) was determined by HPLC-DAD method, as previously described, and expressed as lawsonicin content percentage to 100 mg of powder.

The Actual Extract Content (AEC) was derived by AAC and calculated as:

$AEC\% = AAC_{HEP\text{-}HSE/HEP\text{-}HSE\text{-}46} / AAC_{unprocessed\ HSE}$ x 100 (Esposito et al., 2017)

The extract encapsulation efficiency (EE%) was the ratio of the actual to the theoretical extract

content:

$$EE\% = AEC/TEC \times 100 \text{ (Sansone et al., 2018 a)}$$

Each analysis was made in triplicate and results expressed as average value

A.III 2.2.2. Particle-Size analyses

The dimensions of the raw materials and of all the batches obtained by spray drying were determined with a Laser Light Scattering (LLS) granulometer (Beckman Coulter LS 230, Particle Volume Module Plus, Brea, CA, USA). The powders were suspended in isopropanol and 150 µL of each sample were introduced into the analysis cell in order to obtain an obscuration between 8 and 12%. Particle size distribution were calculated using the mathematical Fraunhofer model. The analyses were conducted in triplicate: the results were expressed as d_{50}, indicating the volume diameter at the 50^{th} percentile of the particle size distribution. The span

was calculated as [(d_{90} - d_{10})/ d_{50}]; a higher span value (>3) indicates an uneven particle size distribution (Sansone et al., 2011).

A.III 2.2.3 Morphological analyses

The morphology of the powders was studied by Scanning Electron Microscopy (SEM): the powders were coated with Au/Pd and then observed using an EVO MA 10 microscope (Carl Zeiss, Oberkochen, Germany) with a secondary electron detector (Carl Zeiss SMT Ltd., Cambridge, UK) equipped with a EMSCD005 metallizator (LEICA, Oberkochen, Germany) producing deposition of a 200–400 Å thick gold layer. To verify the microparticles uniformity, 20 SEM images were taken into account for each observation.

The fluorescent microscopy assays (FM) were performed observing the samples with a Zeiss Axiophot fluorescence microscope, with 40, 63 and 100 x 1.4 NA Plan Apochromat oil immersion objectives (Carl Zeiss Vision, München-Hallbergmoos, Germany).

A.III 2.2.4. Differential Scanning Calorimetry (DSC)

The thermal behavior of raw materials and formulated powders were analyzed by Differential Scanning Calorimetry on an indium calibrated Mettler Toledo DSC 822e (Mettler Toledo, OH, USA). The instrument automatically determined the blank curve. The baseline correction was previously performed to the sample assays. It was considered as the baseline the separation between the region of latent heat from that of sensible heat; graphically it was the startup deflection proportional to the heat capacity of the sample followed by a DSC curve section with no thermal effects. The integral baseline which takes into account the change in the heat capacity with conversion has been considered. Thermograms were recorded by

placing accurately weighed quantities (3–6 mg weighed with a microbalance MTS Mettler Toledo, OH, USA) of each sample in a 40 µL aluminium pan, which was sealed and pierced. The samples underwent one dynamic thermal cycle; they were heated from 25°C to 350°C at a heating rate of 10°C/min. Dehydration, melting temperature (Tm), and heat of fusion (ΔHm) were measured.

A.III 2.2.5 Dissolution/release tests

The dissolution/release tests of the extracts from the formulations were performed in H_2O using a Sotax AT Smart Apparatus (Basel, CH) and equipped with apparatus 2 of USP 31 for dissolution tests: paddle, 75 rpm at 37°C. The duration of the test was 120 min and the samples were taken at 5, 10, 15, 30, 45, 60, 90 and 120 minutes. Only the mean values are reported (standard deviations < 5%). Amount of the extract dissolved was measured as AAC (Actual Active Content) value was calculated by-HPLC method, so as reported in the previous paragraphs. The standard curve was analysed using the linear correlation between concentration and peak area integration (regression equation y = 9579.9 x-19.612, r = 0.9999, at five concentration levels in the range of 0.01-0.00125 mg/mL). All the dissolution/release tests were made in triplicate, each time in 6 vessels; only the mean values are reported (standard deviations < 5%).

A.III.2.3. Stability studies

Stability was performed under harsh storage conditions, according to the ICH (International Conference Harmonization) guidelines. Glass vials with 1.5g of each batch were stored for six months at 40± 2°C; 75± 2% R.H in a climate chamber (Climatic and Thermostatic Chamber, Angelantoni Life Science s.r.l., PG, Italy).

At time 0 and after 6 months, samples of each batch were collected. Extract content was verified by HPLC method, and morphology and DSC analysis were performed to detect changes in the structure and possible degradation events, according to the previously described methods. The free-radical scavenging activity of HEP-HSE-46 was evaluated after 6 months using the previously reported method (powder were dissolved directly in water at 15 mg/mL), and compared with raw extract (HSE), in the same conditions. The first analysis (t_0) has been realized after 48 h or 72 h from the formulation; all measurements were conducted in triplicate.

A.III.3. Statistical Analysis

All results are shown as mean ± standard deviation of three experiments performed in triplicate. Statistical comparison between groups were made using ANOVA followed by the Bonferroni parametric test. Differences were considered significant if $p < 0.05$. The free radical scavenging data was subjected to one-way analysis of variance (ANOVA) followed by and Tukey HSD test ($p < 0.05$), using GraphPad Prism version 7.00 for Windows.

RESULTS AND DISCUSSION
SECTION B

CHEMICAL PROFILE AND BIOLOGICAL ACTIVITY OF CHESTNUT WASTE AND HAZELNUT SKINS

PART I

Chemical profile and biological activity of Chestnut (*Castanea sativa* Miller) Bur extracts. Production of antioxidant extract from Roasted Hazelnut (*Coryllus avellana* L.) Skins

Based on the article: Chestnut (*Castanea sativa* Miller.) burs extracts and functional compounds: UHPLC-UV-HRMS profiling, antioxidant activity, and inhibitory effectts on phytopathogenic fungi. (2019). T. Esposito, R. Celano, C. Pane, A. L. Piccinelli, F. Sansone, P. Picerno, M. Zaccardelli, R. P. Aquino, T. Mencherini. Molecules, 24(2), 302.

Scientific background and research aim

During the present PhD project, Chestnut Spiny Burs (CSB) and Roasted Hazelnut Skins (RHS) were also selected as wastes/by-products from Campania agro-industries.

The Chestnuts (*Castanea sativa* Miller, Fagaceae family), production is widely spread on two macro areas, Asia and Europe, which represent, respectively, 80% and 16% of production. Italy is one of the largest European producers of sweet chestnuts, and Campania region covers about 40% of the national fruit crop (Vella et al., 2018).

Figure 31. Chestnut spiny burs (CSB)

Annually the harvest of edible fruits, consumed as unprocessed fruit or industrially transformed (dry product, flour, and *marron-glacé*) is traditionally made by hand, between September and November (Vella et al., 2018). Leaves, burs, outer and inner teguments are by-products and wastes, usually generated during the harvest and processing phases. Actually, only the inner teguments, produced during the peeling phase of chestnuts, are used as industrial fuel (Fernández-agulló et al., 2014). The CSB are the edible lignocellulosic waste, representing about 20% w/w of the total chestnut weigh, that usually remain in the woodland after the fruit

harvesting and promote the proliferation of insect larvae which cause damages for cultivation, reducing the quantity and quality of fruit production in the following years (Vázquez, et al., 2012).

The strategy of farmers to avoid crop damages is to burn the wastes (Vella et al., 2018). The strategy of researches is to exploit and reuse these solid residues, aiming to reduce both the environmental and economic impacts of the agro-industrial process, also getting new products.

CSB contain a high polyphenol content, with a broad-spectrum of biological activities such as antioxidant ability, antimicrobial efficacy, both against human pathogens (Li et al., 2015; Landete 2011; Yuan et al., 2018) and bacterial and fungal strains causing plant infections, supporting their potential re-use as functional ingredient in cosmetic, pharmaceutical or food products (Balboa et al., 2014; Zhao et al., 2011).

The main causes of postharvest rots of fresh fruits and vegetables during storage and transport are fungal infections, determining significant economic losses in the marketing phase. Widespread use of synthetic fungicides involves the development of resistant strains and raises environmental and human health concerns. Natural antimicrobial derivatives from plants or agro-industrial residues, characterized by a good toxicological and eco-toxicological profile, may represent an attractive alternative. Plant extracts, rich in polyphenols, have gained scientific interest, due to their ability to alterate fungal cell wall integrity (Gatto et al., 2011; Veloz-García et al., 2010). In this project, organic and aqueous extracts from CSB were produced, and, an accurate CSB profiles was carried out, by ultra-high-performance liquid chromatography coupled with UV and high-resolution mass spectrometry detectors (UHPLC-UV-HRMS). The chemical structures of the major constituents were confirmed by 1D- and 2D-NMR experiments after the isolation procedure. The *in vitro* free radical scavenging activity against the radicals $DPPH^{\bullet}$ and $ABTS^{\bullet+}$ of

CSB extracts and marker compounds, as well as, their inhibitive effects on mycelial growth and spore germination of *Alternaria alternata*, *Fusarium solani* and *Botrytis cinerea* were investigated.

Roasted Hazelnut Skins (RHS) were selected as another interesting by-product, generally produced during the industrial roasting process (Piccinelli et al., 2016). The hazelnut edible kernel is consumed whole in its raw (with skin) and peeled (without skin) forms. However, the most common use of the peeled hazelnut is as an ingredient in processed foods, such as bakery, candy, and chocolate products. The skin, which represents about 2.5% of the total hazelnut kernel weight, is usually removed by blanching or roasting to improve the kernel flavour, colour, and crunch and for the use of the kernel in the bakery and confectionery industry (Shaidi et al., 2007). Nowadays, Roasted Hazelnut Skins (RHS) are used without treatment for animal feed.

Figure 32. Hazelnut skins

Several studies have demonstrated that hazelnut by-products contain higher amount of polyphenolic compounds than the edible portion (Alasalvar et al., 2009; Montella et al., 2013; Yuan et al., 2018; Contini et al., 2008, Shahidi et al., 2007). RHS are a rich source of proanthocyanidins (PAs) (Shahidi et al., 2007; Alasalvar et al., 2009;

Gu et al., 2003; Contini et al., 2008). PAs possess not only a strong antioxidant property (Prior et al., 2005), but also antifungal efficacy against *Candida albicans*, inhibiting biofilm formation (Luiz et al., 2015; Rane et al., 2014). The ability to form biofilms on biotic and abiotic surfaces and the hyphal form of growth play key roles during *Candida albicans* human pathogenesis and fungal drug resistance.

For this reason, in a previous work (Piccinelli et al., 2016), we have produced a methanolic extract (RHS-M) by exhaustive maceration. The extract possessed a high content of oligomeric proanthocyanidins (PAs), in particular by B-type oligomers of (epi)-catechin, with strong free radical scavenging activity against DPPH. In addition, RHS-M exhibited a high antifungal activity against *Candida albicans* (MIC_2 = 3.00 μg/mL and MIC_0 = 5.00 μg/mL, corresponding at the lowest concentration that produced an inhibition of growth >50% or completely, respectively). During the present project, on the basis of the demonstrated functional properties, a hydroalcoholic extract of RHS (RHS-H) was produced by Pressurized Liquid Extraction (PLE) technique. PLE is an extraction technique employed as new sustainable alternative to traditional extraction methods, with less amount of organic solvent and reducted time of analysis, using liquid solvents at elevated temperature (above their atmospheric boiling point) and elevated pressure (Castejón, et al., 2018).

PLE is recognized as a "*green*" extraction technique, using GRAS (Generally Recognized As Safe) solvents as ethanol and water, or a mixture of both, suitable for industrial use (Castejón, et al., 2018; Sumere et al., 2018). Moreover, it is conducted in the absence of light, which represents a great advantage in the extraction of sensitive compounds (Alañón, et al., 2017). After the selection of appropriate extraction and operating parameters such as solvent type, solid-to-solvent ratio, extraction time, temperature, pressure particle size, and water content, RHS-H was produced and compared to the conventional methanolic extract (RHS-

M) to understand if the extraction procedure alterate the biological activity of the extract.

B.I.1. CSB Extracts preparation, total phenol content and antioxidant activity

Chestnut spiny burs (CSB) were extracted using three different procedures in order to evaluate the influence of solvent and extraction method on the total polyphenol content, and efficacy against free radicals and phytopathogenic fungi. The methanolic extract (CSB-M) obtained by an exhaustive maceration at room temperature using solvents with increasing polarity was compared in terms of extraction yield and Total Phenol Content (TPC), to CSB-H and CSB-A, extracted by aqueous ethanol 50% under stirring at 45°C, and boiling water, respectively. The selection of ethanol and water is based on their classification as GRAS solvents, able to support the eco-sustainability and the potential application in food industry. In this case, the highest extraction yield (11.6% w/w) was obtained from the employment of aqueous ethanol (50%, v/v). However, according to Piccinelli et al., 2016; the sequential maceration with hexane, chloroform and methanol (CSB-M extract) resulted the most suitable extraction method to obtain a polyphenol rich extract. In fact, as showed by the Folin-Ciocalteu results (**Table 8)**, CSB-M possessed a significantly ($p < 0.05$) higher TPC (26.42 g GAE/100 g extract) than CSB-H and CSB-A (20.60 and 20.26 g GAE/100 g extract, respectively). The degree of linear association between both radical-scavenging activity (DPPH and TEAC assays) and TPC was determined by means of Pearson product moment correlation coefficients (r) calculation. A strong correlation with polyphenols content was observed for antiradical activity, showing correlation coefficients r = -0.9422 and 0.8376 for DPPH and TEAC assays, respectively (negative r value was obtained in that higher antiradical activity corresponded to lower EC_{50} values) (Carpinella et al., 2003). The found correlation could explain the superimposable

activity of CSB-H and CSB-A ($p > 0.05$) against DPPH and ABTS (24.94 and 22.38 µg/mL and TEAC values 3.00 and 2.71 mM Trolox/mg extract, respectively), deriving from the similar TPC (20.60 and 20.26 GAE g/100g extract) (**Table 8**).

All the produced chestnut bur extracts possessed a significant and concentration-dependent free radical scavenging activity (**Table 8**). CSB-M, which is richer in functional compounds (26.42 g GAE/100 g extract), showed the highest scavenging effect against both radicals (EC_{50} 12.64 µg/mL, TEAC value = 3.52 mM Trolox/mg extract). Two of the components detected in CSB extracts (as reported in **B.I.4** paragraph), quercetin 3-O-β-D-glucopyranoside (**25**) and ellagic acid (EA, **27**), were confirmed as strong antiradical compounds. On the contrary, chestanin (**21**) showed less efficacy against $DPPH^{\bullet}$ (EC_{50} 16.62 µg/mL) and $ABTS^{\bullet+}$ (TEAC value 1.05 mM Trolox/mM compound).

Table 8. Free radical-scavenging activity and total phenolic content (TPC) in CSB extracts

	DPPH test (EC_{50}[a] µg/mL extract or phenol) [b]		TEAC Value[c] (mM Trolox/mg extract or mM compound)[b]	TPC [b] g GAE[d]/100g extract
CSB-H	24.94 ± 0.46		3.00 ± 0.22	20.60 ± 0.85
CSB-M	12.64 ± 0.12		3.52 ± 0.13	26.42 ± 0.95
CSB-A	22.38 ± 2.80		2.71 ± 0.71	20.26 ± 0.14
quercetin 3-O-β-D-glucopyranoside (**25**)		2.98 ± 0.84	3.39 ± 0.11	
EA (**27**)		2.40 ± 0.24	4.98 ± 0.21	
Chestanin (**21**)		16.62 ± 0.84	1.05 ± 0.14	
gallic acid[e]		1.23 ± 0.15	3.49 ± 0.21	

[a] EC_{50} =the concentration (in micrograms per milliliter) of sample necessary to decrease the initial DPPH concentration by 50%
[b] Mean ± SD of three determinations; different letters in the same column indicate significantly different ($p < 0.05$)
[c] TEAC value = concentration of standard trolox with the same antioxidant capacity as 1mg/mL of the tested extract or 1mM of the antioxidant compounds
[d] Gallic acid equivalent
[e] Positive control of the $ABTS^{\bullet+}$ and $DPPH^{\bullet}$ assay

B.I.2. UHPLC-UV-(–)-HRMS profiling of CSB extracts

In order to obtain a complete polyphenol profile of CSB extracts, a rapid and sensitive ultra-high-performance liquid chromatography, coupled with photodiode array and high resolution mass spectrometry detectors (UHPLC-PDA-HRMS) method was developed in collaboration with an other research group of the Pharmacy Department of Salerno University. Analyses were performed in negative ion mode due to higher sensibility of detection mode for the most of detected CSB compounds. CSB-M extract displayed more complex and rich composition than CSB-H and CSB-A, and **Figure 33** shows its HRMS and UV profile. Metabolite assignments were established comparing retention time and MS data of detected compounds with standard compounds, whenever available, or interpreting MS data (accurate masses and MS/MS fragment ions) combined with chemo-taxonomic data reported in the literature and databases. 42 compounds were identified by UHPLC-UV-HRMS^n, grouped into two major classes of secondary metabolites: hydrolysable tannins (HTs) and flavonoids (**Table 9**). In chestnut by-products, HTs, a large group of polyphenolic compounds, were reported as one of the main class (Braga et al., 2015). HTs can be divided in simple gallic acid (GA) derivatives, gallotannins and ellagitannins. EA (**27**), the main compound of CSB extracts, and two of its trimethyl glycoconjugates (**28**, trimethyl-ellagic acid hexoside, and **36**, trimethyl-ellagic acid deoxyhexoside) were identified (**Table 9**).

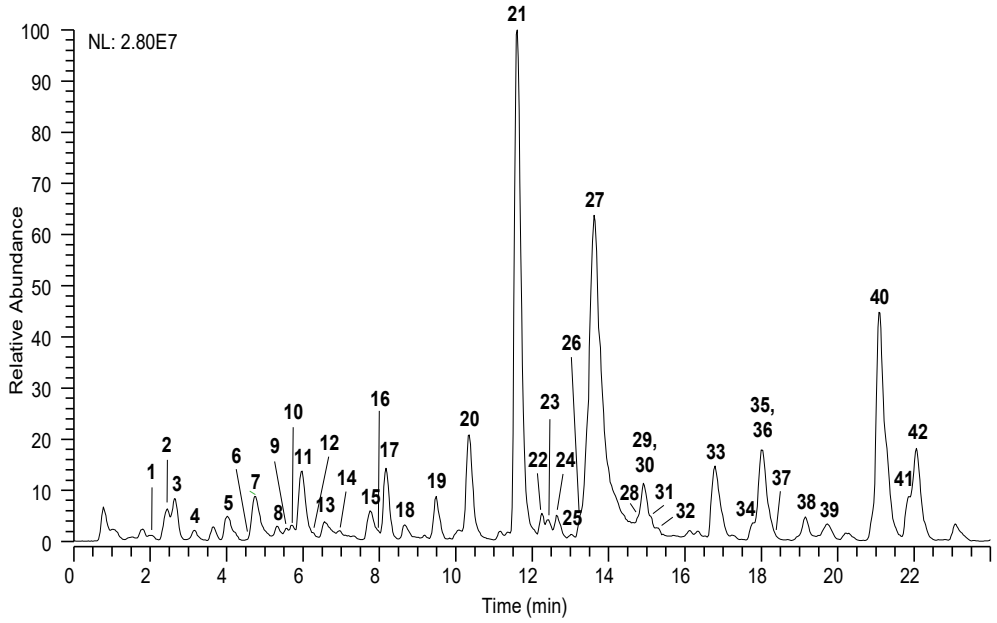

Figure 33. UHPLC-PDA-HRMS profiling of CSB extracts

As simple GA derivateves were identified chestanin (**21**) (the other main component of CSB extracts) and chesnatin (**17**), isochesnatin (**19**), cretanin (**20**) and chestanin isomer (**24**). Their structures were subsequently confirmed by NMR analysis (as reported in section **B.I.3.**) (**Figure 34**). ETs containing exclusively hexahydroxydiphenoyl (HHDP) group as, pedunculagin (**5)**, stachyurin or casuarinin (**12**,) and tellimagrandin I (**8** and **15**) were characterized. In addition, **2** (castalagin or vescalagin) and **4** (methylvescalagin), two methyl esters of chebulagic acid, **14** and **18**, two ETs with valoneoyl group (**1** and **10,** castavaloninic or vescavaloninic acid), cocciferin d2 (**13**) were also detected as constitutes of CSB (**Table 9**). Finally, three ET metabolites, castacrenin A-C isomers (**7**, **9** and **11**) were recognized in CSB, and through the isolation procedure and NMR studies it was possible to differentiate the three isomers. The second representative class of secondary metabolites is CSB was flavonoids, according to data reported in the

literature on chestnut by-products (Braga et al., 2015). All detected flavonoids were identified as flavonol glycoconjugates, particularly, quercetin (**23**, **25**, **26**, and **33**), isorhamnetin (**30-32**, **37**), and kaempferol derivatives (**29**, **34**, **35**, **38-42**) (**Table 9)**. The proposed structure of flavonols were confirmed by comparison with pure compounds (isolated or standards), or tentatively identified on the basis of the accurate masses of precursor and product ions, fragmentation pattern of the aglycone (MS_3 experiments), literature data, and following the spectra interpretation guidelines for flavonoids. This study represents the first report on the profiling of phenolic compounds in chestnut burs.

Table 9. UHPLC-HRMS data of compounds detected in CSB extracts

N[a]	RT (min)	[M-H]$^-$ (*m/z*)	Molecular formula	Error ppm	Diagnostic product ions (*m/z*)[b]	Compound	Ref.
1	1.97	1101.0672	$C_{48}H_{30}O_{31}$	–1.4	**1057** [M–H–CO_2]$^-$	valoneoyl–NHTP–glucose (vescavaloninic/castavaloninic acid)	Moilanen et al., 2013
2	2.45	933.0613	$C_{41}H_{26}O_{26}$	–1.6	915 [M–H–H_2O]$^-$, 889 [M–H–CO_2]$^-$, 871 [M–H–H_2O–CO_2]$^-$, **631** [M–H–EA]$^-$, 613 [M–H–EA–H_2O]$^-$, 587 [M–H–EA–CO_2]$^-$, 569 [M–H–EA–H_2O–CO_2]$^-$	HHDP–NHTP–glucose (castalagin/vescalagin)	García-villalba et al., 2017
3	2.59	783.0663	$C_{34}H_{24}O_{22}$	–1.6	481 [M–H–EA]$^-$, **301** [EA–H]$^-$ ($C_{14}H_5O_8$ 1.8 ppm)	diHHDP-glucose (pedunculagin)	García-villalba et al., 2017
4	3.16	947.0772	$C_{42}H_{28}O_{26}$	–1.4	**915** [M–H–CH_3OH]$^-$	methyl–HHDP–NHTP–glucose (methylvescalagin)	Moilanen et al., 2013
5	4.01	783.0661	$C_{34}H_{24}O_{22}$	–1.9	481 [M–H–EA]$^-$, **301** [EA–H]$^-$ ($C_{14}H_5O_8$ 1.8 ppm)	diHHDP-glucose (pedunculagin)	García-villalba et al 2017
6	4.71	953.0882	$C_{41}H_{30}O_{27}$	–0.9	**909** [M–H–CO_2]$^-$, 785 [M–H–$C_7H_4O_5$]$^-$	galloyl-chebuloyl-HHDP-glucose (chebulagic acid)	Yang et al., 2012
7	4.74	613.0454	$C_{27}H_{18}O_{17}$	–0.9	595 [M–H–H_2O]–, **523** [M–H–$C_3H_6O_3$]$^-$, 493 [M–H–$C_4H_8O_4$]$^-$	castacrenin C	Tanaka et al., 1996
8	5.32	785.0820	$C_{34}H_{26}O_{22}$	–1.4	633 [M–H–galloyl]$^-$, 615 [M–H–GA]$^-$, 483 [M–H–EA]$^-$, **301** ($C_{14}H_5O_8$ 2.1 ppm)	digalloyl-HHDP-glucose (tellimagrandin I)	Regueiro, et al., 2014
9	5.58	613.0455	$C_{27}H_{18}O_{17}$	–0.8	595 [M–H–H_2O]$^-$, **523** [M–H–$C_3H_6O_3$]$^-$, 493 [M–H–$C_4H_8O_4$]$^-$	castacrenin B[f]	Tanaka et al., 1996

10	5.71	1115.0825	$C_{49}H_{32}O_{31}$	–1.3	1097 $[M–H–H_2O]^-$, 1071 $[M–H–CO_2]^-$, **1053** $[M–H–H_2O–CO_2]^-$, 933 $[M–H–C_8H_6O_5]^-$, 569 $[M–H–C_8H_6O_5–EA–CO_2–H_2O]^-$	methylvaloneoyl–NHTP–glucose (vescavaloninic/castavaloninic acid methyl ester)	
11	5.98	613.0454	$C_{27}H_{18}O_{17}$	–0.9	523 $[M–H–C_3H_6O_3]^-$, **493** $[M–H–C_4H_8O_4]^-$	Castacrenin A[f]	Tanaka et al., 1996
12	6.20	935.0769	$C_{41}H_{28}O_{26}$	–1.8	917 $[M–H–H_2O]^-$, 873 $[M–H–H_2O–CO_2]^-$, 783 $[M–H–GA]^-$ **633** $[M–H–EA]^-$,	galloyl-diHHDP-glucose (stachyurin/casuarinin)	Regueiro, et al., 2014
13	6.53	933.0609[d]	$C_{82}H_{52}O_{52}$	1.0	1565 $[M–H–EA]^-$, **915** $[HHDP-NHTP-glucose–H_2O]^-$, 633 $[galloyl-diHHDP-glucose–EA]^-$, 631 $[HHDP-NHTP-glucose–EA]^-$	HHDP-NHTP-glucose-galloyl-diHHDP-glucose (cocciferin d2)	Moilanen et al., 2013
14	6.93	967.1035	$C_{42}H_{32}O_{27}$	–1.3	**785** $[M–H–C_8H_6O_5]^-$	galloyl-methylchebuloyl-HHDP-glucose (chebulagic acid methyl ester)	Lee et al., 2017
15	7.76	785.0822	$C_{34}H_{26}O_{22}$	–1.3	633 $[M–H–galloyl]^-$, 615 $[M–H–GA]^-$, 483 $[M–H–EA]^-$, **301** ($C_{14}H_5O_8$ 2.2 ppm)	digalloyl-HHDP-glucose (tellimagrandin I)	Regueiro, et al., 2014
16	7.97	953.0882	$C_{41}H_{30}O_{27}$	–0.9	**909** $[M–H–CO_2]^-$, 785 $[M–H–C_7H_4O_5]^-$	galloyl-chebuloyl-HHDP-glucose (chebulagic acid)	Yang et al., 2012
17	8.18	637.1028	$C_{27}H_{26}O_{18}$	–1.2	**467** $[M–H–GA]^-$, 305 $[M–H–GA–hex]^-$	Chesnatin[f]	
18	8.65	967.1038	$C_{42}H_{32}O_{27}$	–1.0	**785** $[M–H–C_8H_6O_5]^-$	galloyl-methylchebuloyl-HHDP-glucose (chebulagic acid methyl ester)	Lee et al., 2017
19	9.49	637.1032	$C_{27}H_{26}O_{18}$	–1.0	**593** $[M–H–CO_2]^-$, 469 $[M–H–C_7H_6O_5]^-$	isochesnatin [f]	
20	10.35	469.0972	$C_{20}H_{22}O_{13}$	–1.0	169 $[GA–H]^-$ ($C_7H_5O_5$ 1.8 ppm),	cretanin [f]	
21	11.61	937.1871	$C_{40}H_{42}O_{26}$	–1.0	637 $[M–H–C_{13}H_{16}O_8]^-$, **467** $[M–H–C_{20}H_{22}O_{13}]^-$	chestanin [f]	
22	12.25	351.1076	$C_{17}H_{20}O_8$	0.5	**163** $[M–H–C_8H_{12}O_5]^-$	methyl coumaroyl quinate	
23	12.43	615.0977	$C_{28}H_{24}O_{16}$	–0.5	**463** $[M–H–galloyl]^-$, 301 $[Ag–H]^-$ ($C_{15}H_9O_7$ 0.4 ppm)	quercetin-galloyl-hexoside	García-villalba et al., 2017
24	12.64	937.1865	$C_{40}H_{42}O_{26}$	1.7	**467** $[M–H–C_{20}H_{22}O_{13}]^-$	chestanin isomer [f]	
25	13.48	463.0867	$C_{21}H_{20}O_{12}$	–1.5	301 $[Ag–H]^-$ ($C_{15}H_9O_7$ 1.2 ppm)	quercetin 3-O-β-D-glucopyranoside [f]	

26	13.33	477.0660	$C_{21}H_{18}O_{13}$	–0.8	301 $[Ag–H]^-$ ($C_{15}H_9O_7$ 0.8 ppm)	quercetin hexuronoside	Barros,et al., 2013
27	13.62	300.9982	$C_{14}H_6O_8$	1.1	-	ellagic acid [c]	
28	14.78	551.1026[e]	$C_{23}H_{22}O_{13}$	–1.0	343 $[M–H–Hex]^-$	Ellagic acid 3,3',4-trimethoxy 4'-O-β-D-glucopyranoside [f]	
29	14.91	447.0916	$C_{21}H_{20}O_{11}$	–1.3	327 $[M–H–C_4H_8O_4]^-$, **285** $[Ag–H]^-$ ($C_{15}H_9O_6$ 1.1 ppm)	Astragalin [f]	
30	14.94	491.0815	$C_{22}H_{20}O_{13}$	–1.0	**315** $[Ag–H]^-$ ($C_{16}H_{11}O_7$ 0.6 ppm), 301 $[M–H–Hexu–CH_3]^-$	Isorhamnetin hexuronoside [f]	
31	15.11	477.1024	$C_{22}H_{22}O_{12}$	–0.6	315 $[Ag–H]^-$ ($C_{16}H_{11}O_7$ 1.8 ppm)	isorhamnetin 3-O-β-D-glucopyranoside [f]	
32	15.29	623.1599	$C_{28}H_{32}O_{16}$	–1.2	315 $[Ag–H]^-$ ($C_{16}H_{11}O_7$ 1.6 ppm)	isorhamnetin-rhamnoside-hexoside	García-villalba et al., 2017
33	16.8	609.1231	$C_{30}H_{26}O_{14}$	–1.3	**463** $[M–H–coumaroyl]^-$, 301 $[Ag–H]^-$ ($C_{15}H_9O_7$ 0.8 ppm)]	quercetin 3-O-(6"-O-trans-*p*-coumaroyl)-β-D-glucopyranoside [f]	
34	17.84	593.128	$C_{30}H_{26}O_{13}$	–1.5	447 $[M–H–coumaroyl]^-$, **285** $[Ag–H]^-$ ($C_{15}H_{10}O_6$ 1.2 ppm)	kaempherol coumaroyl hexoside	García-villalba et al., 2017
35	18.00	593.12748	$C_{30}H_{26}O_{13}$	–2.5	447 $[M–H–coumaroyl]^-$, **285** $[Ag–H]^-$ ($C_{15}H_{10}O_6$ 1.7 ppm)	Tiliroside [c]	
36	18.04	535.1076[e]	$C_{23}H_{22}O_{12}$	–1.1	343 $[M–H\ dHex]^-$	Ellagic acid 3,3',4-trimethoxy 4'-O-α-L-rhamnopyranoside [f]	
37	18.22	623.1388	$C_{31}H_{28}O_{14}$	–1.1	477 $[M–H–coumaroyl]^-$, **315** $[Ag–H]^-$ ($C_{16}H_{12}O_7$ 1.5 ppm)	isorhamnetin coumaroyl hexoside	García-villalba et al., 2017
38	19.16	593.1284	$C_{30}H_{26}O_{13}$	–1.0	285 $[Ag–H]^-$ ($C_{15}H_{10}O_6$ 1.5 ppm)	kaempherol coumaroyl hexoside	García-villalba et al., 2017
39	19.74	635.1282	$C_{32}H_{28}O_{14}$	–2.1	**575** $[M–H–acetyl]^-$, 285 $[Ag–H]^-$ ($C_{15}H_{10}O_6$ 2.7 ppm)	kaempherol acetyl coumaroyl hexoside	García-villalba et al., 2017
40	21.09	739.1648	$C_{39}H_{32}O_{15}$	–1.3	593 $[M–H–$ coumaroyl$]^-$, **453** $[M–H–Kaempferol]^-$, 285 $[Ag–H]^-$ ($C_{15}H_{10}O_6$ 2.4 ppm)	kaempferol dicoumaroyl hexoside	García-villalba et al., 2017
41	21.9	781.1753	$C_{41}H_{34}O_{16}$	–1.3	**635** $[M–H–$ coumaroyl$]^-$, 495 $[M–H–Kaempferol]^-$, 285 $[Ag–H]^-$ ($C_{15}H_{10}O_6$ 2.2 ppm)	kaempherol acetyl dicoumaroyl hexoside	García-villalba et al., 2017
42	22.11	781.1747	$C_{41}H_{34}O_{16}$	–2.0	**635** $[M–H–$ coumaroyl$]^-$, 495 $[M–H–Kaempferol]^-$, 285 $[Ag–H]^-$ ($C_{15}H_{10}O_6$ 2.2 ppm)	kaempherol acetyl dicoumaroyl hexoside	García-villalba et al., 2017

Abbreviations: GA: gallic acid; EA: ellagic acid¸dHex: loss of deoxyhexose (−146 Da); Hex: loss of hexose (−162 Da); Hexu: loss of hexuronose (−176 Da); Ag: aglycone.
[a]Compounds are numbered according to their elution order; [b]In bold the base peak of MS/MS spectrum; [c]Compared with reference standards; [d] m/z values corresponding to $[M–2H]^{-2}$; [e]m/z values corresponding to $[M + HCOOH–H]^-$; [f]The identification of these compounds was corroborated by isolation procedure and NMR spectra analysis.

B.I.3. Isolation and chemical characterization of CSB compounds.

In order to isolate the main CSB metabolites, CSB-M was partitioned between n-BuOH and H_2O, and the organic portion was separated by molecular exclusion chromatography (Sephadex LH-20) to collect five main fractions, subsequently analyzed by RP-HPLC chromatography to isolate 16 constituents (**Figure 34**). The chemical structures of purified compounds were elucidated by spectroscopic data in 1D- and 2D- NMR experiments, in comparison with those being in literature. The spectra analysis confirmed the structures proposed by HRMS analysis of the GA (chesnatin **17**, isochesnatin **19**, cretanin **20** and chestanin **21**), and EA derivatives (**28** and **36**), and to differentiate three ET metabolite isomers (castacrenin A-C **7, 9** and **11**) (**Figure 34**). Regarding flavonoids, kaempferol and isorhamnetin glycosides **29**, **30** and **32** were also confirmed (**Figure 34**). Moreover, the structure of flavonols **25**, **31** and **33** were unambiguously assigned to quercetin 3-O-β-D-glucopyranoside, isorhamnetin 3-O-β-D-glucopyranoside, and quercetin 3-O-(6''-O-trans-p-coumaroyl)-β-D-glucopyranoside, respectively, studying the proton coupling constants, 1D-TOCSY, ^{1}H-^{1}H-COSY, HSQC, and HMBC experiments of the glycosidic units (**Figure 34**). The isolation procedure led also to obtain chestanin (**21**) as pure compound. The isolated molecule was employed in the quantitative analysis, because commercial sample was not available. As an example, in the Supplementary Material (**Section S 2**).

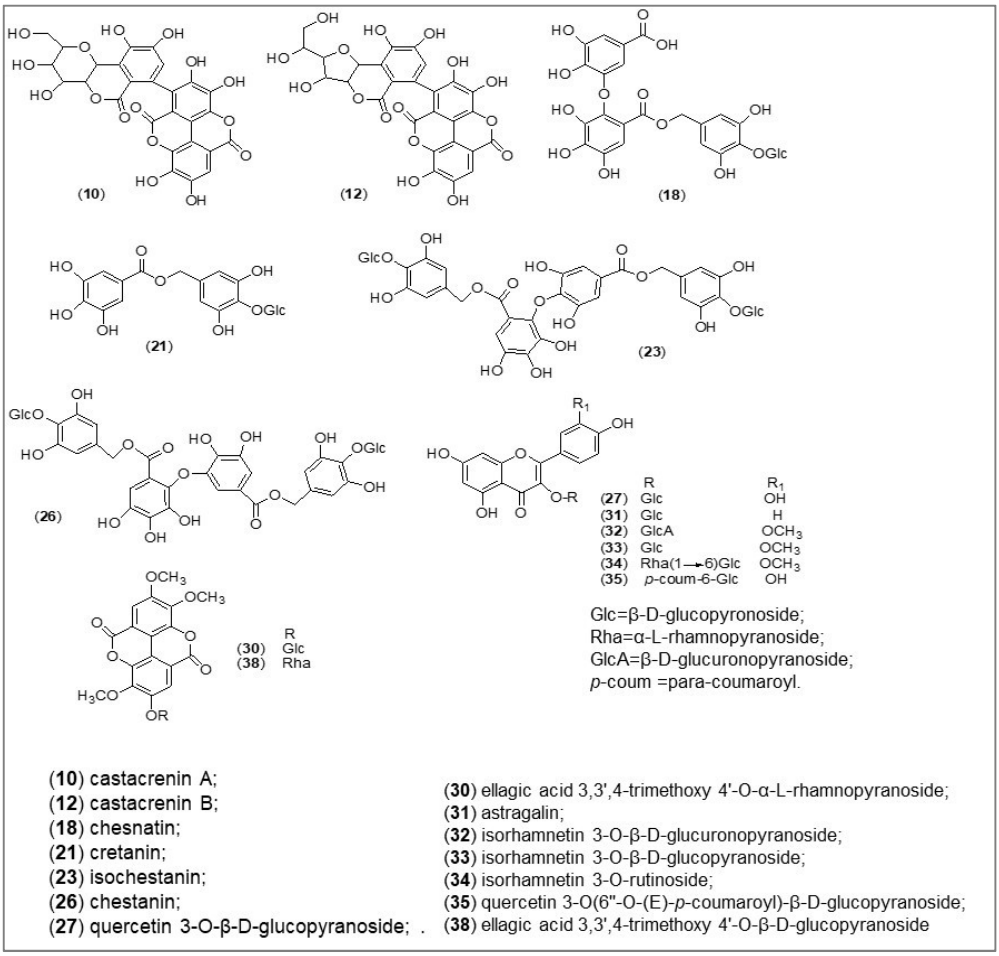

Figure 34. Chemical structure of CSB compounds assigned by 1D- and 2D- NMR experiments

B. I.4. Quantitative analysis of CSB extracts.

Chestanin (**21**) and EA (**27**) were the most abundant compounds of chestnut burs (**Table 10**) as revealed by a HPLC-UV profiling of CSB. Despite in literature is reported the presence of both compounds in chestnut bark and by-products (Fernández-agulló, et al., 2014; Braga et al., 2015). No significant differences were detected in the qualitative profiles of three different CSB extracts (CSB-M, A and H). Thus, a quantitative evaluation using external calibration method was carried

out. Chestanin and EA amounts in CSB extracts depending to the applied extraction conditions (**Table 10**). Among the three extracts, CSB-M extract showed the highest content of both analyzed compounds (79.28 mg g^{-1} of chestanin and 13.34 mg g^{-1} of EA). CSB-H and CSB-A showed instead comparable levels of both compounds (**Table 10**).

Table 10. amount of Chestanin (**21**) and ellagic acid (EA, **27**) in CSB extracts

	Chestanin (mg/g)[a]	EA (mg/g)[a]
CSB-H	3.21 ± 0.32	7.41 ± 1.32
CSB-M	13.34 ± 1.43	79.28 ± 2.87
CSB-A	1.12 ± 0.21	5.20 ± 1.41

[a]Mean ± SD of three determinations

B.I.5. *In vitro* antifungal activity against phytopathogenic fungi

The frequent resistance developed by pathogens against the applied synthetic molecules, regulatory limitations in the use of fungicides, and public concerns about healthy and eco-friendly foods led to the investigation of new and alternative strategies for the control of *Alternaria alternata*, *Botrytis cinerea* and *Fusarium solani* infections occurring during cropping, storage, and commercial phases of vegetable foods. Some scientific researches report the effectiveness of plant extracts, rich in polyphenols, against phytopathogenic fungi, probably related to their ability to altering fungal membrane integrity (Zacchino et al., 2017). EA, one of the most active polyphenols in CSB extracts, has been shown to possess good antioxidant properties and proved to be suitable for postharvest kumquat treatments to preserving fruit quality (Landete, 2011; Mendoza et al., 2013). Thus, the inhibitory effects of CSB-M, CSB-H and CSB-A on mycelial growth and spore

germination of the selected fungi were studied by using an amended-plate technique and a liquid microculture method, respectively, to evaluating the potential use of CSB extracts for the management in field and or postharvest vegetable diseases (Pane et al., 2016). All the extracts (tested in a concentration range from 1 to 70 mg/mL) exhibited a dose-dependent antifungal activity against *A. alternata* and *F. solani* (**Table 11**), resulted as the most sensitive pathogens, with EC_{50} of all extracts varying from 6.04 mg/mL to 15.51 mg/mL, while *B. cinerea* resulted the less sensitive pathogen (**Table 11**). Among the three extracts, CSB-M showed the highest inhibitory effect against the phytopathogens showing the lowest EC_{50} values (**Table 11**) against *A. alternata* and *F. solani* (6.29 mg/mL and 6.04 mg/mL, respectively). In addition, CSB-M completely inhibited the mycelial growth of both *A. alternata* and *F. solani* at 30 mg/mL. On the contrary, CSB-H and CSB-A were not detrimental for *B. cinerea* growth up to 70 mg/mL; the EC_{50} determined for CSB-M was high (64.98 mg/ml, **Table 11**).

Table 11. EC_{50} of CSB extracts inhibiting *Alternaria alternata*, *Botrytis cinerea* and *Fusarium solani* mycelial growth

	EC_{50} growth inhibition (mg mL^{-1})	**95% Fiducial limits**		**Chi-square test (p value) [a]**
		Lower	**Upper**	
Alternaria alternata				
CSB-H	8.71	7.16	10.26	1.00
CSB-M	6.29	5.71	6.87	0.88
CSB-A	14.53	13.59	18.17	0.99
Botrytis cinerea				
CSB-H	>70.00			
CSB-M	64.98	61.85	68.11	0.88
CSB-A	>70.00			
Fusarium solani				
CSB-H	14.13	11.35	16.91	0.55
CSB-M	6.04	5.22	6.85	0.99
CSB-A	15.51	11.19	19.83	0.93

[a] Chi-square value, significant at $P < 0.05$ level.

The inhibitory effect of CSB extracts on the germination of fungal conidia was also investigated. The microorganisms produce spore cells to reproduce and survive in adverse conditions. The spores are usually very resistant even to the strongest treatments (Meng et al., 2010). As resumed in **Table 12**, the phytopathogenic fungi are most sensitive to CSB extracts in the phases of spore germination than those of saprophytic mycelial growth, and confirmed *A. alternata* and *F. solani* as the most sensitive strains (EC_{50} values between 2.22 and 11.17 mg/mL). CSB-M proved to be the most effective extract against *A. alternata* and *F. solani* spores with EC_{50} values of 2.66 mg/mL and 2.22 mg/mL, respectively (**Table 12**), while exhibited weak effect (EC_{50} 16.33 mg/mL, **Table 12**) on *B. cinerea* spores.

Table 12. EC_{50} of CSB inhibiting *Alternaria alternata*, *Botrytis cinerea* and *Fusarium solani* spore germination.

	EC_{50} germination inhibition (mg mL-^{1})[a]	**95% Fiducial limits**		**Chi-square test (p value) [a]**
		Lower	**Upper**	
Alternaria alternate				
CSB-H	11.17	8.91	27.77	0.53
CSB-M	2.66	1.48	8.70	1.00
CSB-A	5.48	1.14	9.82	0.24
Botrytis cinerea				
CSB-H	>50			
CSB-M	16.33	4.85	27.81	0.61
CSB-A	>50.00			
Fusarium solani				
CSB-H	10.52	5.28	15.76	0.72
CSB-M	2.22	1.84	2.60	0.95
CSB-A	6.80	5.18	8.42	0.99

[a] Chi-square value, significant at $P < 0.05$ level

The chemical markers of CSB extracts were identified as chestanin (**21**) and ellagic acid (EA, **27**). To understand if their content possesses a role in the different antifungal behavior of the extracts, the pure compounds were tested separately against the spore germination, and the results were compared with two synthetic fungicides, such as iprodione, used for the control of postharvest diseases caused by *A. alternata* and *B. cinerea*, and carbendazim used against the occurrence of *F. solani* infections (Thomidis et al., 2009) (**Table 13**). EA (**27**) resulted the most active against all fungi, with EC_{50} included between 13.33-112.64 µg/mL. Instead, chestanin (**21**) was the less active, with EC_{50} value against *A. alternata* of 561.56 µg/mL, and higher than 2 mg/mL against *B. cinerea* and *F. solani*.

In literature several biological properties of EA are reported such as antioxidant, antimicrobial, and anti-inflammatory activities (Gatto et al., 2011; Veloz-Garcia et al., 2010). The antimicrobial activity of EA was investigated against different *Candida* strains, with a MIC value ranging from 25 to 100 μg/mL and against phytopathogenic fungi *F. solani* and *B. cinerea* at concentrations of 1 mg/mL and 390 μg/mL, respectively (Osorio et al., 2010; Mendoza et al., 2013). In a previous research, EA showed a dual behavior against *B. cinerea*, resulting detrimental for germ tube length and mycelial growth and ineffective on spore germination at low concentration (18 ppm); whereas the higher dose of the compound incited both germination and *in vitro* growth (90 ppm) (Tao et al., 2010). The obtained results in the present research, supported by data reported in literature, could let suggest that EA contributed to the highest effectiveness of CSB-M in both performed assays. However, the different magnitude antifungal effect of CSB extracts against target fungal species seem to be more related to the TPC than to a single isolated compound. Indeed, EC_{50} calculated on germination and plate growth of *A. alternata* and *F. solani* was well correlated with TPC (Pearson coefficient from -0.72 to -0.99).

Table 13. EC_{50} of pure compounds compared to synthetic fungicides (iprodione, and carbendazim) inhibiting *Alternaria alternata*, *Botrytis cinerea* and *Fusarium solani* spore germination.

	EC_{50} growth inhibition (µg mL^{-1})	**95% Fiducial limits**		**Chi-square test (p value) [a]**
		Lower	**Upper**	
Alternaria alternata				
EA (**27**)	13.33	12.77	13.90	0.99
Chestanin (**21**)	561.56	544.57	578.54	0.92
Iprodione	0.85	0.70	0.99	1.00
Botrytis cinerea				
EA (**27**)	112.64	8.89	219.11	1.00
Chestanin (**21**)	>2000			
Iprodione	37.36	18.90	58.10	0.99
Fusarium solani				
EA (**27**)	21.27	15.57	26.43	1.00
Chestanin (**21**)	>2000			
Carbendazim	14.29	6.03	21.97	0.99

[a] Chi-square value, significant at $P < 0.05$ level

B.I.6. Production of hydroalcoholic extract from Roasted Hazelnut Skins, total phenol content and free radical scavenging activity

A non-conventional extraction method was applied to recovery polyphenols from Roasted Hazelnut Skins. The obtained results in terms of process yield, TPC and antioxidant activity of the extract (RHS-H) were compared with those of extract produced with a conventional exhaustive maceration at room temperature (RHS-M) and reported in a previous research (Piccinelli et al., 2016). RHS-H was obtained by Pressurized Liquid Technique (PLE), at 125°C, using aqueous ethanol concentration (30%, v/v), 5 extraction cycles and 5 static cycles. As showed in **Table 14**, RHS-H process yield (32.0 w/w) resulted 4 times higher than RHS-M (7.8 % w/w). This can be due to the combined use of high pressure and temperature

in PLE, which forcing the solvent between the pores of the matrix, increases the interaction between compounds and solvent, promoting their higher solubility and consequently an enhanced recovery of active molecules (Alañón, et al., 2017; Dai and Mumper, 2010). In fact, RHS-H polyphenols content resulted improved than RHS-M (308.4 µg and 249.2 µg GAE/mg extract, respectively), producing a strongest free radical scavenging activity (EC_{50} 7.9 µg/mL) (**Table 14**). Thus, PLE extraction procedure did not modify the efficacy of the RHS, and this support its potential use to obtain antioxidant extracts from agro-food wastes and by products, with potential use as functional ingredient (Alañón, et al., 2017).

Table 14 Extraction yield, free radical-scavenging activity and total phenolic content (TPC), and in RHS-H extract compared to RHS-M

	Extraction yield % w/w	DPPH test EC_{50} [a] (µg/mL) [b]	Total phenolic content [b] µg GAE [d]/mg extract
RHS-M*	7.82 ± 0.82	10.61 ± 0.72	249.22 ± 0.11
RHS-H	32.01 ± 0.22	7.91 ± 0.22	308.43 ± 0.10
α-tocopherol [c]		10.11 ± 1.21	

[a] EC_{50}=concentration of sample necessary to decrease the initial DPPH concentration by 50%; [b]Mean ± SD of three determinations, [c]Positive control of the DPPH assay[d] Gallic acid equivalent, * extract reported by Piccinelli et al., 2016

B.I.7. Conclusion

Chestnut Spiny Burs and Roasted Hazelnut Skins were selected as interesting matrices to be subjected to technological transformation. The chemical study of chestnut burs led to identify several compounds, mainly gallic and ellagic acid derivatives, hydrolysable tannins, and glycosylated flavonols in organic and aqueous extracts. All CSB extracts showed a significant antioxidant effect and inhibitory activity against plant pathogens. Moreover, a hydroalcoholic extract from Roasted Hazelnut Skins was produced by Pressurized Liquid Technique (PLE). RHS-H exhibited a high extraction yield and improved antioxidant activity against DPPH, due to the higher recovery of phenol compounds. PLE resulted an optimal environmental-friendly technique, suitable for the extraction of active molecules, using no-toxic and less amount of solvent. The significant free radical scavenging activity of both extracts, and the antifungal effects against phytopathogenic fungi of CSB extracts, support their potential use as new functional ingredients for the design and development of food active packaging films.

Part II

Design and Development of new packaging films loaded with Chestnut Spiny Burs and Roasted Hazelnut Skins hydroalcoholic extracts

Scientific background and research aim

One of the main challenge of the food industry is to employ renewable and eco-friendly materials as packaging systems, able to replace the petroleum derivatives, and, at the same time, to preserve food quality longer (Mir et al., 2018; Vieira et al., 2016). For this purpose, the development of edible films based on natural polymers and active extracts from fruit and vegetable or by-products is a potential alternative, to prolong the shelf-life, without altering the organoleptic and nutritional properties of foods (Jaramillo et al., 2016). Because of oxidations and microbial spoilage are the major drawbacks affecting foodstuffs quality, the use of natural extracts, with antioxidant and antimicrobial activity, is preferred (Boldini et al., 2013). In this context, as previously described (Section B, part I), the polyphenol-rich extracts from Roasted Hazelnut Skins (RHS-H) and Chestnut Spiny Burs (CSB-H) are interesting and promising active ingredients. Therefore, the aim of this project part was to design and develop an active edible films by including antioxidant and antimicrobial extracts in it. Among biopolymers, pullulan created great interest for its multiple properties: it is water-soluble, non-toxic, biodegradable, and compatible for human purposes (Pinto et al., 2013; Trovatti et al., 2012, Silva et al., 2018). However, pullulan has good film-forming abilities, and the obtained films result transparent, flexible, odourless, and with good mechanical properties that make them easy handling for consumers and producers (Pinto et al., 2013; Trovatti et al., 2012; Silva et al., 2018). The challenge of the research was to combine the functional properties of CSB-H and RHS-H with the filmogenic ability of pullulan in producing flexible and bioactive films by casting technique. The effects of CSB-H and RHS-H addition on mechanical properties, thickness, infrared spectroscopy characteristics, and optical properties, were evaluated. Moreover, the antioxidant and antibacterial activities against Gram-positive and Gram-negative foodborne pathogens, were also investigated

B.II.1. Preparation of Pullulan CSB-H or RHS-H films

A research period at CICECO, Aveiro Institute of Materials, Chemistry Department of Aveiro University (Portugal), provided the design, development, and characterization of edible films based on pullulan (PL), as film-forming polymer, and CSB-H and RHS-H extracts (reported in Section B, part I), as active additives. PL is a non-ionic, biodegradable exopolysaccharide obtained from fermentation of black yeast *Aureobasidium pullulans* fungus. It is made up of maltotriose units, units of three α-1,4-linked glucose molecules, which are polymerised in a linear way through α-1,6-links (**Figure 35**). The alternation of α-1,4 and α-1,6- linkages in a single compound, makes PL soluble in water and a high flexibility to its structure (Fernandes et al., 2014; Xiao et al., 2017).

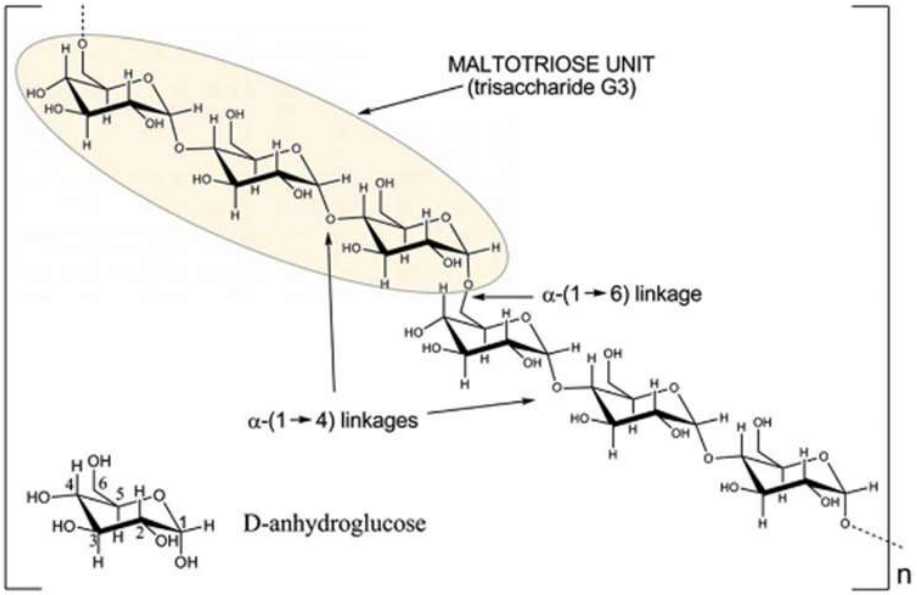

Figure 35. Chemical structure of pullulan (Farris et al., 2014)

This type of bonds gives it the ability to form films that are transparent, with a low permeability to oil and oxygen (Silva et al., 2018; Fernandes et al., 2014). It appears as a white powder, odourless, tasteless, non-hygroscopic, and impermeable to oxygen. PL is also non-toxic, non-mutant and non-carcinogenic (Fernandes et al., 2014; Niu et al., 2019).

It is widely used in the production of food films, because it is an edible polymer and the films generated result transparent, flexible, elastic, easy to handle, with good barrier properties against oxygen and humidity (Silva et al., 2018). It possesses functional properties like adhesiveness, film forming ability, enzymatically mediated degradability. It also has a low caloric value, suitable for vegetarians, diabetics, and subjects with restricted diets, and result resistant to oil and heat-sealable (Diab et al., 2001; Vuddanda et al., 2017).

In recent years, PL has been used also in various pharmaceutical applications, drug delivery and biomedical applications such as targeting, surface modification, nanoparticles, gene delivery, cancer therapy, bio-imaging, plasma expander and tissue engineering. It is also used for the production of hard capsules as an alternative to glycerine (Vuddanda et al., 2017).

As plasticizer was selected glycerol (Gly, $C_3H_8O_3$), suitable for water soluble polymer. It is a polyol with three hydroxyl groups in the structure, responsible for its water solubility and its hygroscopic nature. It is non-toxic, biocompatible, transparent, odourless, with a slight sweet taste (Basiak et al., 2018). When it is loaded in the film matrix, it increases the volume of polymer structure and promote the molecular mobility of the polymeric molecules, through the formation of inter and intramolecular bonds, reducing the plastic properties in favour of the elastic ones.

Moreover, the addition of Gly in the edible films provides them high mechanical properties, excellent barrier ability, and enhance thermal stability (Cao et al., 2018).

Several works reported that Gly has a better plasticizing effect than sorbitol, which is widely used in the food industry as a sweetener, stabilizer, and leavening agent, which instead makes the films less resistant and extendable. This behaviour is due to the higher molecular weight of sorbitol and it appears in solid form at room temperature, unlike Gly which is liquid (Otoni et al., 2017).

PL was used at 6% (w/w) and Gly was added at 10%, w/w. Gly not only change the three-dimensional molecular organization of polymer, reduces film fragility, and makes films more flexibles and easier to handle, but also improves the extracts dissolution into the polysaccharide solution, resulting easy to fold even when CSB-H and RHS-H were added at 10% w/w (Silva et al., 2018; Gheribi et al., 2018; Silva-Weiss et al., 2013). Films were casted into acrylic plates as molds (5x5 cm^2), and **Table 15** resumed their composition.

Adding natural extracts change the original color of the polymeric solution, because of both the own color of the raw extract, and interactions between film-forming polymers and extract components (Talon et al., 2017; Wang et al., 2016; Siripatrawan and Vitchayakitti, 2016). In our case, after the drying process (in a ventilated oven at 30 °C for 24 h), the blank films (PL and PL-Gly) appeared transparent, while as the amount of CSB-H and RHS-H increased from 1% to 10%, the films became darker, showing at 10% of extract a strong brownish color (**Figure 36** and **37**). On the other hand, all films showed a homogeneous distribution of CSB-H and RHS-H, and no bubbles or brittle areas were visible, at all the extract employed concentrations.

Table 15. Composition of prepared films

Sample	PL (mg)	Gly (%)[a]	CSB (%)[a]	RHS (%)[a]
PL	480	-	-	-
PL-Gly	480	10.0	-	-
PL-Gly-CSB-H_1%	480	10.0	1.0	-
PL-Gly-CSB-H_5%	480	10.0	5.0	-
PL-Gly-CSB-H_10%	480	10.0	10.0	-
PL-Gly-RHS-H_1%	480	10.0	-	1.0
PL-Gly-RHS-H_5%	480	10.0	-	5.0
PL-Gly-RHS-H_10%	480	10.0	-	10.0

[a] (w/w) relative to PL

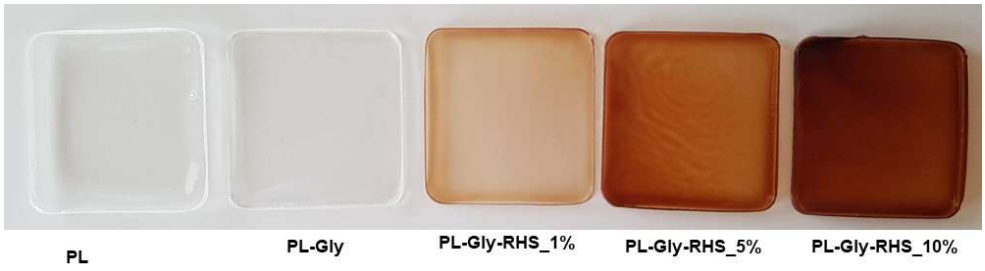

Figure 36. Photographs (by digital camera CANON EOS 600D) of films loaded with RHS-H (composition in **Table 15)**

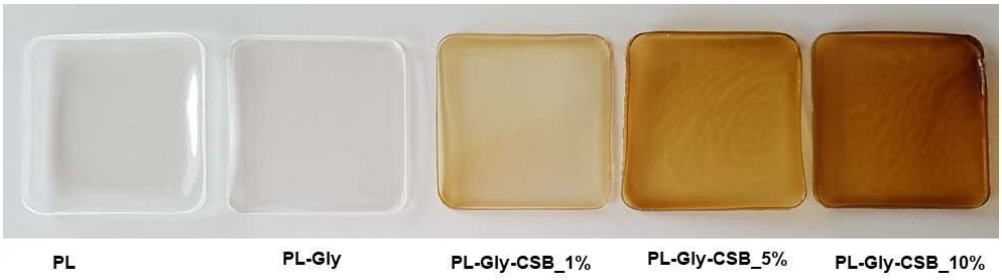

Figure 37. Photographs (by digital camera CANON EOS 600D) of films loaded with CSB-H (composition in **Table 15**)

B.II.2. Characterization of films

B.II.2.1. Optical properties: internal transmittance

Protecting food from the negative effect of UV-vis light is an important property required to edible films to prevent the deterioration of foodstuffs, their nutritional value and active components (Norajat et al., 2010; Talon et al., 2010). Active ingredients, such as natural extracts, may cause significant changes of barrier properties of films (Mir et al., 2018; Aparicio-Fernández et al., 2018). For this reason, the optical properties of films were evaluated scanning the films in the range of 200-800 nm, to find out the percentage of transmitted light. According to Silva et al., 2018, blank films (PL; PL-Gly) were optically transparent with a transmittance value of 90% in visible range (400-700 nm) and of 7-87% in ultraviolet range (200-400 nm) (**Figures 38** and **39**). On the contrary, as increase the CSB-H and RHS-H concentration, the transmittance values decrease in both ranges (**Figures 38** and **39**). At 10% (w/w), RHS-H and CSB-H induced a reduction of transmittance in visible range (55-2% and 70-0%, respectively) and a completely light absorption in UV range (transmittance values 0-2%) (**Figures 38** and **39**). Several authors confirmed our results, reporting as adding extracts in edible films reduces the light transmission in UV and visible range, especially when added at high concentrations (Akhatar et al., 2012; Norajat et al., 2010; Wang et al., 2016). The improved ultraviolet light barrier properties of loaded films suggest their use to protect food from lipid photo-oxidation, discoloration and nutrient losses prolonging their shelf-life (Wang et al., 2016; Liu et al., 2017).

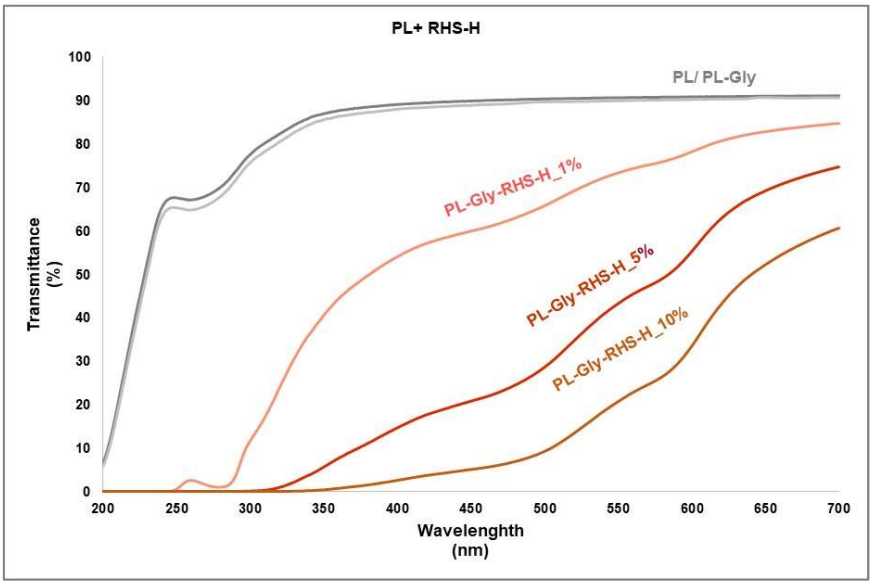

Figure 38. UV-vis spectra of blank (PL; PL-Gly) and RHS-H-loaded films

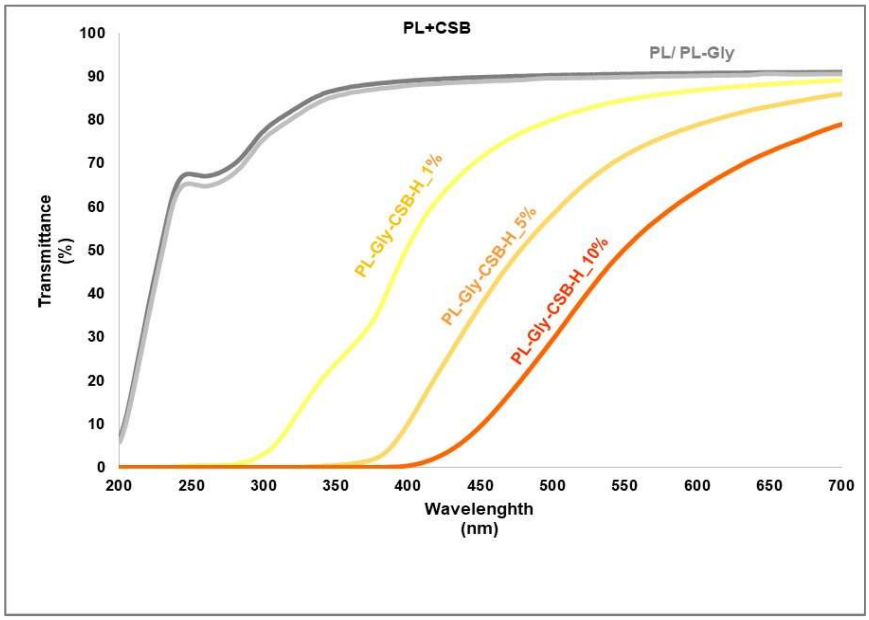

Figure 39. UV-vis spectra of blank (PL; PL-Gly) and CSB-H-loaded films

B.II.2.2. Thickness and mechanical properties

The thickness of films is an important feature to evaluate their physical properties. Incorporating CSB-H and RHS-H increased the film thickness, from 77.0 ± 1.0 µm to 98.0 ± 17.0 µm and 110.0 ± 19.0 µm, respectively (**Table 16**). It depends on both the introduction of high solid content and potential extract/polymer interactions, altering the organized structure of the blank film matrix (Mir et al., 2018; Norajat et al., 2010). In our case, the cross-links among the high molecular weight polyphenols of CSB-H and RHS-H could increase the distance within the pullulan chains. At least, the homogeneous distribution of extracts into the polymeric matrix, also at highest loaded concentration, is proved by the low standard deviations (Wang et al., 2016; Talon et al., 2017; Siripatrawan and Vitchayakitti, 2016).

Table 16. Composition and thickness of prepared films

Sample	Thickness (µm)	Tensile Strength (TS)* (MPa)	Elongation at break (ES) * (%)	Young's Modulus* (GPa)
PL	77.00 ± 1.02	69.04 ± 7.96 ^{a}	4.08 ± 0.76 ^{a}	3.41 ± 0.20 ^{a}
PL-Gly	78.01 ± 4.05	61.60 ± 11.02 ^{ab}	3.22 ± 0.80 ^{ab}	2.79 ± 0.29 ^{b}
PL-Gly-RHS_1%	96.04 ± 12.03	58.24 ± 13.65 ^{ab}	3.47 ± 0.48 ^{ab}	2.75 ± 0.44 ^{b}
PL-Gly-RHS_5%	100.04 ± 6.02	55.59 ± 2.88 ^{ab}	2.63 ± 0.16 ^{b}	2.73 ± 0.13 ^{b}
PL-Gly-RHS_10%	98.02 ± 17.02	46.64 ± 4.43 ^{b}	2.29 ± 0.20 ^{b}	2.66 ± 0.21 ^{b}
PL-Gly-CSB_1%	86.01 ± 4.00	64.33 ± 5.11 ^{a}	3.71 ± 0.52 ^{ab}	2.72±0.24 ^{b}
PL-Gly-CSB_5%	103.03 ± 18.01	56.68 ± 10.64 ^{a}	2.72 ± 0.29 ^{bc}	2.66 ± 0.33 ^{b}
PL-Gly-CSB_10%	110.01 ± 19.02	57.41 ± 7.36 ^{a}	2.35 ± 0.19 ^{c}	2.96 ± 0.21 ^{ab}

*One-way analysis of variance (ANOVA) followed by and Tukey HSD test; means followed by the same letters are not significantly different ($p > 0.05$)

Mechanical properties were analyzed to predict the integrity of edible films after extracts incorporation, and under stress and elongation conditions defining their

final applications (Cao et al., 2007) (**Table 16**). The Young's modulus defines the elasticity of films when a force was applied; tensile strength predicts the maximum tensile stress that film can support before breaking and failing, and elongation at break indicate films flexibility, the ability to resist changes of their shape without cracking (Sanchez-Gonzalez et al., 2010). The obtained results (**Table 16**) showed that the three parameters (YM, TS, and EB) resulted unchanged, after CSB-H and RHS-H incorporation in plasticized films ($p > 0.05$), showing how the extracts did not deeply affect elastic properties, workability and flexibility of the films (**Figure 40**) (Silva-Weiss et al., 2018).

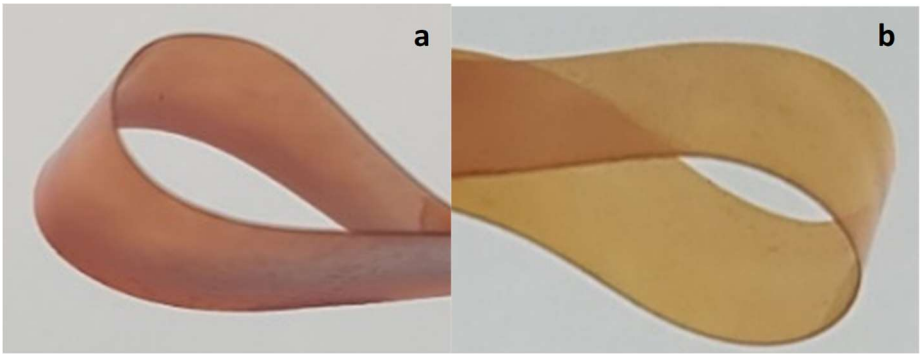

Figure 40. Films loaded with 10% of RHS-H (**a**) and CSB-H (**b)**

The addition of CSB-H and RHS-H at 10% (w/w), induced only a moderate ($p > 0.05$) reduction of EB (of about 27% for CSB-H, and 29% for RHS-H) and of TS ($p>0.05$) (of about 7% for CSB-H, and 24% for RHS-H), compared to plasticized PL film, suggesting that the films were less stretchable and resistant to break than the control film (Boldini et al., 2013; Gimenez et al., 2013; Pastor et al., 2013).

B.II.2.3. FTIR-ATR

FTIR analysis of either raw extracts and blank films was recorded. The obtained results were compared with extract loaded films (concentration of 10% w/w) to evaluate potential intermolecular bonds occurring between extract and pullulan. As depicted in **Figures 41 a** and **b**, **42**, and **43**, the blank film profiles, had a very strong absorption band at 3310 cm^{-1} (O-H stretching), 2927 cm^{-1} (CH and CH_2 stretching), 1646 cm^{-1} (bending motion of adsorbed water (H-O-H), 1150 to 1060 cm^{-1} (C-O-C stretching of glycosidic bridges) and 754 cm^{-1}(a-glycosidic bond stretching), due to the pullulan structure (Silva et al., 2018; Talon et al., 2017). No additional peaks were detected in the spectra of the films containing 5 and 1% of CSB-H and RHS-H, because this amount added in films is much lower than that of pullulan (**Figure 41 a** and **b).**

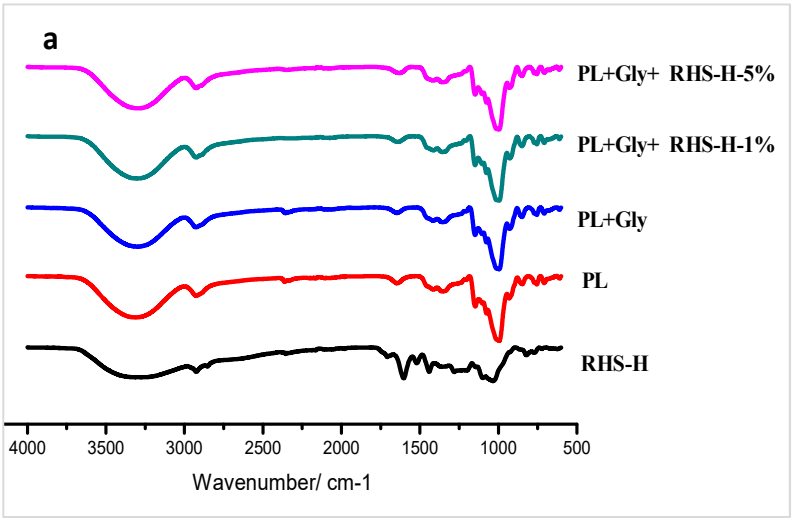

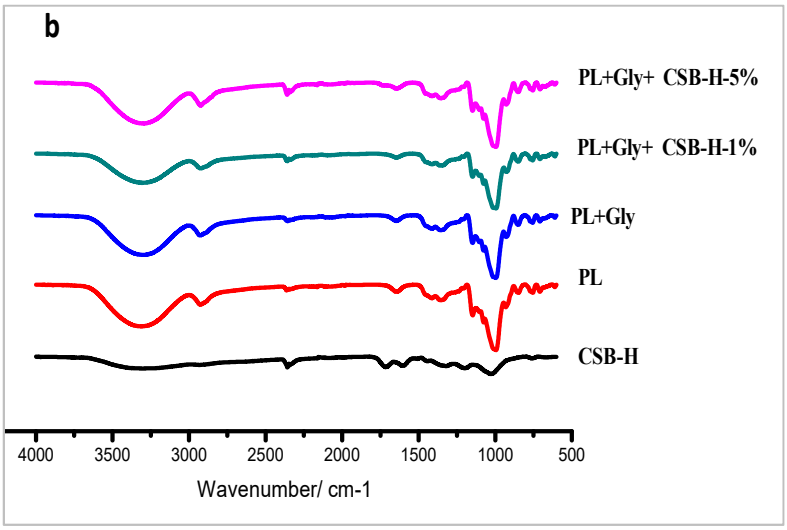

Figure 41. FTIR spectra of raw extracts (**a** RHS-H and **b** CSB-H), blank films (**a** and **b** PL and PL-Gly) and loaded film (PL-Gly-RHS-H_1%, PL-Gly-RHS-H_5%, **Figure a**; PL-Gly-CSB-H_1%, PL-Gly-CSB-H_5%, **Figure b**)

At the contrary, new peaks which were not related to pullulan structure, (**Figure 42**) were detected in the 10% RHS-H film loaded spectra regions of 1607-1622 cm^{-1}, 1507-1523 cm^{-1} and 1468-1463 cm^{-1}, associated to C=C skeletal in plane vibrations. As reported elsewhere (Ricci et al., 2015), the spectral regions 1620 to 1610 cm^{-1} are affected by the elongation of C4-C8 inter-flavonoid linkage during the condensation process in proanthocyanidins (higher intensity corresponds to an extensive degree of polymerization). Moreover, new peak was also identified in the region 1266-1297 cm^{-1} attributed to C-O stretching absorption and relative OH deformations (Ricci et al., 2015), suggesting the presence of polyphenols.

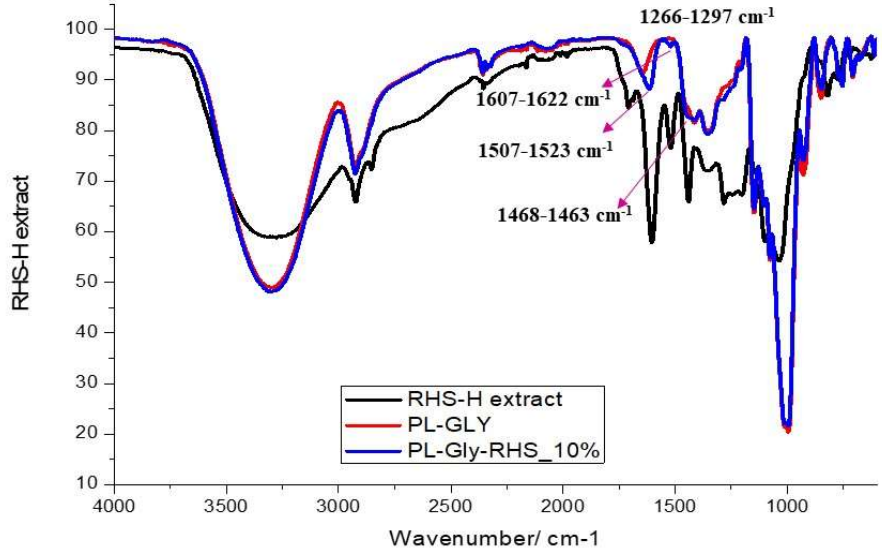

Figure 42. FTIR spectra of raw extract (RHS-H black line), blank film (PL-Gly, red line) and loaded film (PL-Gly-RHS-H_10%, blue line)

Additional peak was also observed in the CSB-H (10%) film spectra (**Figure 43**); the spectra region was 1708-1747 cm^{-1} probably due to C=O stretching vibration of esters, typical of derivatives of gallic acid and indicate the structure of hydrolysable tannins (Wang et al., 2016).

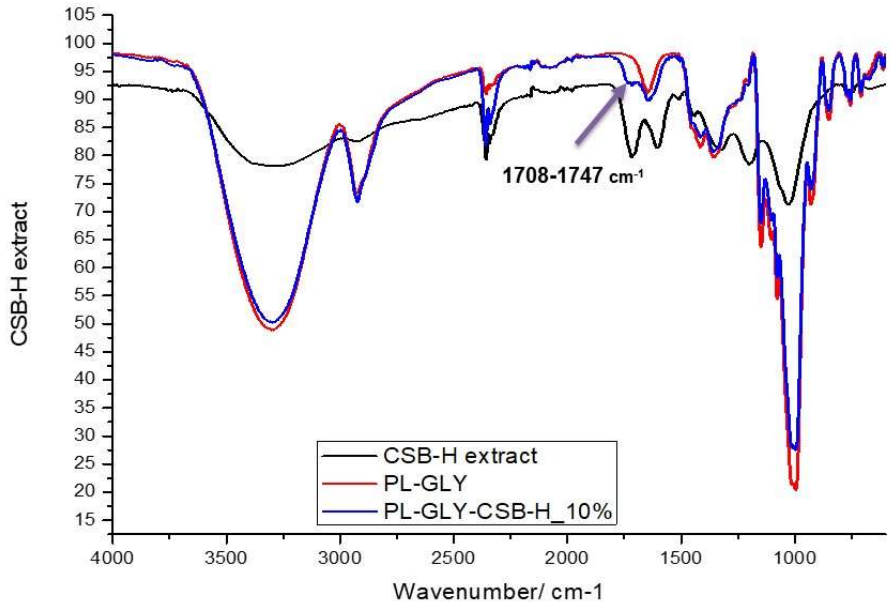

Figure 43. FTIR spectra of raw extract (CSB-H black line), blank film (PL-Gly, red line) and loaded film (PL-Gly-CSB-H_10%, blue line)

B.II.3. Functional properties of films

B.II.3.1. Antioxidant activity

The new challenge of food industry is the use of active packaging as carriers of natural antioxidant and antimicrobial ingredients (Benbettaïeb et al., 2018). CSB-H and RHS-H raw extracts showed a strong scavenging activity against the radical DPPH (EC_{50} 24.94 µg/mL and 7.91 µg/mL, respectively). To understand if PL and extract antioxidant compounds were compatible and to verify their homogeneous distribution, the DPPH assay was employed, according to Silva et al 2018 (Silva et al., 2018). 1x1 cm^2 of films (in triplicate) with different concentrations of RHS-H and CSB-H were tested and compared with the raw extracts and blank films (in the same conditions). PL films did not show DPPH radical scavenging activity (RSA

0%). On the contrary, CSB-H and RHS-H maintained their antioxidant activity within the film, exhibiting RSA% higher than 90% (**Figure 44 a** and **b**) at all three tested concentrations. This also proved that the film matrix allows the effective release of the active extracts.

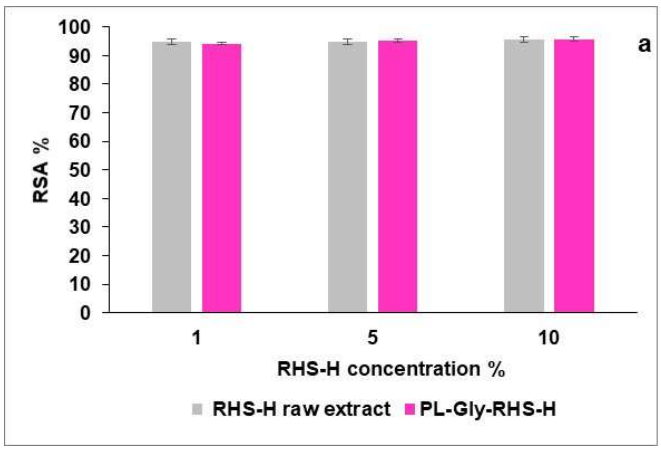

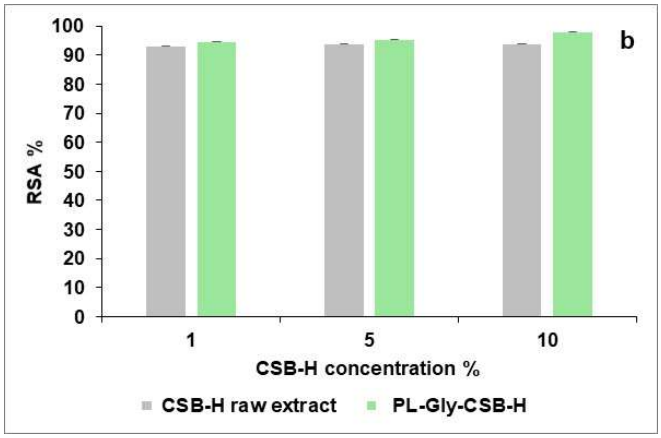

Figure 44. DPPH scavenging activity of RHS-H raw extract and PL/RHS-H films (**a**) and CSB-H raw extract and PL-Gly-CSB-H films; values are the mean of three independent experiments; error bars represent the standard deviation

Several works reported that the addition of extracts, rich in phenolic compounds, improved the scavenging ability of the films against the DPPH$^{\bullet}$ (Akhtar et al., 2012; Siripatrawan and Vitchayakitti, 2016; Norajat et al., 2010; Talon et al., 2017). The results support the use of films based on CSB-H and RHS-H for antioxidant food packaging.

B.II.3.2 Antimicrobial activity

The microbial spoilage is another important cause of the low food shelf-life. The modern packaging strategies seek to replace synthetic substances with natural antimicrobial additives (Bodini et al., 2013). For this reason, the realized films have been tested against two bacteria, *S. aureus* (Gram positive) and *E. coli* (Gram negative), responsible of foodborne diseases (Silva et al., 2018). As depicted in **Figures 45** and **46**, PL blank films did not inhibit the growth of the bacteria. Films did not show any efficacy against *E. coli*. On the contrary, the increase in the extract concentration increased the film effect against *S. aureus*. Several studies reported that *S. aureus* is more sensitive to the action of extracts than *E. coli*, because Gram negative bacteria possesses an additional external membrane that prevent the diffusion of molecules through its lipopolysaccharide layer (Silva et al., 2018). RHS-H at 1% (0.48 mg/mL), 5% (2.4 mg/mL) and 10% (4.8 mg/mL) and the films loaded with the same concentration of the extract (5x5 cm^2) were tested against *S. aureus*. In particular, at 5% and 10%, RHS-H showed a strong antimicrobial activity, with 6 log CFU reduction after only 6 h and 8 log CFU reduction after 12 h (**Figure 45**). At 6 hours, the extract maintains the same effectiveness even when incorporated into the film (**Figure 45**).

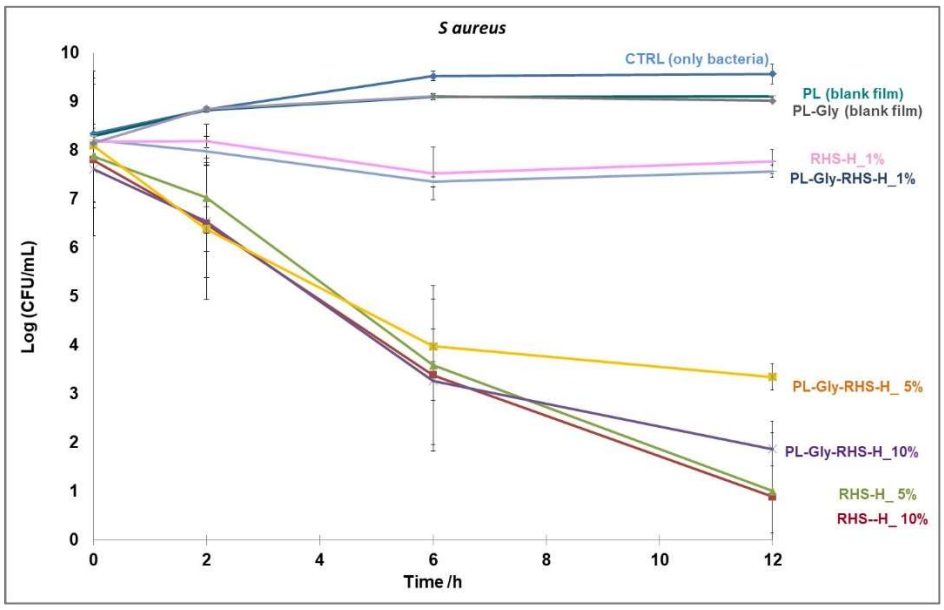

Figure 45. Antibacterial activity of PL and PL-Gly (grey); RHS-H at 1%, 5% and 10% (blue, green and red lines, respectively), PL-Gly-RHS-H_1, 5 and 10% (pink, yellow and purple lines, respectively) after 0, 2, 6 and 12 hours; values are the mean of three independent experiments; error bars represent the standard deviation

CSB-H and film loaded with (10% w/w) of extract were tested against *S. aureus,* slightly modifying the protocol, in order to test the final CSB-H concentration of 12 mg/mL of (raw or loaded in the film). The results displayed a reduction of about 3 log after 12 h from the beginning of the test (**Figure 46**). The effectiveness of composite film resulted completely superimposable, demonstrating, also in this case, a good interaction between PL and CSB-H and its effective release from the film matrix. In both cases, the extracts improve antimicrobial efficacy of films, supporting their potential use in the preservation of food from microbial spoilage (Bodini et al., 2013).

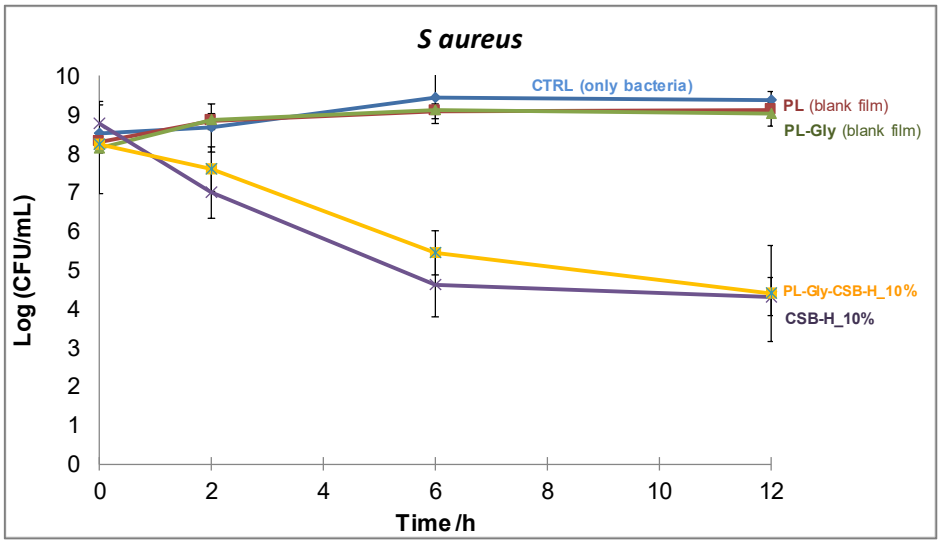

Figure 46. Antibacterial activity of PL (red line), PL-Gly (green line); CSB-H_10% (purple line) and PL/CSB-H_10% (yellow line) after 0, 2, 6 and 12 hours; values are the mean of three independent experiments; error bars represent the standard deviation

B.II.4. Conclusion

In recent years, the development of active edible films with natural compounds, such as polyphenols, is considered a potential tool to improve safety of food and increase its shelf life. Therefore, in this PhD project, the hydroalcoholic extracts from Roasted Hazelnut Skin (RHS-H) and Chestnut Spiny Burs (CSB-H) was included, at 1, 5, and 10% (w/w), in a plasticized pullulan solution to produce food packaging films. The addition of RHS-H and CSB-H reduced the light transmittance of films in the visible and UV ranges, which can contribute to the reduction of food deterioration. Moreover, the addition of both extracts does not affect the mechanical properties of the films, also improving their antioxidant and antimicrobial activities. All the results suggest that RHS-H and CSB-H can be used as natural antioxidant and antimicrobial agents in flexible bioactive films promoting the reuse of a food waste and by-product to reduce the environmental impact and to increase the eco-sustainability of the food processing industry.

MATERIALS AND METHODS
OF
SECTION B

B.III.1.1. Chemicals and reagents.

Analytical grade *n*-hexane, chloroform ($CHCl_3$), methanol (MeOH) and ethanol (EtOH), dimethyl sulfoxide (DMSO), methanol deuterated (CD_3OD), Folin-Ciocalteu phenol reagent, 1,1-diphenyl-2-picrylhydrazyl radical (DPPH), 2, 2′-azino-bis (3-ethylbenzothiazoline)-6 sulphonic acid (ABTS), Trolox, ellagic acid, carbendazim 97% (Carbendazim PESTANAL®), iprodione (Iprodione PESTANAL^{TM}), and HPLC-grade methanol (MeOH) were purchased from Sigma-Aldrich (Milan, Lombardia, Italy). Potato Dextrose Agar (PDA) and Potato Dextrose Broth (PDB) were purchased from Thermo Fisher Diagnostics S.p.A (Milano, Italia). HPLC-grade water (18 mΩ) was prepared by a Milli-Q_{50} purification system (Millipore Corp., Bedford, MA).

Glycerol (≥99.5%, Sigma-Aldrich, USA), Pullulan powder (PL, 98%, MW 272 kDa, B&K Technology Group, China), 2,2-diphenyl-1-picrylhydrazyl (DPPH, Aldrich, USA), Brain-Heart Infusion Broth (BHI, Liofilchem, Italy), Phosphate buffer solution (PBS, pH 7.4, Sigma-Aldrich, USA), Luria Bertani medium (LB, Liofilchem, Italy), Tryptic Soy Broth (TSB, Liofilchem, Italy), and Trypticase Soy Agar (TSA, Sigma-Aldrich, USA) were used. Methanol and ethanol were supplied by VWR (Carnaxide Portugal). Ultrapure water (18 MΩ) was prepared by a Milli-Q purification system (Millipore, Bedford, MA, USA). *E. coli* (ATCC 13706) and *S. aureus* (ATCC 6538) were provided by DSMZ e Deutsche Sammlung von Mikroorganismen und Zellkulturen GmbH (German Collection of Microorganisms and Cell Cultures).

B.III.1.2. General experimental procedures.

A Bruker DRX-600 NMR spectrometer, operating at 599.19 MHz for ^{1}H and 150.858 MHz for ^{13}C, using the TopSpin 3.2 software package, was used for NMR

experiments in CD_3OD. Chemical shifts are expressed in δ (parts per million) referring to the solvent peaks δ_H 3.31 and δ_C 49.05 for CD_3OD, with coupling constants, *J*, in Hertz. Conventional pulse sequences were used for ^1H-^1H DQF-COSY, ^1H-^{13}C HSQC, and HMBC experiments (Kerbab et al., 2015). HPLC analyses were performed on a Platin Blue UHPLC system (KNAUER GmbH, Berlin, Germany) consisting of two Ultra High-Pressure Pumps, an autosampler, a column temperature manager and a diode array detector, coupled to a LTQ Orbitrap XL (Thermo Scientific, San Jose, CA) equipped with an electrospray ionization (ESI) probe. The data were acquired and processed with Xcalibur 2.7 software from Thermo Scientific. Chromatography was performed over Sephadex LH-20 (Pharmacia, Uppsala, Sweden). Thin-layer chromatography (TLC) analysis was performed with Macherey−Nagel precoated silica gel 60 F_{254} plates (Delchimica, Naples, Italy), and the spray reagent cerium sulfate (saturated solution in dilute H_2SO_4) and UV (254 and 366 nm) were used for the spot visualization. Semireparative HPLC separations were conducted on a Waters 590 series pumping system, equipped with a Waters R401 refractive index detector, a Rheodyne injector (100 µL loop), and Luna C_8 (250 x 10 mm i.d., 10 µm, Phenomenex, Inc.) and C_{18} Synergy Fusion–RP 4 µm 80A (250 x 10.0 mm, Phenomenex, Inc.) as columns.

B.III.1.3. Chestnut Spiny Burs (CSB) and Hazelnut skins materials (RHS)

CSB were collected in a chestnut plantation (Società Cooperativa Agricola "Castagne di Montella") in Montella (AV), Italy, during the chestnut (*Castanea sativa* Miller specie) collection in the middle of October 2016. CSB were air-dried till equilibrium humidity.

RHS samples were kindly supplied by an Italian hazelnut processing industry (Hazelnuts South Italy Manufacturing S.r.l., Baiano, Avellino, Italy). RHS is the waste of the daily industrial processing, consisting of two Campania varieties (90%

Mortarella and 10% Lunga San Giovanni). RHS material was finely blended using a knife mill Grindomix GM 200 (Retsch, Bergamo, Italy), at 8000 rpm, for 4 minutes.

B.III.1.4. Preparation of CSB

Dried CSB (1000 gr) were sequentially defatted with *n*-hexane and chloroform, and extracted (at 25°C) with methanol to give 71.7 g of residue (CSB-M). The extraction yield, gravimetrically determined (balance Denver Instruments-PK-201, max 2400 g d = 0.1 g; +15/30 °C), and expressed as the weight percentage of the dry matter compared to the total amount of the started powder, was 7.2 %, w/w. A portion of CSB-M was partitioned between *n*-butanol and water to obtain a *n*-BuOH-soluble portion (CSB-B). A sample (50 g) of dried CSB was extracted with 50% of aqueous ethanol (2500 mL) by homogenization with an Ultra-Turrax T-25 (IKA ULTRA-TURRAX T25 digital), at 10000 rpm, for 4 min. The homogenate was transferred in an orbital shaker with temperature control (45°C), and the shaking rate was set at 300 rpm for 30 minutes. The resulted extract was filtered through a sieve with pore size 45 μm. The solvent was evaporated by a Buchi R-210 rotavapor (Buchi Italia srl, Milan, Italy) for the alcoholic portion, and by lyophilizer (Alpha 1–2 LD freeze dryer, Martin Christ, Germany) for the aqueous one, to obtain a dry powder (CSB-H, extraction yield of 11.6 %, w/w). An aqueous extract was prepared boiling 2 g of dried CSB at 100°C for 10 min with 200 ml of distilled water. The mixture was left to stand at room temperature, for 5 min, then filtered through cheesecloth, and freeze-dried using a lyophilize to obtain the dried CSB-A extract (yield of 1.3 %, w/w).

B.III.1.5. Preparation of the RHS extract

A Dionex Accelerated Solvent Extractor (ASE) 200 System (Dionex, Sunnyvale, CA) equipped with a solvent controller unit, with 11 mL stainless steel cells (Restek, Italy) was used. One gram of RHS powder was placed into cells and homogenated with glass beads. The extraction was performed with the followed parameters: solvent 30% v/v ethanol, purge 100 sec, pressure 1500 psi, temperature 125°C, 5 cycle of extraction and static time of 5 minutes. The sample was flushed with 150% nitrogen. The organic solvent was removed under vacuum at 40°C by a rotary evaporator (Rotavapor R-200, Buchi Italia s.r.l, Cornaredo, Italy), while the aqueous part was lyophilized (freeze dryer Alpha 1-2 LD, Christ, Germany) to obtain the dried RHS-H extract. The extraction yield, determined gravimetrically (equilibrium Denver Instruments-PK-201, max 2400 gd = 0.1 g, +15/30 ° C) and expressed as a percentage of dry extract compared to the total amount of the initial powder, was 32% w/w.

B.III.1.6. Quantitative determination of Total Phenol Content (TPC) of CSB and RHS-H extracts

The TPC of CSB-M, CSB-H, CSB-A, and RHS-H was determined using the Folin-Ciocalteu colorimetric method (Esposito et al., 2017). Briefly, 50 µL of the sample was added to 500 µL of H_2O and 500 µL of Folin-Ciocalteau reagent. After 3 minutes 500 µL of Na_2CO3 (10%, w/v) was included. Finally, the absorbance of the samples was read after 1h, at 723 nm (Thermo Evolution 201 UV–visible spectrophotometer, Thermo Fisher Scientific Italia, Milan, Italy). The results were expressed as Gallic Acid Equivalents (GAE µmol/mg extract, means ± SD of three determinations) calculated by calibration curve ($y = 0.0294x - 0.0747$, $R^2 = 0.999$) derivateves **Table 13**.

B.III.1.7. Bleaching of the free-radical 1,1-Diphenyl-2-picrylhydrazyl (DPPH Test) of CSB and RHS-H.

The radical scavenging activities of CSB-M, CSB-H, CSB-A, CSB pure compounds, and RHS-H were assayed using the stable 1,1-diphenyl-2-picrylhydrazyl radical ($DPPH^{\bullet}$), according to reported procedures in Piccinelli et al., 2016. Briefly, 1.5 mL of $DPPH^{\bullet}$ solution (25 mg/mL in methanol, prepared daily) was added to 37.5 µL of various concentrations of CSB samples in MeOH, EtOH:H_2O 1:1, v/v, or H_2O solutions (ranged from 0.5 to 100 µg/mL), and RHS-H sample in EtOH:H_2O 30% (v/v) solution (ranged from 50 to 6.25 µg/mL). The mixtures were kept in the dark for 10 min at room temperature, and the decrease in absorbance was measured at 517 nm (Thermo Evolution 201 UV–visible spectrophotometer, Thermo Fisher Scientific Italia, Milan, Italy), against a blank consisting of an equal volume of solvent alone. Gallic acid was used as positive control. The $DPPH^{\bullet}$ concentration in the reaction medium was calculated from a calibration curve (range = 5-36 µg/mL), analyzed by linear regression (y = 0.0228x-0.0350, R^2 = 0.9999). EC_{50} (mean effective scavenging concentration) was determined as the concentration (in micrograms per milliliter) of sample necessary to decrease the initial $DPPH^{\bullet}$ concentration by 50%. All tests were performed in triplicate. A lower EC_{50} value indicates stronger antioxidant activity.

B.III.1.8. Trolox Equivalent Antioxidant Capacity (TEAC) assay of CSB derivatives

TEAC assay was performed according to the method of Re et al., 1999. The radical cation $ABTS^{\bullet+}$ was generated by mixing (1:1, v/v) $ABTS^{\bullet+}$ (7.0 mM) and potassium

persulfate (2.45 mM). The mixture was allowed to stand overnight at room temperature in the dark to form the radical $ABTS^{\bullet+}$, and it was used within 2 days. The radical working solution was prepared by diluting the stock solution with PBS (pH 7.4) to an absorbance of 0.70 ± 0.05 at 734 nm. 15 µL of extracts (0.000625-0.01 mg/mL) or compounds (0.0015-0.0075 mM) solutions were mixed with 1485 µL of $ABTS^{\bullet+}$ working solution. The decrease of absorbance was measured at 734 nm by a Thermo Evolution 201 UV–visible spectrophotometer (Thermo Fisher Scientific Italia, Milan, Italy), after 1 minute of incubation at room temperature, in reference to a blank (PBS without $ABTS^{\bullet+}$). The scavenging percentage of $ABTS^{\bullet+}$ was calculated relating to Trolox (a water-soluble analogue of vitamin E adopted as an antioxidant standard). Antioxidant activity was expressed as mmol Trolox equivalent (TE)/mg extract or mmol compound. A high TEAC value indicated a high level of antioxidant activity.

B.III.1.9. UHPLC-UV-ESI-HRMS analysis of CSB extracts

UHPLC separation was achieved with a Kinetex C_{18} (100 x 2.1 mm i.d., 2.6 µm) column protected by a C18 Guard Cartridge (2.1 mm i.d.), both from Phenomenex (Torrance, CA, USA) held at 30°C. The mobile phase consisted of water (A) and MeOH (B), both containing 0.1% HCOOH. The following elution gradient was used: 0-6 min, 5-20% B; 6-10 min, 20-35%, B; 10-15 min, 35-50% B; 15-22 min, 50-70% B; 22-27 min, 70-98% B. After each injection, the column was washed with 100% B for 4 min and re-equilibrated (5 min). A flow rate of 0.4 mL/min and an injection volume of 5 µL were used. Detection by diode array was performed at three wavelengths: 254, 278 and 330 nm and the UV spectra were recorded over a 200-600 nm range. The HRMS and HRMS/MS were performed with an ESI source operating in the ion negative mode. High-purity nitrogen (N_2) was used as both

drying gas and nebulizing gas, and ultra-high pure helium (He) as the collision gas. The operating parameters were optimized as follows: source voltage 3.5 kV, capillary voltage –72 V, tube lens voltage –41.4 V, capillary temperature 280ºC, sheath and auxiliary gas flow (N_2) 32 e 10 (arbitrary units), respectively. The MS profile was recorded in full scan mode (scan time = 1 micro scans and maximum inject time 500 ms) with resolving power of 60000. For the HRMS/MS acquisitions, a data-dependent method, setting the normalized collision energy in the ion trap of 35%, was used.

B.III.1.10. Quantitative HPLC Analysis of CSB extracts

The HPLC and detection by diode array equipment and conditions were the same used for qualitative analysis. The UV chromatograms were recorded at 254 and 278 nm for quantification of ellagic acid (EA) and chestanin, respectively. Calibration external standard method was used to quantify two compounds in CSB extracts (1 and 3 mg mL^{-1}). Mixtures of 2 reference standards at different concentrations (six levels in triplicate; EA range 1.5-50 μg/mL; chestanin range 25-400 μg/mL) were used to produce calibration curves. UV peak areas of the external standard (at each concentration) were plotted against the corresponding standard concentrations (μg/mL) using weighed linear regression to generate standard curves. For the linear regression of external standards, R^2 values were 0.9987 and 0.9993 for EA and chestanin, respectively. The amount of the compounds was finally expressed as micrograms per milligram of extracts. Data are reported in **Table 10** as mean standard deviation (SD) of triplicate determinations.

B.III.1.11. Isolation and Identification of CSB Compounds

A portion of CSB-B (2.0 g) was fractionated over a Sephadex LH-20 column (1 m × 3 cm i.d.) with MeOH as eluent at flow rate 1 mL/min. Fractions of 8 mL each were collected and combined in six major groups (**I-VI)** on their TLC analysis [(Si-gel, n-BuOH–AcOH–H2O (60:15:25)]. Fractions **I-V** were purified by RP-HPLC on a Luna C_8 column (flow rate 2.0 mL/min). Fraction **I** (100.1 mg) was chromatographed with the elution solvent MeOH/H_2O 6.5:3.5 v/v, giving compound (**36**) (1.3 mg, t_R = 15 min). Fraction **II** (152.8 mg) was separated using MeOH/H_2O 5.5:4.5 v/v as solvent system to obtain compounds (**29**) (3.3 mg, t_R = 9 min), (**31**) (1.1 mg, t_R = 10 min), and (**28**) (1.8 mg, t_R = 18 min. Fraction **III** (184.1 mg) was purified with MeOH/H_2O 5:5 v/v as solvent system and afforded compounds (**21**) (6.9 mg, t_R =9 min), (**20**) (3.1 mg, t_R = 11 min), (**25**) (3.7 mg, t_R = 12 min), (**30**) (1.2 mg, t_R = 14 min) and (**32**) (1.0 mg, t_R = 16 min). Fraction **IV** (200.4 mg) was separated using as solvent system MeOH/H_2O 2:8 v/v giving compounds (**21**) (3.9 mg, t_R = 10 min), (**17**) (3.7 mg, t_R = 14 min), and (**20**) (2.9 mg, t_R = 38 min). Fraction **V** (114.0 mg) was purified with a solvent system MeOH/H_2O 4:6 v/v and gave compounds (**21**) (6.4 mg, t_R = 14 min), and (**33**) (1.8 mg, t_R = 23 min). Finally, fraction **VI** (253.6 mg) was purified by RP-HPLC using MeOH/H_2O 3.5:6.5 v/v on a C_{18} Synergy Fusion column, (flow rate 1.8 mL/min) to obtain compounds (**11**) (2.2 mg, t_R = 12 min), (**9**) (11.5 mg, t_R = 14 min), and (**21**) (22.2 mg, t_R = 28 min).

The NMR data of all the isolated compounds corresponded to those reported in the literature (Tanaka et al., 1996; Ozawa et al., 1979; Feng et al., 1988; Jaramillo et al., 2011; Nasser et al., 2008; Ren et al., 2011; Benhamed et al., 2014; Merfort & Wendisch 1988). The ESI-MS data are reported in **Table 9**.

B.III.1.12. Antifungal activity

B.III.1.12.1. Fungal pathogens

The strains of the pathogens *Alternaria alternata*, *Botrytis cinerea* and *Fusarium solani* were taken from CREA-Pontecagnano (Salerno, Italy) collection, maintained at 20°C on PDA slant.

B.III.1.12.2. In vitro antifungal assays

The inhibitory effect of CSB-H CSB-M and CSB-A extracts on mycelial growth of *A. alternata*, *B. cinerea,* and *F. solani* was assayed using an amended plate technique (Badawy, & Abdelgaleil, 2014). Extracts were previously sterilized through 2-hours UV exposition (ƛ 254 nm). CSB-M was dissolved in DMSO, then poured in sterile 0.1× PDA, while CSB-H and CSB-A were directly dissolved into sterile 0.1× PDA until to obtain the final concentrations in the range 30-70 mg/mL to assay *B. cinerea*, and in the range 2.5-50 mg/mL to assess the susceptibility of the remaining two fungi. The final concentration of DMSO in the plates never exceed 2.5%. Not amended plates were used as control. A fungal plug (0.5 cm diameter) taken from the edge of a fresh culture, was transferred onto the centre of the plate. Plates were incubated in the dark at 25°C according to a randomized design. Each treatment was tested in triplicate and the experiment was conducted twice. The mycelial growth diameter was measured when fungus completely covered the control plates. The inhibition percentage of fungal growth was calculated as follows:

$$\text{Fungal growth inhibition (\%)} = 100 * [DC-DT/DC]$$

where DC and DT are the average diameters of fungal colony in the control and in the treated plates, respectively. The EC_{50} values were calculated by linear regression of Probit of the fungal inhibition percentage and the log of the extract concentrations (Badawy & Abdelgaleil, 2014). The EC_{50} was defined as the concentration required to inhibit fungal growth by 50% of the control.

B.III.1.12.3. Spore germination assay

In order to collect conidia of *A. alternata, F. solani,* and *B. cinerea*, each fungus was transferred onto PDA in Petri dishes (9 cm diameter) and incubated at 25°C for 7-10 d in darkness. The sporulated plates were then flooded with sterile distilled water and gently rubbed with a sterile bent plastic rod to release conidia. Conidia suspensions were filtered on synthetic filtering wool to remove mycelia fragments, then concentration was determined using a Burker chamber and adjusted to 1×10^6 conidia mL^{-1} by dilution (Pane et al., 2016). To assay the effects of CSB and pure compounds on fungal conidia germination, a 0.1× PDB microculture method was used. The stock solutions of CSB-M, EA (pure compound), and commercial fungicides (iprodione and carbendazim) were prepared in DMSO. The extracts CSB-H and CSB-A were dissolved directly into PDB, while chestanin (pure compound) was solubilized into water. Aliquots of spore suspension (10 µL, 10^6 spores/mL) were pipetted in 1.5 mL-tubes containing final concentration 0.1×PDB supplemented with extract, pure compound or commercial fungicide solutions (final volume 100 µL). Extracts were assayed at concentrations ranging between 10-50 mg/mL, 15-50 mg/mL and 5-30 mg/mL, for *A. alternata*, *B. cinerea* and *F. solani*, respectively. While, pure compounds were used at concentrations included in the range 0.005-1 mg/mL in *A. alternata* experiments and 0.010-2 mg/mL with the other two fungi. The commercial fungicides dissolved into DMSO were used as positive controls and tested at concentration of 0.00025-0.25 mg/mL, while DMSO

(2.5%) and not-amended cultures were used as negative controls. Treatments were three-replicated. Tubes were incubated at 25°C for 24 h according to a complete randomized design. After that, the samples were observed under the light microscope (Leitz, Wetzlar, Germany) (40× magnification) to examine the occurrence of germination. A spore was considered germinated when the length of the germ tube equaled or exceeded the length of the spore. At least 100 spores of each replicate were observed, then the percentage of the spore germination inhibition was calculated as follows:

$$\text{Spore Germination inhibition (\%)} = 100 * [\%\ GC_{sample} - \%GC_{control} / \%\ GC_{sample}]$$

where GC sample and GC control are average percentage of germinated conidia of treatment and control (only vehicle), respectively. The experiment was repeated. The EC_{50} values were determined as the extract concentration inhibiting germination at 50% of the untreated control.

B.III.2.1. Preparation of films

Films were prepared by Casting technique using the method reported by Silva et al., 2018, with some modifications. 6% w/v of pullulan (PL) was dispersed in a glycerol (Gly) aqueous solution (10% w/v) and left under mechanical stirring 12 h, at room temperature. Afterwards, 1, 5 and 10% of RHS or CSB-H (w/w, based on pullulan weight) was added to the polysaccharide solutions and mixed overnight at 25°C, to improve extract dissolution. The resulting suspensions were put in acrylic plates (5x5 cm^2) as molds, and dried at 30°C in a ventilated oven overnight. The obtained films were removed from the molds and stored in desiccators until their

use. The films without extract were used as control. All films were prepared in triplicate.

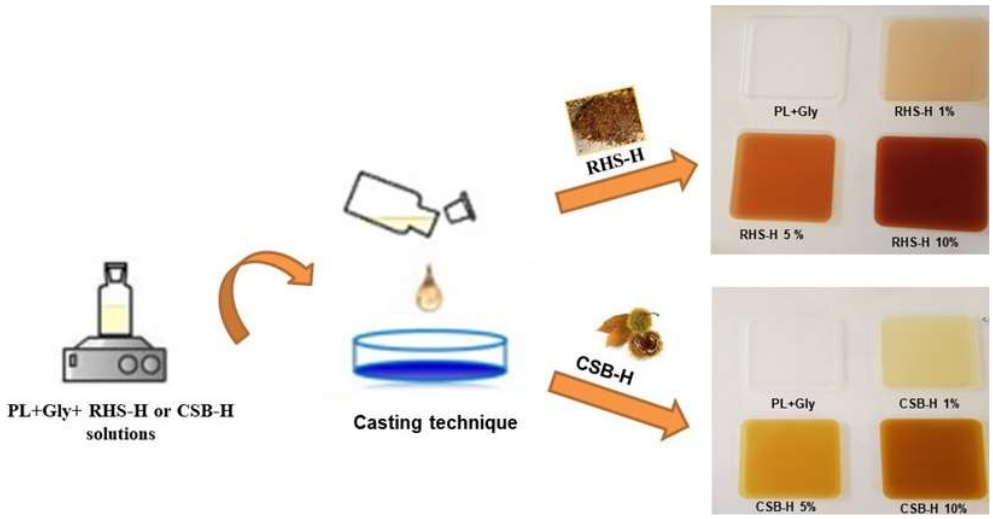

Figure 47. Films preparation by Casting technique

B.III.2.2. Film characterization

B.III.2.2.1. Optical properties: internal transmittance

The barrier properties of the films were evaluated in ultraviolet (UV) and visible range, between 200-700 nm, using a Shimadzu UV-1800 UV e Vis spectrophotometer (Shimadzu Corp., Kyoto, Japan) equipped with a quartz window plate with 10 mm diameter, bearing the holder in the vertical position. Spectra were recorded at room temperature, in steps of 1 nm. Films of 50 × 10 mm^2, previously conditioned in the desiccator at 25°C for 48h, were used directly in spectrophotometer test cell and three measurements were performed.

B.III.2.2.2. Thickness Analysis

A hand-held digital micrometer (Mitutoyo, Mitutoyo Corporation, Japan) was used to measured films thickness, with an accuracy of 0.001 mm. All measurements were randomly performed at 3 different positions of rectangular film strips (50 x 10 mm^2) and the average value was calculated.

Figure 48. Digital micrometer Mitutoyo

B.III.2.2.3. Mechanical properties

Tensile strength, Young's modulus, and Elongation at break were calculated using an Instron 5966 Series machine (Instron Corporation, USA), at a cross-head velocity of 10 mm min^{-1}, and using a static load cell of 500 N, under ambient conditions (**Figures 49 a** and **b)**. Five rectangular strips (50 x 10 mm^2), previously stored in desiccator for 48h, were used for each film sample and the average value was considered. The test consists in subjecting the rectangular strip to a tensile force along its axis, with a controlled deformation speed, up to the breaking. Films properties were evaluated (**Figure 50**) studying the three tensile parameter, calculated from stress-strain curve by Bluehill 3 material testing software.

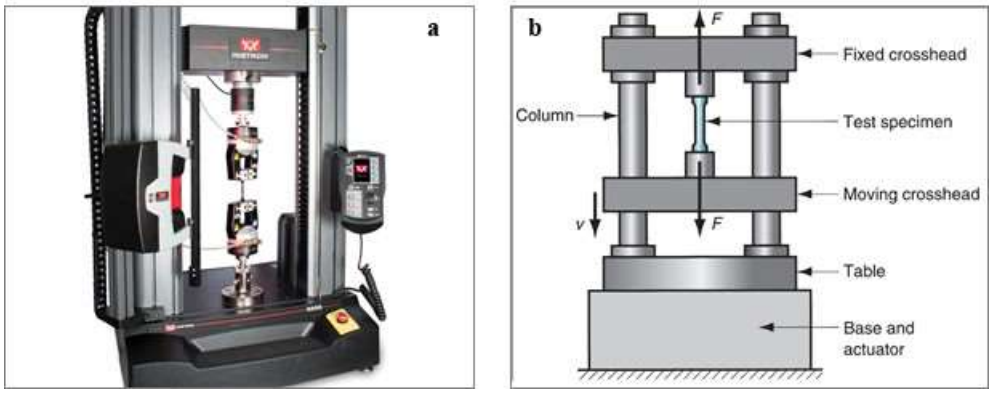

Figures 49. (a) Instron 5966 Series machine and (**b**) operating mechanism

Young's modulus (E) can be used to predict the elasticity of materials and it is calculated by drawing a tangent to the initial linear portion of the stress strain curve, and dividing the tensile stress and tensile stress. The result is expressed in gigapascals (GPa). The tensile strength (TS) is the maximum tensile stress recorded during elongation of the testing piece till breaking moment, and it is calculated by dividing the load at break by the original minimum cross sectional area. The result is expressed in megapascals (MPa). The Elongation at break (EB) is the strain at which the sample breaks when tested in tension. A higher percentage usually indicates a better quality material when combined with a good Tensile Strength (Anderson Simsek, 2019).

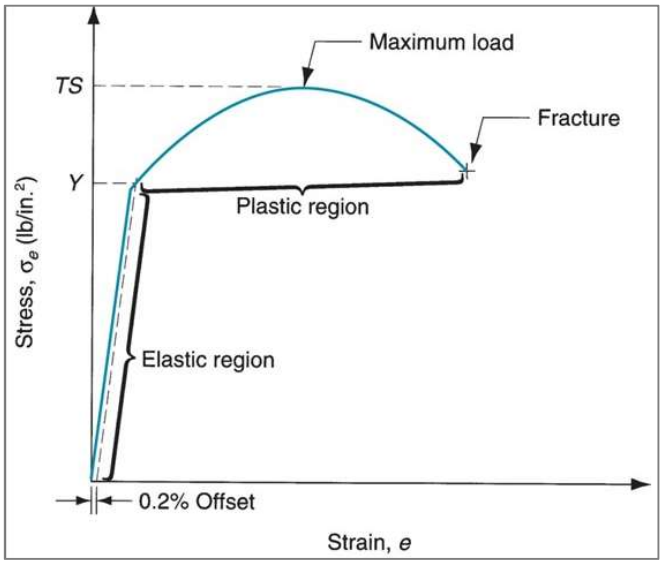

Figure 50. Typical Stress-Strain Plot

B.III.2.2.4. FTIR-ATR analysis

The FTIR-ATR spectra were performed with a Perkin-Elmer Spectrum BX FTIR spectrophotometer (Perkin-Elmer Inc., USA) equipped with a single horizontal Golden Gate ATR cell, in the range from 600 to 4000 cm^{-1}, with a resolution of 4 cm^{-1}, collected from 16 scans.

B.III.2.4. Antioxidant Activity

The free radical scavenging efficacy of the films was evaluated by DPPH test, according to Silva et al., 2018, with some modifications. A methanolic solution 0.2 mM of DPPH was prepared daily and left under magnetic stirring, in the dark, for 2 h. The films loaded with RHS-H and CSB-H at 1, 5 and 10% were cut (1x1 cm^2), immersed in 2 mL of distilled water, and mixed 5' with vortex, to improve the dissolution of films and extracts (**Figure 51**). Afterwards, 2 mL of methanol and

0.250 mL of the DPPH solution were added to the solutions, homogeneously mixed, and left in the dark, at 25°C, for 30' (when the steady state of reaction was achieved). After the incubation period, the suspensions were centrifuged at 5000 rpm for 5 minutes, at 20°C, and the absorbance of the supernatant was read at 517 nm, using a Shimadzu UV-1800 spectrophotometer. The free radical scavenging activity of the films containing RHS-H and CSB-H were compared with blank films and with the raw extract tested from 0.05 to 0.5 mg/mL (corresponding to 1, 5 and 10% added into the films).

The Radical Scavenging Activity (RSA) was measured as follows

$$\%RSA=100\ (A_0-A_s)/\ A_0,$$

where A_0 is the absorbance of vehicle and A_s is the absorbance of the samples.

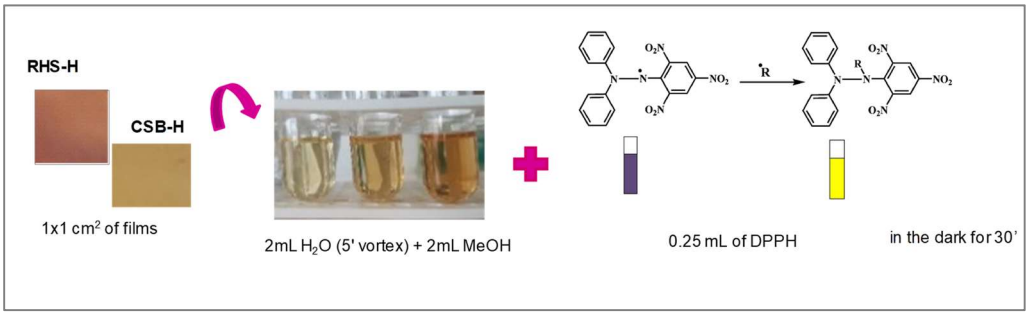

Figure 51. DPPH protocol to evaluate antioxidant activity of films

B.III.2.5. Antibacterial activity

The antimicrobial activities of films were tested against *S. aureus* and *E. coli.* For CSB-H was texted only the film containing 10% of extract, while for RHS-H all the films prepared. The data were compared with raw extracts evaluated in the same concentrations used in the films, blank films (PL and PL-Gly) and control (only bacteria in the medium). The strains were stored at -80°C, and before each

experiment, *S. aureus* was grown in 30 mL of Luria Bertani medium (Liofilchem, Italy), while *E. coli* in 30 mL of Tryptic Soy Broth (Liofilchem, Italy), for 24 h, at 37ºC, at 120 r.p.m. In order to obtain a concentration of 10^8 Colony Forming Unit per mL (CFU mL^{-1}), 100 µL of *S. aureus* suspension and 300 µL of *E. coli* culture were transferred in 30 mL of fresh medium, and grown for 10 h and 18h, respectively, at 37°C, at 120 rpm. Both bacterial cultures were ten-fold diluted in the corresponding growth medium to obtain a finally concentration of 10^6 CFU. Films samples (5x5 cm^2) and raw extracts were placed in contact with bacterial suspension (10 mL for RHS-H and 4 mL for CSB-H samples), previously distributed in sterilized glass beakers, under stirring (120 rpm), and protected from light with aluminum foil. At 0, 2, 6 and 12 h 100 µL of each sample were serially diluted in PBS (pH 7.4) and plated in duplicate in Tryptic Soy Agar medium. The petri plates were incubated for 24 h at 37ºC. Three independent experiments were performed.

B.III.3. Statistical analysis

The free radical scavenging, TPC data and results reported in section B part II were subjected to one-way analysis of variance (ANOVA), followed by Tukey HSD test ($p \leq 0.05$), using GraphPad Prism version 7.00 for Windows. The Log-Dose-Response curves allowed determination of EC_{50} values for the fungal bioassay, according to the Probit analysis. The 95% confidence limits for the range of EC_{50} values were determined, and they were considered to be significantly different, if the 95% confidence limits did not overlap. The Chi-square test was performed to compare observed with expected dose-response dataset and the resulting *p* level (> 0.05), associated to each EC_{50} value, indicates the goodness of fit between the distributions (Badawy and Abdelgaleil, 2014).

GENERAL CONCLUSION

This PhD project involved the production of three polar extracts, resulted rich in polyphenols, obtained from waste and by-products recovered from wastes/by-products from Campania agro-industries. Specifically, a polar extract was produced from hazelnut shells (HSE), which showed a cytotoxic against three tumor cell lines. The spray drying technique was employed to convert the raw HSE into a stable, easy handling, functional microparticles powder suitable to be enclosed in a topical or oral dosage forms. Instead, the hydroalcoholic extracts obtained from Chestnut Spiny Burs (CSB-H) and Roasted Hazelnut Skins (RHS-H), displaying a good antioxidant and antifungal activity, were successfully used as active ingredients in the production of film prototypes with antimicrobial and antioxidant efficacy to improve food preservation. The conducted study supports the exploitation and the reuse of waste and by-products as a resource for the development of new active ingredients or products useful for human or food purposes.

REFERENCES

Akhtar, M. J., Jacquot, M., Jasniewski, J., Jacquot, C., Imran, M., Jamshidian, M., Paris, C. & Desobry, S. (2012). Antioxidant capacity and light-aging study of HPMC films functionalized with natural plant extract. Carbohydrate polymers, 89(4), 1150-1158.

Alañón, M. E., Alarcón, M., Marchante, L., Díaz-Maroto, M. C., & Pérez-Coello, M. S. (2017). Extraction of natural flavorings with antioxidant capacity from cooperage by-products by green extraction procedure with subcritical fluids. Industrial Crops and Products, 103, 222-232.

Alasalvar, C., Karamać, M., Kosinska, A., Rybarczyk, A., Shahidi, F., & Amarowicz, R. (2009). Antioxidant activity of hazelnut skin phenolics. Journal of Agricultural and Food Chemistry, 57(11), 4645-4650.

Ameer, K., Shahbaz, H. M., & Kwon, J. H. (2017). Green extraction methods for polyphenols from plant matrices and their byproducts: A review. Comprehensive Reviews in Food Science and Food Safety, 16(2), 295-315.

Anderson, C., & Simsek, S. (2019). Mechanical profiles and topographical properties of films made from alkaline extracted arabinoxylans from wheat bran, maize bran, or dried distillers grain. Food Hydrocolloids, 86, 78-86.

Aparicio-Fernández, X., García-Gasca, T., Yousef, G. G., Lila, M. A., González de Mejia, E., & Loarca-Pina, G. (2006). Chemopreventive activity of polyphenolics from black Jamapa bean (*Phaseolus vulgaris* L.) on HeLa and HaCaT cells. Journal of agricultural and food chemistry, 54(6), 2116-2122.

Aparicio-Fernández, X., Vega-Ahuatzin, A., Ochoa-Velasco, C. E., Cid-Pérez, S., Hernández-Carranza, P., & Ávila-Sosa, R. (2018). Physical and Antioxidant Characterization of Edible Films Added with Red Prickly Pear (*Opuntia ficus-indica* L.) cv. San Martín Peel and/or Its Aqueous Extracts. Food and Bioprocess Technology, 11(2), 368-379.

Augustin, M. A., & Hemar, Y. (2009). Nano-and micro-structured assemblies for encapsulation of food ingredients. Chemical society reviews, 38(4), 902-912.

Augustin, M. A., Sanguansri, L., & Lockett, T. (2013). Nano-and micro-encapsulated systems for enhancing the delivery of resveratrol. Annals of the New York Academy of Sciences, 1290(1), 107-112.

Badawy, M. E., & Abdelgaleil, S. A. (2014). Composition and antimicrobial activity of essential oils isolated from Egyptian plants against plant pathogenic bacteria and fungi. Industrial Crops and Products, 52, 776-782.

Balboa, E. M., Soto, M. L., Nogueira, D. R., González-López, N., Conde, E., Moure, A., Vinardell M. P., Mitjans, M. & Domínguez, H. (2014). Potential of antioxidant extracts produced by aqueous processing of renewable resources for the formulation of cosmetics. Industrial Crops and Products, 58, 104-110.

Barros, L., Alves, C. T., Dueñas, M., Silva, S., Oliveira, R., Carvalho, A. M., Henriques, M.; Santos-buelga, C.; & Ferreira, I. C. (2013). Characterization of phenolic compounds in wild medicinal flowers from Portugal by HPLC–DAD–ESI/MS and evaluation of antifungal properties. Industrial Crops and Products, 44, 104-110.

Basiak, E., Lenart, A., & Debeaufort, F. (2018). How Glycerol and Water Contents Affect the Structural and Functional Properties of Starch-Based Edible Films. Polymers, 10(4), 412.

Benahmed, M., Akkal, S., Elomri, A., Laouer, H., Vérité, P., & Seguin, E. (2014). Constituents from Bupleurum montanum (Coss. & Dur.)(Apiaceae). Arabian Journal of Chemistry, 7(6), 1065-1069.

Benbettaïeb, N., Debeaufort, F., & Karbowiak, T. (2018). Bioactive edible films for food applications: mechanisms of antimicrobial and antioxidant activity. Critical reviews in food science and nutrition, 1-25.

Beneke, C., Viljoen, A., & Hamman, J. (2009). Polymeric plant-derived excipients in drug delivery. Molecules, 14(7), 2602-2620.

Benyounes, K., Remli, S., & Benmounah, A. (2018, June). Rheological behavior of Hydroxyethylcellulose (HEC) Solutions. In Journal of Physics: Conference Series (Vol. 1045, No. 1, p. 012008). IOP Publishing.

Bettiol, F., & Cecchi, M. (2013). Manuale delle preparazioni cosmetiche e dermatologiche: teoria, pratica e normativa aggiornata al nuovo Regolamento CE. Tecniche nuove.

Blanco-Pascual, N., & Gómez-Estaca, J. (2016). Production and processing of edible packaging. Edible Food Packaging: Materials and Processing Technologies, 36, 153.

Bodini, R. B., Sobral, P. J. A., Favaro-Trindade, C. S., & Carvalho, R. A. (2013). Properties of gelatin-based films with added ethanol–propolis extract. LWT-Food Science and Technology, 51(1), 104-110.

Boopathi, K., & Ramasamy, P. (2015). Synthesis, growth and characterization of a new metal–organic NLO material: Dibromo bis (l-proline) Cd (II). Journal of Molecular Structure, 1080, 37-43.

Bouarab Chibane, L., Degraeve, P., Ferhout, H., Bouajila, J., & Oulahal, N. (2018). Plant antimicrobial polyphenols as potential natural food preservatives. Journal of the Science of Food and Agriculture.

Braga, N., Rodrigues, F., & PP Oliveira, M. B. (2015). *Castanea sativa* by-products: a review on added value and sustainable application. Natural product research, 29(1), 1-18.

Brejnholt, S. M. (2009). Pectin. Food Stabilisers, Thickeners and Gelling Agents, Wiley-Blackwell: 237-265.

Bustos, M. C., Rocha-Parra, D., Sampedro, I., de Pascual-Teresa, S., & León, A. E. (2018). The Influence of Different Air-Drying Conditions on Bioactive Compounds and Antioxidant Activity of Berries. Journal of agricultural and food chemistry, 66(11), 2714-2723

Cal, K., & Sollohub, K. (2010). Spray drying technique. I: Hardware and process parameters. Journal of pharmaceutical sciences, 99(2), 575-586.

Cao, L., Liu, W., & Wang, L. (2018). Developing a green and edible film from Cassia gum: The effects of glycerol and sorbitol. Journal of Cleaner Production, 175, 276-282.

Cao, N., Fu, Y., & He, J. (2007). Mechanical properties of gelatin films cross-linked, respectively, by ferulic acid and tannin acid. Food Hydrocolloids, 21(4), 575-584.

Carpinella, M. C., Giorda, L. M., Ferrayoli, C. G., & Palacios, S. M. (2003). Antifungal effects of different organic extracts from *Melia azedarach* L. on phytopathogenic fungi and their isolated active components. Journal of Agricultural and Food Chemistry, 51(9), 2506-2511.

Castejón, N., Luna, P., & Señoráns, F. J. (2018). Alternative oil extraction methods from Echium plantagineum L. seeds using advanced techniques and green solvents. Food chemistry, 244, 75-82.

Castro-Muñoz, R., Yanez-Fernandez, J., & Fila, V. (2016). Phenolic compounds recovered from agro-food by-products using membrane technologies: an overview. Food chemistry, 213, 753-762.

Cazon, P., Velazquez, G., Ramírez, J. A., & Vázquez, M. (2017). Polysaccharide-based films and coatings for food packaging: A review. Food Hydrocolloids, 68, 136-148.

Cazón, P., Velazquez, G., Ramírez, J. A., & Vázquez, M. (2017). Polysaccharide-based films and coatings for food packaging: A review. Food Hydrocolloids, 68, 136-148.

Chaitanya, G. V., Alexander, J. S., & Babu, P. P. (2010). PARP-1 cleavage fragments: signatures of cell-death proteases in neurodegeneration. Cell Communication and Signaling, 8(1), 31.

Chang, Y. X., Yang, J. J., Pan, R. L., Chang, Q., & Liao, Y. H. (2014). Anti-hygroscopic effect of leucine on spray-dried herbal extract powders. Powder Technology, 266, 388-395.

Chatzidaki, M. D., Mitsou, E., Yaghmur, A., Xenakis, A., & Papadimitriou, V. (2015). Formulation and characterization of food-grade microemulsions as carriers of natural phenolic antioxidants. Colloids and Surfaces A: Physicochemical and Engineering Aspects, 483, 130-136.

Chen, J., Shen, Y., Chen, C., & Wan, C. (2019). Inhibition of Key Citrus Postharvest Fungal Strains by Plant Extracts In Vitro and In Vivo: A Review. Plants, 8(2), 26.

Chung, C. P., Hsu, C. Y., Lin, J. H., Kuo, Y. H., Chiang, W., & Lin, Y. L. (2011). Antiproliferative lactams and spiroenone from adlay bran in human breast cancer cell lines. Journal of agricultural and food chemistry, 59(4), 1185-1194.

Ciarmiello, L. F., Mazzeo, M. F., Minasi, P., Peluso, A., De Luca, A., Piccirillo, P., Siciliano, R. A., Carbone, V., 2014. Analysis of Different European Hazelnut (*Corylus avellana* L.) Cultivars: Authentication, Phenotypic Features, and Phenolic Profiles. J. Agric. Food Chem. 62, 6236–6246

Ciemniewska-Żytkiewicz, H., Verardo, V., Pasini, F., Bryś, J., Koczoń, P., & Caboni, M. F. (2015). Determination of lipid and phenolic fraction in two

hazelnut (*Corylus avellana* L.) cultivars grown in Poland. Food chemistry, 168, 615-622.

Contini, M., Baccelloni, S., Massantini, R., & Anelli, G. (2008). Extraction of natural antioxidants from hazelnut (*Corylus avellana* L.) shell and skin wastes by long maceration at room temperature. Food Chemistry, 110(3), 659-669.

Crestini, C., Caponi, M. C., Argyropoulos, D. S., & Saladino, R. (2006). Immobilized methyltrioxo rhenium (MTO)/H_2O_2 systems for the oxidation of lignin and lignin model compounds. Bioorganic & medicinal chemistry, 14(15), 5292-5302.

Daglia, M. (2012). Polyphenols as antimicrobial agents. Current opinion in biotechnology, 23(2), 174-181.

Dai, J., & Mumper, R. J. (2010). Plant phenolics: extraction, analysis and their antioxidant and anticancer properties. Molecules, 15(10), 7313-7352.

De Cicco, F., Porta, A., Sansone, F., Aquino, R. P., & Del Gaudio, P. (2014). Nanospray technology for an in situ gelling nanoparticulate powder as a wound dressing. International journal of pharmaceutics, 473(1-2), 30-37.

De Corato, U. (2019). Improving the shelf-life and quality of fresh and minimally-processed fruits and vegetables for a modern food industry: A comprehensive critical review from the traditional technologies into the most promising advancements. Critical reviews in food science and nutrition, 1-36.

Delgado, T., Malheiro, R., Pereira, J. A., & Ramalhosa, E. (2010). Hazelnut (*Corylus avellana* L.) kernels as a source of antioxidants and their potential in relation to other nuts. Industrial Crops and Products, 32(3), 621-626.

Demirbas, A. (2011). Waste management, waste resource facilities and waste conversion processes. Energy Conversion and Management, 52(2), 1280-1287.

Di Domenico, F., Foppoli, C., Coccia, R., & Perluigi, M. (2012). Antioxidants in cervical cancer: chemopreventive and chemotherapeutic effects of polyphenols. Biochimica et Biophysica Acta (BBA)-Molecular Basis of Disease, 1822(5), 737-747.

Diab, T., Biliaderis, C. G., Gerasopoulos, D., & Sfakiotakis, E. (2001). Physicochemical properties and application of pullulan edible films and coatings in fruit preservation. Journal of the Science of Food and Agriculture, 81(10), 988-1000

Diamantopoulos, P. T., Sofotasiou, M., Papadopoulou, V., Polonyfi, K., Iliakis, T., & Viniou, N. A. (2014). PARP1-driven apoptosis in chronic lymphocytic leukemia. BioMed research international, 2014.

Domínguez, R., Barba, F. J., Gómez, B., Putnik, P., Kovačević, D. B., Pateiro, M., Santos, E. M., & Lorenzo, J. M. (2018). Active packaging films with natural antioxidants to be used in meat industry: A review. Food Research International, 113, 93-101.

Đorđević, V., Balanč, B., Belščak-Cvitanović, A., Lević, S., Trifković, K., Kalušević, A., Kostić, I., Komes, D., Bugarski, B., & Nedović, V. (2015). Trends in encapsulation technologies for delivery of food bioactive compounds. Food Engineering Reviews, 7(4), 452-490.

Dreyer, H. C., Dukovska-Popovska, I., Yu, Q., & Hedenstierna, C. P. (2019). A ranking method for prioritising retail store food waste based on monetary and environmental impacts. Journal of Cleaner Production, 210, 505-517.

Ersus, S., & Yurdagel, U. (2007). Microencapsulation of anthocyanin pigments of black carrot (*Daucus carota* L.) by spray drier. Journal of Food Engineering, 80(3), 805-812.

Espitia, P. J. P., Du, W. X., de Jesús Avena-Bustillos, R., Soares, N. D. F. F., & McHugh, T. H. (2014). Edible films from pectin: Physical-mechanical and antimicrobial properties-A review. Food hydrocolloids, 35, 287-296.

Esposito, T., Celano, R., Pane, C., Piccinelli, A. L., Sansone, F., Picerno, P., Zaccardelli, M., & Mencherini, T. (2019). Chestnut (*Castanea sativa* Miller.) Burs Extracts and Functional Compounds: UHPLC-UV-HRMS Profiling, Antioxidant Activity, and Inhibitory Effects on Phytopathogenic Fungi. Molecules, 24(2), 302.

Esposito, T., Sansone, F., Franceschelli, S., Del Gaudio, P., Picerno, P., Aquino, R. P., & Mencherini, T. (2017). Hazelnut (*Corylus avellana* L.) shells extract: phenolic composition, antioxidant effect and cytotoxic activity on human cancer cell lines. International journal of molecular sciences, 18(2), 392.

Farris, S., Unalan, I. U., Introzzi, L., Fuentes-Alventosa, J. M., & Cozzolino, C. A. (2014). Pullulan-based films and coatings for food packaging: Present applications, emerging opportunities, and future challenges. Journal of Applied Polymer Science, 131(13).

Feng, H., Nonaka, G. I., & Nishioka, I. (1988). Hydrolysable tannins and related compounds from *Castanea mollissima*. Phytochemistry, 27(4), 1185-1189.

Fernandes, S. C., Sadocco, P., Causio, J., Silvestre, A. J., Mondragon, I., & Freire, C. S. (2014). Antimicrobial pullulan derivative prepared by grafting with 3-aminopropyltrimethoxysilane: Characterization and ability to form transparent films. Food hydrocolloids, 35, 247-252.

Fernández-Agulló, A., Freire, M. S., Antorrena, G., Pereira, J. A., & González-Álvarez, J. (2014). Effect of the extraction technique and operational

conditions on the recovery of bioactive compounds from chestnut (*Castanea sativa*) bur and shell. Separation Science and Technology, 49(2), 267-277.

Galanakis, C. M. (2012). Recovery of high added-value components from food wastes: conventional, emerging technologies and commercialized applications. Trends in Food Science & Technology, 26(2), 68-87.

Galanakis, C. M. (2013). Emerging technologies for the production of nutraceuticals from agricultural by-products: a viewpoint of opportunities and challenges. Food and Bioproducts Processing, 91(4), 575-579.

Gallagher, P. G., Bao, Y., Prorock, A., Zigrino, P., Nischt, R., Politi, V., Mauch, C., Dragulev, B., & Fox, J. W. (2005). Gene expression profiling reveals cross-talk between melanoma and fibroblasts: implications for host-tumor interactions in metastasis. Cancer research, 65(10), 4134-4146.

Gallo, L., Ramírez-Rigo, M. V., Wilson, E., Piña, J., Allemandi, D., & Bucalá, V. (2013). Spray-Dried Cascara Sagrada extract for direct compression: tablet formulation and a simple HPLC method for tablet performance evaluation. Int J Res Pharm Biomed. Sci, 4, 1360-1370.

Ganesan, A. R., Shanmugam, M., & Bhat, R. (2018). Producing novel edible films from semi refined carrageenan (SRC) and ulvan polysaccharides for potential food applications. International journal of biological macromolecules, 112, 1164-1170.

Ganesan, K., & Xu, B. (2017). A critical review on polyphenols and health benefits of black soybeans. Nutrients, 9(5), 455.

Ganiari, S., Choulitoudi, E., & Oreopoulou, V. (2017). Edible and active films and coatings as carriers of natural antioxidants for lipid food. Trends in food science & technology, 68, 70-82.

García-Villalba, R., Espín, J. C., Tomás-Barberán, F. A., & Rocha-Guzmán, N. E. (2017). Comprehensive characterization by LC-DAD-MS/MS of the

phenolic composition of seven Quercus leaf teas. Journal of Food Composition and Analysis, 63, 38-46.

Gatto, M. A., Ippolito, A., Linsalata, V., Cascarano, N. A., Nigro, F., Vanadia, S., & Di Venere, D. (2011). Activity of extracts from wild edible herbs against postharvest fungal diseases of fruit and vegetables. Postharvest Biology and Technology, 61(1), 72-82.

Gheribi, R., Puchot, L., Verge, P., Jaoued-Grayaa, N., Mezni, M., Habibi, Y., & Khwaldia, K. (2018). Development of plasticized edible films from *Opuntia ficus-indica* mucilage: A comparative study of various polyol plasticizers. Carbohydrate polymers, 190, 204-211.

Giampieri, F., Quiles, J. L., Orantes-Bermejo, F. J., Gasparrini, M., Forbes-Hernandez, T. Y., Sánchez-González, C., Llopis, J., Rivas-García, L., Afrina, S., Varela-López, A., Cianciosi, D., Reboredo-Rodrigueza, P., Torres Fernández-Piñarc, C., Iglesiase, R. C., Ruize, R., Aparicio, S., Crespo, J., Lopez, L. D., Xiaog, J., Battino, M., & Cianciosi, D. (2018). Are by-products from beeswax recycling process a new promising source of bioactive compounds with biomedical properties? Food and Chemical Toxicology, 112, 126-133.

Gimbun, J., Nguang, S. L., Pang, S. F., Yeong, Y. L., Kee, K. L., & Chin, S. C. (2018). Assessment of phenolic compounds stability and retention during spray drying of Phyllanthus niruri extracts. Industrial & Engineering Chemistry Research.

Giménez, B., de Lacey, A. L., Pérez-Santín, E., López-Caballero, M. E., & Montero, P. (2013). Release of active compounds from agar and agar–gelatin films with green tea extract. Food Hydrocolloids, 30(1), 264-271.

Gómez-Guillén, M. C., Pérez-Mateos, M., Gómez-Estaca, J., López-Caballero, E., Giménez, B., & Montero, P. (2009). Fish gelatin: a renewable material for

developing active biodegradable films. Trends in Food Science & Technology, 20(1), 3-16.

Gore, P. M., Zachariah, S., Gupta, P., & Balasubramanian, K. (2016). Multifunctional nano-engineered and bio-mimicking smart superhydrophobic reticulated ABS/fumed silica composite thin films with heat-sinking applications. RSC Advances, 6(107), 105180-105191.

Gu, L., Kelm, M. A., Hammerstone, J. F., Zhang, Z., Beecher, G., Holden, J., & Prior, R. L. (2003). Liquid chromatographic/electrospray ionization mass spectrometric studies of proanthocyanidins in foods. Journal of Mass Spectrometry, 38(12), 1272-1280.

Han, J. H. (2014). Edible films and coatings: a review. In Innovations in Food Packaging (Second Edition) (pp. 213-255).

Hanani, Z. N., Yee, F. C., & Nor-Khaizura, M. A. R. (2019). Effect of pomegranate (*Punica granatum* L.) peel powder on the antioxidant and antimicrobial properties of fish gelatin films as active packaging. Food Hydrocolloids, 89, 253-259.

Haruna, M., Koube, T., Ito, K., & Murata, H. (1982). Balanophonin, a new neo-lignan from Balanophora japonica Makino. Chemical and Pharmaceutical Bulletin, 30(4), 1525-1527.

Hassan, B., Chatha, S. A. S., Hussain, A. I., Zia, K. M., & Akhtar, N. (2018). Recent advances on polysaccharides, lipids and protein based edible films and coatings: A review. International journal of biological macromolecules, 109, 1095-1107.

Horodytska, O., Valdés, F. J., & Fullana, A. (2018). Plastic flexible films waste management–a state of art review. Waste management.

Huang, X. X., Zhou, C. C., Li, L. Z., Peng, Y., Lou, L. L., Liu, S., Li, D. M., Ikejima, T. & Song, S. J. (2013). Cytotoxic and antioxidant dihydrobenzofuran

neolignans from the seeds of *Crataegus pinnatifida*. Fitoterapia, 91, 217-223.

Huang, Y. H., Zeng, W. M., Li, G. Y., Liu, G. Q., Zhao, D. D., Wang, J., & Zhang, Y. L. (2014). Characterization of a new sesquiterpene and antifungal activities of chemical constituents from *Dryopteris fragrans* (L.) Schott. Molecules, 19(1), 507-513.

Hyung, W., Kim, Y., Chung, C. H., & Haam, S. (2008). Drowning-out crystallization of l-proline: Effect of anti-solvent composition and processing parameters on crystal size and shape. Powder Technology, 186(2), 137-144.

ICH Topic Q 1 A (R2) Note for Guidance on Stability Testing: Stability Testing of new Drug Substances and Products, (CPMP/ICH/2736/99) European Medicines Agency 2003

Iyer, R., Hegde, S., Zhang, Y. E., Dinunzio, J., Singhal, D., Malick, A., & Amidon, G. (2013). The impact of hot melt extrusion and spray drying on mechanical properties and tableting indices of materials used in pharmaceutical development. Journal of pharmaceutical sciences, 102(10), 3604-3613.

Jaramillo, C. M., Gutiérrez, T. J., Goyanes, S., Bernal, C., & Famá, L. (2016). Biodegradability and plasticizing effect of yerba mate extract on cassava starch edible films. Carbohydrate polymers, 151, 150-159.

Jaramillo, K., Dawid, C., Hofmann, T., Fujimoto, Y., & Osorio, C. (2011). Identification of antioxidative flavonols and anthocyanins in Sicana odorifera fruit peel. Journal of agricultural and food chemistry, 59(3), 975-983.

Jiménez, A., Requena, R., Vargas, M., Atarés, L., & Chiralt, A. (2018). Food Hydrocolloids as Matrices for Edible Packaging Applications. In Role of Materials Science in Food Bioengineering (pp. 263-299).

Jin, Q., Yang, L., Poe, N., & Huang, H. (2018). Integrated processing of plant-derived waste to produce value-added products based on the biorefinery concept. Trends in food science & technology.

Jyothi, N. V. N., Prasanna, P. M., Sakarkar, S. N., Prabha, K. S., Ramaiah, P. S., & Srawan, G. Y. (2010). Microencapsulation techniques, factors influencing encapsulation efficiency. Journal of microencapsulation, 27(3), 187-197.

Kammerer, D. R., Kammerer, J., Valet, R., & Carle, R. (2014). Recovery of polyphenols from the by-products of plant food processing and application as valuable food ingredients. Food Research International, 65, 2-12.

Kardos, G. R., Wastyk, H. C., & Robertson, G. P. (2015). Disruption of proline synthesis in melanoma inhibits protein production mediated by the GCN2 pathway. Molecular Cancer Research, molcanres-0048.

Karonen, M., Loponen, J., Ossipov, V., & Pihlaja, K. (2004). Analysis of procyanidins in pine bark with reversed-phase and normal-phase high-performance liquid chromatography–electrospray ionization mass spectrometry. Analytica Chimica Acta, 522(1), 105-112.

Kedare, S. B., & Singh, R. P. (2011). Genesis and development of DPPH method of antioxidant assay. Journal of food science and technology, 48(4), 412-422.

Kerbab, K., Mekhelfi, T., Zaiter, L., Benayache, S., Benayache, F., Picerno, P., Mencherini, T., Sansone, F. & Rastrelli, L. (2015). Chemical composition and antioxidant activity of a polar extract of *Thymelaea microphylla* Coss. et Dur. Natural product research, 29(7), 671-675.

Kim, T. H., Ito, H., Hayashi, K., Hasegawa, T., Machiguchi, T., & Yoshida, T. (2005). Aromatic Constituents from the Heartwood of Santalum album L. Chemical and pharmaceutical bulletin, 53(6), 641-644.

Kowalska, H., Czajkowska, K., Cichowska, J., & Lenart, A. (2017). What's new in biopotential of fruit and vegetable by-products applied in the food processing industry. Trends in Food Science & Technology, 67, 150-159.

Krishnan, N., Dickman, M. B., & Becker, D. F. (2008). Proline modulates the intracellular redox environment and protects mammalian cells against oxidative stress. Free Radical Biology and Medicine, 44(4), 671-681.

Kulkarni Vishakha, S., Butte Kishor, D., & Rathod Sudha, S. (2012). Natural polymers–A comprehensive review. International journal of research in pharmaceutical and biomedical sciences, 3(4), 1579-1613.

Kumar, K., Yadav, A. N., Kumar, V., Vyas, P., & Dhaliwal, H. S. (2017). Food waste: a potential bioresource for extraction of nutraceuticals and bioactive compounds. Bioresources and Bioprocessing, 4(1), 18.

Laine, P., Kylli, P., Heinonen, M., & Jouppila, K. (2008). Storage stability of microencapsulated cloudberry (*Rubus chamaemorus*) phenolics. Journal of Agricultural and Food Chemistry, 56(23), 11251-11261.

Landete, J. M. (2011). Ellagitannins, ellagic acid and their derived metabolites: a review about source, metabolism, functions and health. Food research international, 44(5), 1150-1160.

Leal, J., Teixeira-Santos, L., Pinho, D., Afonso, J., Carvalho, J., de Lourdes Bastos, M., Albino-Teixeira, A., Fraga, S., & Sousa, T. (2019). l-proline supplementation improves nitric oxide bioavailability and counteracts the blood pressure rise induced by angiotensin II in rats. Nitric Oxide, 82, 1-11.

Lee, D. Y., Kim, H. W., Yang, H., & Sung, S. H. (2017). Hydrolyzable tannins from the fruits of *Terminalia chebula* Retz and their α-glucosidase inhibitory activities. Phytochemistry, 137, 109-116.

Lee, J. S., Kim, H. J., Park, H., & Lee, Y. S. (2002). New diarylheptanoids from the stems of *Carpinus cordata*. Journal of natural products, 65(9), 1367-1370.

Li, A. N., Li, S., Zhang, Y. J., Xu, X. R., Chen, Y. M., & Li, H. B. (2014). Resources and biological activities of natural polyphenols. Nutrients, 6(12), 6020-6047.

Li, L., & Seeram, N. P. (2010). Maple syrup phytochemicals include lignans, coumarins, a stilbene, and other previously unreported antioxidant phenolic compounds. Journal of agricultural and food chemistry, 58(22), 11673-11679.

Li, Y. C., & Kuo, Y. H. (2000). Four new compounds, ficusal, ficusesquilignan A, B, and ficusolide diacetate from the heartwood of *Ficus microcarpa*. Chemical and pharmaceutical bulletin, 48(12), 1862-1865.

Li, Z. J., Guo, X., Dawuti, G., & Aibai, S. (2015). Antifungal activity of ellagic acid in vitro and in vivo. Phytotherapy Research, 29(7), 1019-1025.

Liu, C., Lin, J. J., Yang, Z. Y., Tsai, C. C., Hsu, J. L., & Wu, Y. J. (2014). Proteomic study reveals a co-occurrence of gallic acid-induced apoptosis and glycolysis in B16F10 melanoma cells. Journal of agricultural and food chemistry, 62(48), 11672-11680.

Liu, J., Liu, S., Wu, Q., Gu, Y., Kan, J., & Jin, C. (2017). Effect of protocatechuic acid incorporation on the physical, mechanical, structural and antioxidant properties of chitosan film. Food Hydrocolloids, 73, 90-100.

Liu, X., Chen, T., Liu, L., & Li, G. (2006). Electrochemical characteristics of heme proteins in hydroxyethylcellulose film. Sensors and Actuators B: Chemical, 113(1), 106-111.

Liu, Y., Borchert, G. L., Surazynski, A., Hu, C. A., & Phang, J. M. (2006). Proline oxidase activates both intrinsic and extrinsic pathways for apoptosis: the role of ROS/superoxides, NFAT and MEK/ERK signaling. Oncogene, 25(41), 5640.

Lo, C., Lai, T. Y., Yang, J. H., Yang, J. S., Ma, Y. S., Weng, S. W., Chen, Y. Y., Lin, J. G. & Chung, J. G. (2010). Gallic acid induces apoptosis in A375. S2 human melanoma cells through caspase-dependent and-independent pathways. International journal of oncology, 37(2), 377-385.

Lozano, F. J., & Lozano, R. (2018). Assessing the potential sustainability benefits of agricultural residues: biomass conversion to syngas for energy generation or to chemicals production. Journal of Cleaner Production, 172, 4162-4169.

Lozano-Navarro, J. I., Díaz-Zavala, N. P., Velasco-Santos, C., Melo-Banda, J. A., Páramo-García, U., Paraguay-Delgado, F., & Zapién-Castillo, S. (2018). Chitosan-Starch Films with Natural Extracts: Physical, Chemical, Morphological and Thermal Properties. Materials, 11(1), 120.

Luiz, R. L. F., Vila, T. V. M., de Mello, J. C. P., Nakamura, C. V., Rozental, S., & Ishida, K. (2015). Proanthocyanidins polymeric tannin from Stryphnodendron adstringens are active against Candida albicans biofilms. BMC complementary and alternative medicine, 15(1), 68.

Manchanda, S., Chandra, A., Bandopadhyay, S., Deb, P. K., & Tekade, R. K. (2018). Formulation Additives Used in Pharmaceutical Products: Emphasis on Regulatory Perspectives and GRAS. In Dosage Form Design Considerations (pp. 773-831). Academic Press.

Mansour, A., Celano, R., Mencherini, T., Picerno, P., Piccinelli, A. L., Foudil-Cherif, Y., Csupor, D., Rahili, G., Yahi, N., Nabavi, S.M., Aquino, R. P., & Rasytrelli, L. (2017). A new cineol derivative, polyphenols and norterpenoids from Saharan myrtle tea (*Myrtus nivellei*): Isolation, structure determination, quantitative determination and antioxidant activity. Fitoterapia, 119, 32-39.

Martín, Á., Varona, S., Navarrete, A., & Cocero, M. J. (2010). Encapsulation and co-precipitation processes with supercritical fluids: applications with essential oils. The Open Chemical Engineering Journal, 4(1).

Mehta, R. G., Murillo, G., Naithani, R., & Peng, X. (2010). Cancer chemoprevention by natural products: how far have we come?. Pharmaceutical research, 27(6), 950-961.

Mellinas, C., Valdés, A., Ramos, M., Burgos, N., Garrigós, M. D. C., & Jiménez, A. (2016). Active edible films: Current state and future trends. Journal of Applied Polymer Science, 133(2).

Mencherini, T., Picerno, P., Festa, M., Russo, P., Capasso, A., & Aquino, R. (2011). Triterpenoid constituents from the roots of *Paeonia rockii* ssp. rockii. Journal of natural products, 74(10), 2116-2121.

Mendoza, L., Yañez, K., Vivanco, M., Melo, R., & Cotoras, M. (2013). Characterization of extracts from winery by-products with antifungal activity against Botrytis cinerea. Industrial Crops and Products, 43, 360-364.

Meng, X., Yang, L., Kennedy, J. F., & Tian, S. (2010). Effects of chitosan and oligochitosan on growth of two fungal pathogens and physiological properties in pear fruit. Carbohydrate Polymers, 81(1), 70-75.

Merfort, I., & Wendisch, D. (1988). Flavonolglucuronide aus den Blüten von Arnica montana1. Planta medica, 54(03), 247-250.

Mir, S. A., Dar, B. N., Wani, A. A., & Shah, M. A. (2018). Effect of plant extracts on the techno-functional properties of biodegradable packaging films. Trends in Food Science & Technology

Mirabella, N., Castellani, V., & Sala, S. (2014). Current options for the valorization of food manufacturing waste: a review. Journal of Cleaner Production, 65, 28-41.

Moilanen, J., Sinkkonen, J., & Salminen, J. P. (2013). Characterization of bioactive plant ellagitannins by chromatographic, spectroscopic and mass spectrometric methods. Chemoecology, 23(3), 165-179.

Monrad, J. K., Howard, L. R., King, J. W., Srinivas, K., & Mauromoustakos, A. (2010). Subcritical solvent extraction of anthocyanins from dried red grape pomace. Journal of agricultural and food chemistry, 58(5), 2862-2868.

Montella, R.; Coïsson, J. D.; Travaglia, F.; Locatelli, M.; Bordiga, M.; Meyrand, M.; Arlorio. (2013). M. Identification and characterisation of water and alkali soluble oligosaccharides from hazelnut skin (*Corylus avellana* L.). Food Chem. 140, 717−725.

Moreno, T., de Paz, E., Navarro, I., Rodríguez-Rojo, S., Matías, A., Duarte, C., Sanz-Buenhombre M., & Cocero, M. J. (2016). Spray drying formulation of polyphenols-rich grape marc extract: evaluation of operating conditions and different natural carriers. Food and Bioprocess Technology, 9(12), 2046-2058.

Mujtaba, M., Morsi, R. E., Kerch, G., Elsabee, M. Z., Kaya, M., Labidi, J., & Khawar, K. M. (2018). Current advancements in chitosan-based film production for food technology; A review. International journal of biological macromolecules.

Munin, A., & Edwards-Lévy, F. (2011). Encapsulation of natural polyphenolic compounds; a review. Pharmaceutics, 3(4), 793-829.

Murugesan, R., & Orsat, V. (2012). Spray drying for the production of nutraceutical ingredients—a review. Food and Bioprocess Technology, 5(1), 3-14.

Nasser, A. L. M.; Carli, C. B. A.; Rodrigues, C. M.; Maia, D. C. G.; Carlos, I. Z.; Eberlin, M. N.; Hiruma-Lima, A.; Vilegas, W. (2008). Identification of Ellagic Acid Derivatives in Methanolic Extracts from Qualea Species. Z Naturforsch C. 63 (11–12), 794–800.

Natarajan, S. K., Zhu, W., Liang, X., Zhang, L., Demers, A. J., Zimmerman, M. C., Simpson, M. A., Becker, D. F. (2012). Proline dehydrogenase is essential for proline protection against hydrogen peroxide-induced cell death. Free radical biology and medicine, 53(5), 1181-1191.

Negi, A., Dobhal, K., & Ghildiyal, P. (2018). Antioxidant Potential and Effect of Extraction Solvent on Total Phenol Content, Flavonoids Content and Tannin Content of Ficus palmata Forssk. Int. J. Pharm. Sci. Rev. Res, 49(2), 19-24.

Nesterenko, A., Alric, I., Silvestre, F., & Durrieu, V. (2013). Vegetable proteins in microencapsulation: A review of recent interventions and their effectiveness. Industrial crops and products, 42, 469-479.

Niedzwiecki, A., Roomi, M., Kalinovsky, T., & Rath, M. (2016). Anticancer efficacy of polyphenols and their combinations. Nutrients, 8(9), 552.

Niu, B., Shao, P., Chen, H., & Sun, P. (2019). Structural and physiochemical characterization of novel hydrophobic packaging films based on pullulan derivatives for fruits preservation. Carbohydrate polymers, 208, 276-284.

Norajit, K., Kim, K. M., & Ryu, G. H. (2010). Comparative studies on the characterization and antioxidant properties of biodegradable alginate films containing ginseng extract. Journal of Food Engineering, 98(3), 377-384.

Osorio, E.; Flores, M.; Hernández, D.; Ventura, J.; Rodríguez, R.; Aguilar, C. N. (2010). Biological Efficiency of Polyphenolic Extracts from Pecan Nuts Shell (*Carya Illinoensis*), Pomegranate Husk (*Punica Granatum*) and Creosote Bush Leaves (*Larrea Tridentata* Cov .) against Plant Pathogenic Fungi. Indudtrial Crops and Products, 31, 153–157.

Ostroschi, L. C., de Souza, V. B., Echalar-Barrientos, M. A., Tulini, F. L., Comunian, T. A., Thomazini, M., Baliero, J.C.C., Roudaut, G., Genovese, M.I., & Favaro-Trindade, C. S. (2018). Production of spray-dried proanthocyanidin-rich cinnamon (*Cinnamomum zeylanicum*) extract as a

potential functional ingredient: Improvement of stability, sensory aspects and technological properties. Food Hydrocolloids, 79, 343-351.

Otoni, C. G., Avena-Bustillos, R. J., Azeredo, H. M., Lorevice, M. V., Moura, M. R., Mattoso, L. H., & McHugh, T. H. (2017). Recent advances on edible films based on fruits and vegetables—a review. Comprehensive Reviews in Food Science and Food Safety, 16(5), 1151-1169.

Ozawa, T.; Takino, Y. (1979). Carbon-13 Nuclear Magnetic Resonance Spectra of Phenolic Glycosides Isolated from Chestnut Galls. Agric. Biol. Chern. 43 (6), 1173–1177.

Ozkan, G., Franco, P., De Marco, I., Xiao, J., & Capanoglu, E. (2019). A review of microencapsulation methods for food antioxidants: Principles, advantages, drawbacks and applications. Food chemistry, 272, 494-506.

Pane, C.; Fratianni, F.; Parisi, M.; Nazzaro, F.; Zaccardelli, M. (2016). Control of Alternaria Post-Harvest Infections on Cherry Tomato Fruits by Wild Pepper Phenolic-Rich Extracts. *Crop Protection*, *84*, 81–87.

Pastor, C., Sánchez-González, L., Cháfer, M., Chiralt, A., & González-Martínez, C. (2010). Physical and antifungal properties of hydroxypropylmethylcellulose based films containing propolis as affected by moisture content. Carbohydrate Polymers, 82(4), 1174-1183.

Pfaltzgraff, L. A., Cooper, E. C., Budarin, V., & Clark, J. H. (2013). Food waste biomass: a resource for high-value chemicals. Green Chemistry, 15(2), 307-314.

Piccinelli, A. L.; Pagano, I.; Esposito, T.; Mencherini, T.; Porta, A.; Petrone, A. M.; Gazzerro, P.; Picerno, P.; Sansone, F.; Rastrelli, L. (2016). HRMS Profile of a Hazelnut Skin Proanthocyanidin-Rich Fraction with Antioxidant and Anti-*Candida Albicans* Activities. Journal of Agricultural and Food Chemistry, 64 (3), 585–595.

Picerno, P., Mencherini T., Sansone, F., Del Gaudio, P., Granata, I., Porta, A. & Aquino, R. (2011). P. Screening of a polar extract of *Paeonia rockii*: composition and antioxidant and antifungal activities. J. Ethnopharm. 138, 705-712.

Pineros-Hernandez, D., Medina-Jaramillo, C., López-Córdoba, A., & Goyanes, S. (2017). Edible cassava starch films carrying rosemary antioxidant extracts for potential use as active food packaging. Food Hydrocolloids, 63, 488-495.

Pinto, D., Rodrigues, F., Braga, N., Santos, J., Pimentel, F. B., Palmeira-de-Oliveira, A., & Oliveira, M. B. P. (2017). The *Castanea sativa* bur as a new potential ingredient for nutraceutical and cosmetic outcomes: preliminary studies. Food & function, 8(1), 201-208.

Pinto, R. J., Almeida, A., Fernandes, S. C., Freire, C. S., Silvestre, A. J., Neto, C. P., & Trindade, T. (2013). Antifungal activity of transparent nanocomposite thin films of pullulan and silver against Aspergillus niger. Colloids and Surfaces B: Biointerfaces, 103, 143-148.

Plazzotta, S., Manzocco, L., & Nicoli, M. C. (2017). Fruit and vegetable waste management and the challenge of fresh-cut salad. Trends in food science & technology, 63, 51-59.

Ponrasu, T., Jamuna, S., Mathew, A., Madhukumar, K. N., Ganeshkumar, M., Iyappan, K., & Suguna, L. (2013). Efficacy of L-proline administration on the early responses during cutaneous wound healing in rats. Amino acids, 45(1), 179-189.

Prasad, S., Gupta, S. C., & Tyagi, A. K. (2017). Reactive oxygen species (ROS) and cancer: role of antioxidative nutraceuticals. Cancer letters, 387, 95-105.

Prior, R. L., & Gu, L. (2005). Occurrence and biological significance of proanthocyanidins in the American diet. Phytochemistry, 66(18), 2264-2280.

Prota, L., Santoro, A., Bifulco, M., Aquino, R. P., Mencherini, T., & Russo, P. (2011). Leucine enhances aerosol performance of naringin dry powder and its activity on cystic fibrosis airway epithelial cells. International journal of pharmaceutics, 412(1-2), 8-19.

Ran, X. L., Zhang, M., Wang, Y., & Adhikari, B. (2018). Novel technologies applied for recovery and value addition of high value compounds from plant byproducts: A review. Critical reviews in food science and nutrition, 1-12.

Rane, H. S., Bernardo, S. M., Howell, A. B., & Lee, S. A. (2013). Cranberry-derived proanthocyanidins prevent formation of Candida albicans biofilms in artificial urine through biofilm-and adherence-specific mechanisms. Journal of Antimicrobial Chemotherapy, 69(2), 428-436.

Ravindran, R., & Jaiswal, A. K. (2016). Exploitation of food industry waste for high-value products. Trends in Biotechnology, 34(1), 58-69.

Rawson, A., Patras, A., Tiwari, B. K., Noci, F., Koutchma, T., & Brunton, N. (2011). Effect of thermal and non thermal processing technologies on the bioactive content of exotic fruits and their products: Review of recent advances. Food Research International, 44(7), 1875-1887.

Re, R., Pellegrini, N., Proteggente, A., Pannala, A., Yang, M., & Rice-Evans, C. (1999). Antioxidant activity applying an improved ABTS radical cation decolorization assay. Free radical biology and medicine, 26(9-10), 1231-1237.

Regueiro, J., Sánchez-González, C., Vallverdú-Queralt, A., Simal-Gándara, J., Lamuela-Raventós, R., & Izquierdo-Pulido, M. (2014). Comprehensive

identification of walnut polyphenols by liquid chromatography coupled to linear ion trap–Orbitrap mass spectrometry. Food chemistry, 152, 340-348.

Ricci, A., Olejar, K. J., Parpinello, G. P., Kilmartin, P. A., & Versari, A. (2015). Application of Fourier transform infrared (FTIR) spectroscopy in the characterization of tannins. Applied Spectroscopy Reviews, 50(5), 407-442.

Rice-Evans, C. A., Miller, N. J., & Paganga, G. (1996). Structure-antioxidant activity relationships of flavonoids and phenolic acids. Free radical biology and medicine, 20(7), 933-956.

Roomi, M. W., Kalinovsky, T., Roomi, N. W., Ivanov, V., Rath, M., & Niedzwiecki, A. (2008). Suppression of growth and hepatic metastasis of murine B16FO melanoma cells by a novel nutrient mixture. Oncology reports, 20(4), 809-817.

Salarbashi, D., Bazeli, J., & Tafaghodi, M. (2019). Environment-friendly green composites based on soluble soybean polysaccharide: A review. International journal of biological macromolecules, 122, 216-223.

Salgado, P. R., Ortiz, C. M., Musso, Y. S., Di Giorgio, L., & Mauri, A. N. (2015). Edible films and coatings containing bioactives. Current Opinion in Food Science, 5, 86-92.

Sánchez, J., Curt, M. D., Robert, N., & Fernández, J. (2019). Biomass Resources. In The Role of Bioenergy in the Bioeconomy (pp. 25-111). Academic Press.

Sánchez-González, L., Cháfer, M., Chiralt, A., & González-Martínez, C. (2010). Physical properties of edible chitosan films containing bergamot essential oil and their inhibitory action on *Penicillium italicum*. Carbohydrate polymers, 82(2), 277-283.

Sansone, F., Mencherini, T., Picerno, P., Lauro, M. R., Cerrato, M., & Aquino, R. P. (2019). Development of Health Products from Natural Sources. Current medicinal chemistry, doi: 10.2174/0929867325666180926152139.

Sansone, F., Esposito, T., Lauro, M. R., Picerno, P., Mencherini, T., Gasparri, F., De Santis, S., Chieppa, M., Cirillo, C., and Aquino, R.P. (2018a). Application of Spray Drying Particle Engineering to a High-Functionality/Low-Solubility Milk Thistle Extract: Powders Production and Characterization. Molecules. 23, 1716.

Sansone, F., Esposito, T., Mencherini, T., Lauro, M. R., Del Gaudio, P., Picerno, P., Pepe, G, & Aquino, R. P. (2018b). Particle technology applied to a lactose/NaCMC blend: Production and characterization of a novel and stable spray-dried ingredient. Powder Technology, 329, 304-312.

Sansone, F., Picerno, P., Mencherini, T., Porta, A., Lauro, M. R., Russo, P., & Aquino, R. P. (2014a). Technological properties and enhancement of antifungal activity of a *Paeonia rockii* extract encapsulated in a chitosan-based matrix. Journal of Food Engineering, 120, 260-267.

Sansone, F., Mencherini, T., Picerno, P., Esposito, T., Del Gaudio, P., Russo, P., Pepe, G., Lauro, M. R., & Aquino, R. P. (2014b). Microencapsulation by spray drying of *Lannea microcarpa* extract: technological characteristics and antioxidant activity. Journal of Pharmacy & Pharmacognosy Research, 2(4).

Sansone F., Picerno P, Mencherini M., Russo P., Gasparri F., Giannini V, Lauro M.R., Puglisi G., Aquino R. P. (2013). Enhanced technological and permeation properties of a microencapsulated soy isoflavones extract. Journal of Food Engineering. 115 298–305.

Sansone, F., Picerno, P., Mencherini, T., Villecco, F., D'Ursi, A. M., Aquino, R. P., & Lauro, M. R. (2011). Flavonoid microparticles by spray-drying: Influence of enhancers of the dissolution rate on properties and stability. Journal of Food Engineering, 103(2), 188-196.

Santacruz, S., Rivadeneira, C., & Castro, M. (2015). Edible films based on starch and chitosan. Effect of starch source and concentration, plasticizer, surfactant's hydrophobic tail and mechanical treatment. Food Hydrocolloids, 49, 89-94.

Santana-Méridas, O., González-Coloma, A., & Sánchez-Vioque, R. (2012). Agricultural residues as a source of bioactive natural products. Phytochemistry reviews, 11(4), 447-466.

Schieber, A., Stintzing, F. C., & Carle, R. (2001). By-products of plant food processing as a source of functional compounds—recent developments. Trends in Food Science & Technology, 12(11), 401-413.

Shahidi, F., Alasalvar, C., & Liyana-Pathirana, C. M. (2007). Antioxidant phytochemicals in hazelnut kernel (*Corylus avellana* L.) and hazelnut by-products. Journal of Agricultural and Food Chemistry, 55(4), 1212-1220.

Shishir, M. R. I., & Chen, W. (2017). Trends of spray drying: a critical review on drying of fruit and vegetable juices. Trends in food science & technology, 65, 49-67.

Shit, S. C., & Shah, P. M. (2014). Edible polymers: challenges and opportunities. Journal of Polymers, 2014

Shu, B., Yu, W., Zhao, Y., & Liu, X. (2006). Study on microencapsulation of lycopene by spray-drying. Journal of Food Engineering, 76(4), 664-669.

Siemann, U. (2005). Solvent cast technology–a versatile tool for thin film production. In Scattering methods and the properties of polymer materials (pp. 1-14). Springer, Berlin, Heidelberg.

Silva, N. H., Vilela, C., Almeida, A., Marrucho, I. M., & Freire, C. S. (2018). Pullulan-based nanocomposite films for functional food packaging: Exploiting lysozyme nanofibers as antibacterial and antioxidant reinforcing additives. Food Hydrocolloids, 77, 921-930.

Silva-Weiss, A., Ihl, M., Sobral, P. J. A., Gómez-Guillén, M. C., & Bifani, V. (2013). Natural additives in bioactive edible films and coatings: functionality and applications in foods. Food Engineering Reviews, 5(4), 200-216.

Singh, A., & Van den Mooter, G. (2016). Spray drying formulation of amorphous solid dispersions. Advanced drug delivery reviews, 100, 27-50.

Siripatrawan, U., & Vitchayakitti, W. (2016). Improving functional properties of chitosan films as active food packaging by incorporating with propolis. Food Hydrocolloids, 61, 695-702.

Siripatrawan, U., & Vitchayakitti, W. (2016). Improving functional properties of chitosan films as active food packaging by incorporating with propolis. Food Hydrocolloids, 61, 695-702.

Slatnar, A., Mikulic-Petkovsek, M., Stampar, F., Veberic, R., & Solar, A. (2015). Identification and quantification of phenolic compounds in kernels, oil and bagasse pellets of common walnut (*Juglans regia* L.). Food Research International, 67, 255-263.

Sollohub, K., & Cal, K. (2010). Spray drying technique: II. Current applications in pharmaceutical technology. Journal of pharmaceutical sciences, 99(2), 587-597.

Song, Q., Li, J., & Zeng, X. (2015). Minimizing the increasing solid waste through zero waste strategy. Journal of Cleaner Production, 104, 199-210.

Sosnik, A., & Seremeta, K. P. (2015). Advantages and challenges of the spray-drying technology for the production of pure drug particles and drug-loaded polymeric carriers. Advances in colloid and interface science, 223, 40-54.

Srinivasa, P. C., & Tharanathan, R. N. (2007). Chitin/chitosan—Safe, ecofriendly packaging materials with multiple potential uses. Food reviews international, 23(1), 53-72.

Stévigny, C., Rolle, L., Valentini, N., Zeppa, G., 2007. Optimization of extraction of phenolic content from hazelnut shell using response surface methodology. J. Sci. Food Agric. 87, 2817–2822.

Suderman, N., Isa, M. I. N., & Sarbon, N. M. (2018). The effect of plasticizers on the functional properties of biodegradable gelatin-based film: A review. Food bioscience, 24, 111-119.

Sumere, B. R., de Souza, M. C., dos Santos, M. P., Bezerra, R. M. N., da Cunha, D. T., Martinez, J., & Rostagno, M. A. (2018). Combining pressurized liquids with ultrasound to improve the extraction of phenolic compounds from pomegranate peel (*Punica granatum* L.). Ultrasonics Sonochemistry

Tabasum, S., Noreen, A., Maqsood, M. F., Umar, H., Akram, N., Chatha, S. A. S., & Zia, K. M. (2018). A review on versatile applications of blends and composites of pullulan with natural and synthetic polymers. International journal of biological macromolecules.

Talanian, R. V., Brady, K. D., & Cryns, V. L. (2000). Caspases as targets for anti-inflammatory and anti-apoptotic drug discovery. Journal of medicinal chemistry, 43(18), 3351-3371.

Talón, E., Trifkovic, K. T., Nedovic, V. A., Bugarski, B. M., Vargas, M., Chiralt, A., & González-Martínez, C. (2017). Antioxidant edible films based on chitosan and starch containing polyphenols from thyme extracts. Carbohydrate polymers, 157, 1153-1161.

Tanaka, T., Ueda, N., Shinohara, H., Nonaka, G. I., Fujioka, T., Mihashi, K., & Kouno, I. (1996). C-Glycosidic Ellagitannin Metabolites in the Heartwood of Japanese Chestnut Tree (*Castanea crenate* SIEB. et ZUCC.). Chemical and pharmaceutical bulletin, 44(12), 2236-2242.

Tao, S.; Zhang, S.; Tsao, R.; Charles, M. T.; Yang, R. and Khanizadeh, S. (2010). Archives of Phytopathology and Plant Protection *In Vitro* Antifungal

Activity and Mode of Action of Selected Polyphenolic Antioxidants on *Botrytis Cinerea*. Archives of Phytopathology and Plant Protection. 43 (16). 1564–1578.

Tencati, A., Pogutz, S., Moda, B., Brambilla, M., & Cacia, C. (2016). Prevention policies addressing packaging and packaging waste: Some emerging trends. Waste management, 56, 35-45.

Thomidis, T., Michailides, T., & Exadaktylou, E. (2009). Contribution of pathogens to peach fruit Rot in northern Greece and their sensitivity to iprodione, carbendazim, thiophanate-methyl and tebuconazole fungicides. Journal of Phytopathology, 157(3), 194-200.

Tolve, R., Galgano, F., Caruso, M. C., Tchuenbou-Magaia, F. L., Condelli, N., Favati, F., & Zhang, Z. (2016). Encapsulation of health-promoting ingredients: applications in foodstuffs. International journal of food sciences and nutrition, 67(8), 888-918.

Tontul, I., & Topuz, A. (2017). Spray-drying of fruit and vegetable juices: effect of drying conditions on the product yield and physical properties. Trends in Food Science & Technology, 63, 91-102.

Trovatti, E., Fernandes, S. C., Rubatat, L., da Silva Perez, D., Freire, C. S., Silvestre, A. J., & Neto, C. P. (2012). Pullulan–nanofibrillated cellulose composite films with improved thermal and mechanical properties. Composites Science and Technology, 72(13), 1556-1561.

Tuyen, C. K., Nguyen, M. H., & Roach, P. D. (2010). Effects of spray drying conditions on the physicochemical and antioxidant properties of the Gac (*Momordica cochinchinensis*) fruit aril powder. Journal of food engineering, 98(3), 385-392.

Umaraw, P., & Verma, A. K. (2017). Comprehensive review on application of edible film on meat and meat products: An eco-friendly approach. Critical reviews in food science and nutrition, 57(6), 1270-1279.

Vázquez, G., Fernández-Agulló, A., Gómez-Castro, C., Freire, M. S., Antorrena, G., & González-Álvarez, J. (2012). Response surface optimization of antioxidants extraction from chestnut (*Castanea sativa*) bur. Industrial Crops and Products, 35(1), 126-134.

Vella, F. M., Laratta, B., La Cara, F., & Morana, A. (2018). Recovery of bioactive molecules from chestnut (Castanea sativa Mill.) by-products through extraction by different solvents. Natural product research, 32(9), 1022-1032.

Veloz-García, R., Marín-Martínez, R., Veloz-Rodríguez, R., Rodríguez-Guerra, R., Torres-Pacheco, I., González-Chavira, M. M., Anaya-López, J. L., Guevara-Olvera, L., Feregrino-Pérez, A. A., Loarca-Piña, G., & Guevara-González, R. G. (2010). Antimicrobial activities of cascalote (*Caesalpinia cacalaco*) phenolics-containing extract against *fungus Colletotrichum lindemuthianum*. Industrial crops and products, 31(1), 134-138.

Vieira, J. M., Flores-López, M. L., de Rodríguez, D. J., Sousa, M. C., Vicente, A. A., & Martins, J. T. (2016). Effect of chitosan–Aloe vera coating on postharvest quality of blueberry (*Vaccinium corymbosum*) fruit. Postharvest Biology and Technology, 116, 88-97.

Vilela, C., Kurek, M., Hayouka, Z., Röcker, B., Yildirim, S., Antunes, M. D. C., Nilsen-Nygaard, J., Pettersen, M., K., & Freire, C. S. (2018). A concise guide to active agents for active food packaging. Trends in Food Science & Technology.

Vuddanda, P. R., Montenegro-Nicolini, M., Morales, J. O., & Velaga, S. (2017). Effect of plasticizers on the physico-mechanical properties of pullulan based

pharmaceutical oral films. European Journal of Pharmaceutical Sciences, 96, 290-298.

Wang, H., Hu, D., Ma, Q., & Wang, L. (2016). Physical and antioxidant properties of flexible soy protein isolate films by incorporating chestnut (*Castanea mollissima*) bur extracts. LWT-Food Science and Technology, 71, 33-39.

Wang, Y., Lu, Z., Lv, F., & Bie, X. (2009). Study on microencapsulation of curcumin pigments by spray drying. European Food Research and Technology, 229(3), 391-396.

Wróblewska-Krepsztul, J., Rydzkowski, T., Borowski, G., Szczypiński, M., Klepka, T., & Thakur, V. K. (2018). Recent progress in biodegradable polymers and nanocomposite-based packaging materials for sustainable environment. International Journal of Polymer Analysis and Characterization, 23(4), 383-395.

Xiao, Q., Lim, L. T., Zhou, Y., & Zhao, Z. (2017). Drying process of pullulan edible films forming solutions studied by low-field NMR. Food chemistry, 230, 611-617.

Yang, B., Kortesniemi, M., Liu, P., Karonen, M., & Salminen, J. P. (2012). Analysis of hydrolyzable tannins and other phenolic compounds in emblic leafflower (*Phyllanthus emblica* L.) fruits by high performance liquid chromatography–electrospray ionization mass spectrometry. Journal of agricultural and food chemistry, 60(35), 8672-8683.

Yang, J., Han, S., Zheng, H., Dong, H., & Liu, J. (2015). Preparation and application of micro/nanoparticles based on natural polysaccharides. Carbohydrate polymers, 123, 53-66.

Yang, Y., & Zhang, T. (2019). Antimicrobial Activities of Tea Polyphenol on Phytopathogens: A Review. Molecules, 24(4), 816.

You, B. R., & Park, W. H. (2010). The effects of mitogen-activated protein kinase inhibitors or small interfering RNAs on gallic acid-induced HeLa cell death in relation to reactive oxygen species and glutathione. Journal of agricultural and food chemistry, 59(2), 763-771.

Yuan, B., Lu, M., Eskridge, K. M., Isom, L. D., & Hanna, M. A. (2018). Extraction, identification, and quantification of antioxidant phenolics from hazelnut (*Corylus avellana* L.) shells. Food Chemistry, 244, 7-15.

Zacchino, S. A., Butassi, E., Di Liberto, M., Raimondi, M., Postigo, A., & Sortino, M. (2017). Plant phenolics and terpenoids as adjuvants of antibacterial and antifungal drugs. Phytomedicine, 37, 27-48.

Zainudin, B. H., Wong, T. W., & Hamdan, H. (2018). Design of low molecular weight pectin and its nanoparticles through combination treatment of pectin by microwave and inorganic salts. Polymer Degradation and Stability, 147, 35-40.

Zhao, S., Liu, J. Y., Chen, S. Y., Shi, L. L., Liu, Y. J., & Ma, C. (2011). Antioxidant potential of polyphenols and tannins from burs of Castanea mollissima Blume. Molecules, 16(10), 8590-8600.

Zlotogorski, A., Dayan, A., Dayan, D., Chaushu, G., Salo, T., & Vered, M. (2013). Nutraceuticals as new treatment approaches for oral cancer: II. Green tea extracts and resveratrol. Oral oncology, 49(6), 502-506.

SITOGRAPHY

- ✓ Directive 2008/98/EC of the European Parliament and of the Council of 19 November 2008 on waste from http://data.europa.eu/eli/dir/2008/98/oj
- ✓ European Commission 2010 from ec.europa.eu/environment/eussd/pdf/bio_foodwaste_report

- ✓ FAOstat Agriculture data. Available from: http://faostat3.fao.org. Accessed 12 May 2016.
- ✓ www.epa.gov//rcc

SECTION S

Supplementary Material

NMR and HRESIMS analysis of HSE and CSB-M compounds

A Bruker DRX-600 NMR spectrometer, operating at 599.19 MHz for ^{1}H and 150.858 MHz for ^{13}C, using the TopSpin 3.2 software package, was used for NMR experiments in CD_3OD. Chemical shifts are expressed in δ (parts per million) referring to the solvent peaks δ_H 3.31 and δ_C 49.05 for CD_3OD, with coupling constants, *J*, in Hertz. ^{1}H-^{1}H DQF-COSY, ^{1}H-^{13}C HSQC, and HMBC experiments were obtained using conventional pulse sequences (Kerbab et al 2015). HRESIMS experiments were performed by a LTQ Orbitrap XL spectrometer (Thermoquest, San Jose, CA, USA) equipped with an electrospray ionization (ESI) probe. The data were acquired and processed with Xcalibur 2.7 software (Thermoquest, San Jose, CA, USA).

Table S.1. ^{1}H and ^{13}C NMR data of compound **1** (lawsonicin) from HSE in CD_3OD[a]

Position	δ_C	δ_H (*J* in Hz)[b]
1	134.3	-
2	110.3	6.97, d, (2.0)
3	148.9	-
4	146.9	-
5	115.6	6.78, d, (8.4)
6	119.0	6.85, dd (2.0, 8.4)
7	88.6	5.52, d, (6.4)
8	55.1	3.49, dd, (12.6, 6.4)
9	64.8	3.82, 3.86, m
1’	136.9	-
2’	113.5	6.75, br,s
3’	144.6	-
4’	147.9	-
5’	129.4	-
6’	117.5	6.75, br,s
7’	32.5	2.65, t, (7.2)
8’	35.2	1.85, tt, (7.2, 2.4)
9’	62.0	3.58, t, (6.4)
3-OCH_3	55.8	3.84,s
3’-OCH_3	56.2	3.88, s

[a]assignments confirmed by 2D-DQF-COSY, HSQC, HMBC experiments; [b]^{1}H-^{1}H coupling constants measured in Hz using 2D-DQF-COSY spectra

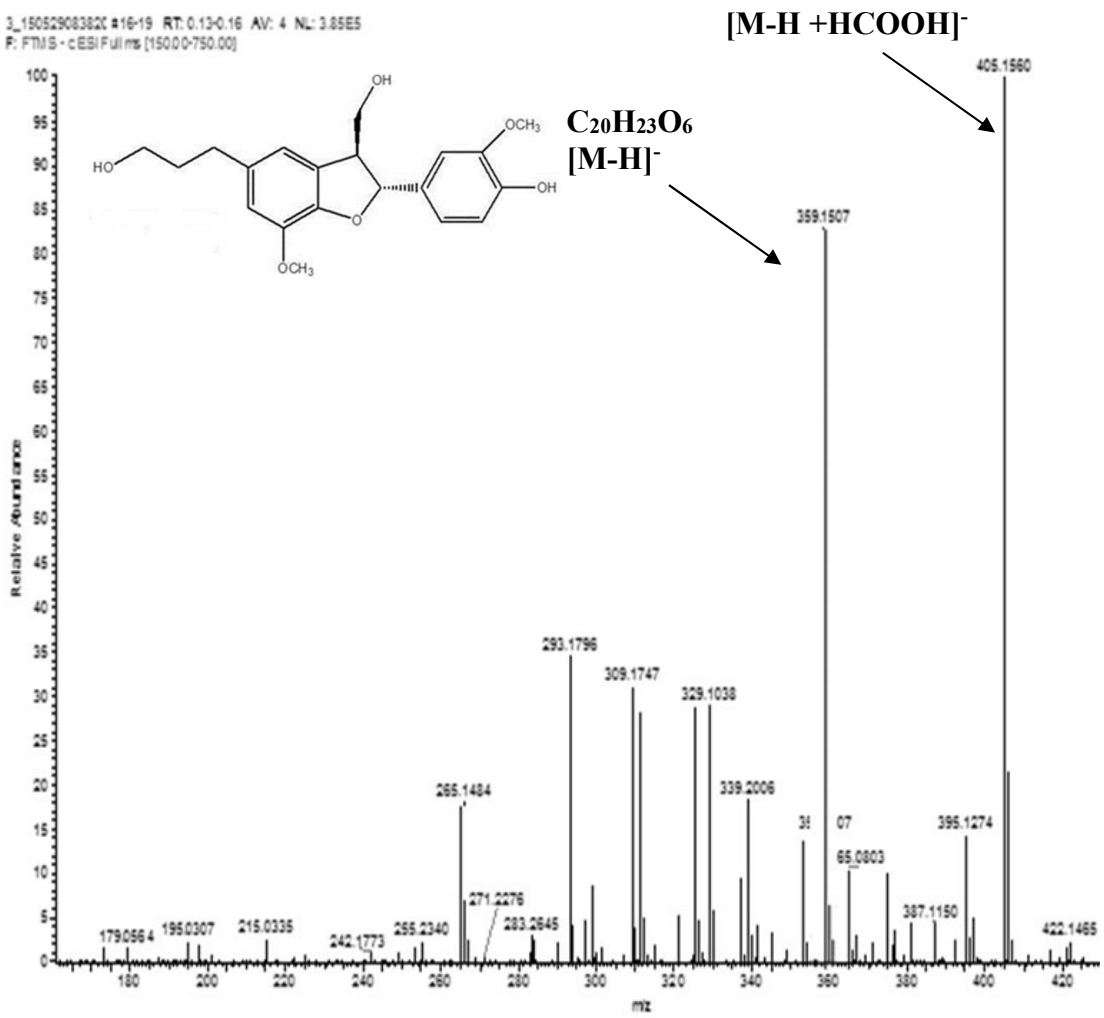

Figure S.1. *HRESIMS spectrum of compound **1***

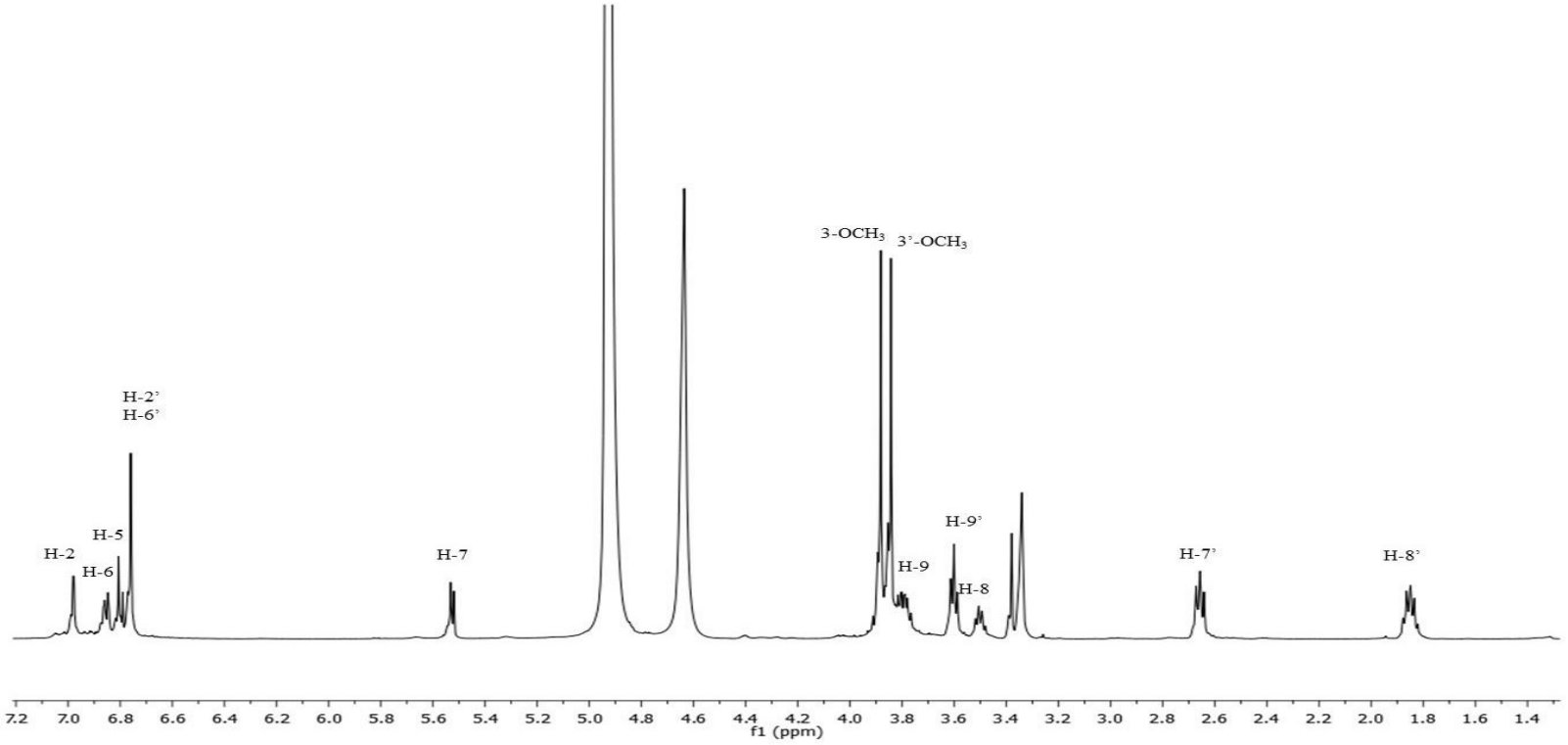

Figure S.2. *^{1}H NMR spectrum of compound **1***

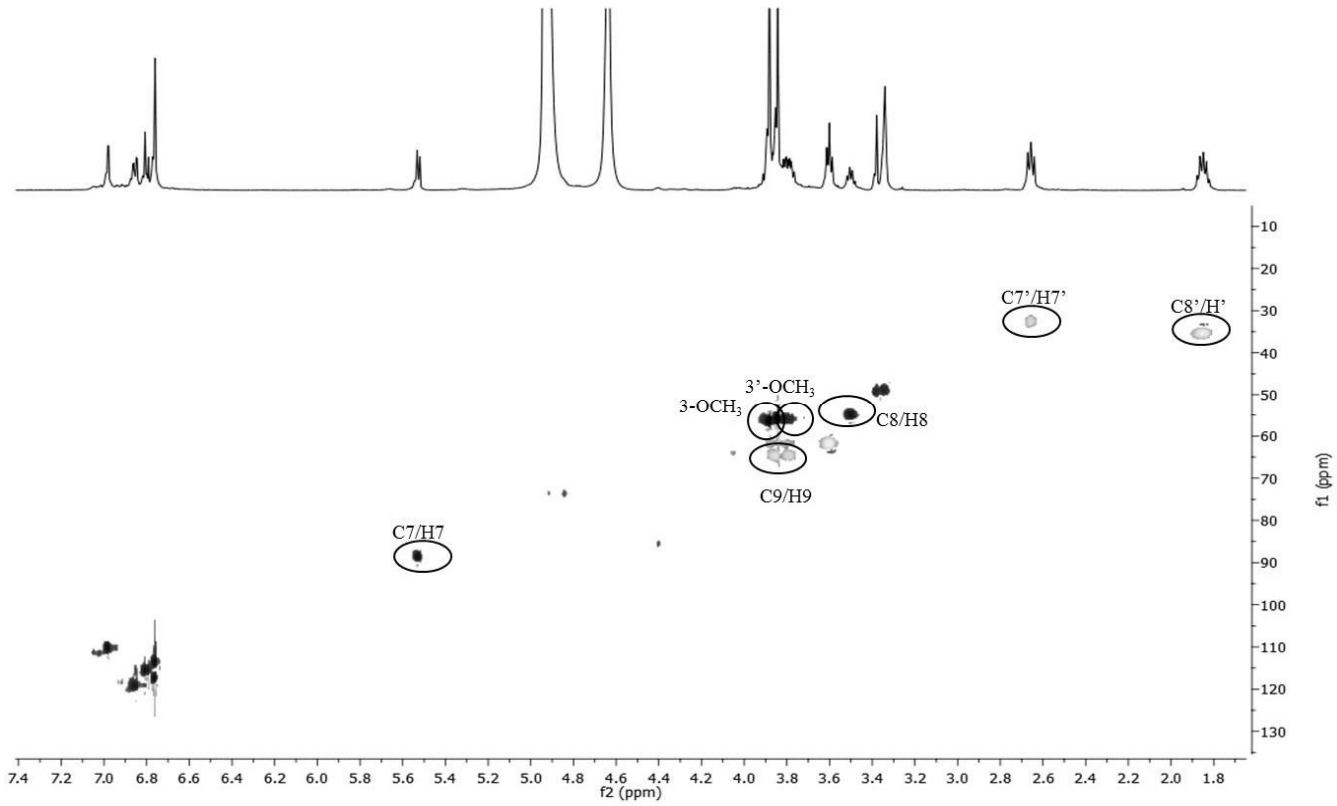

Figure S.3. *HSQC spectrum of compound **1***

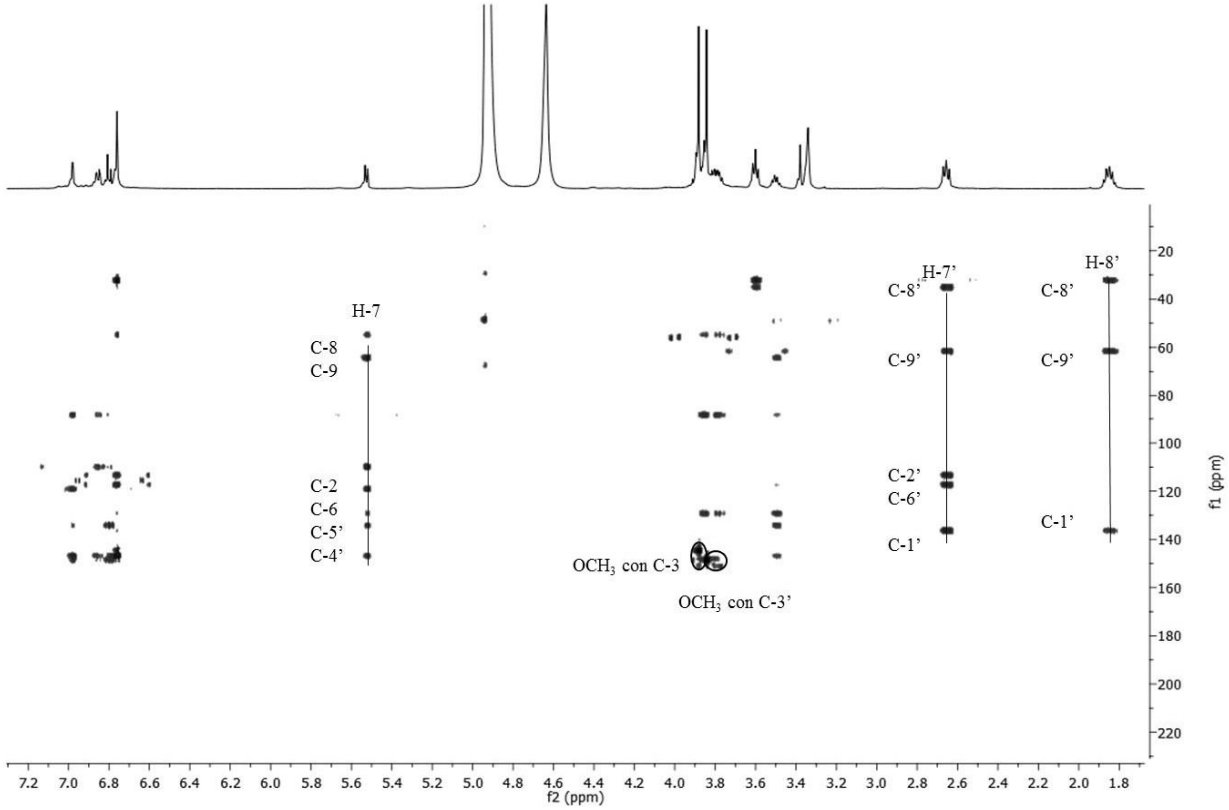

Figure S.4. *HMBC spectrum of compound **1***

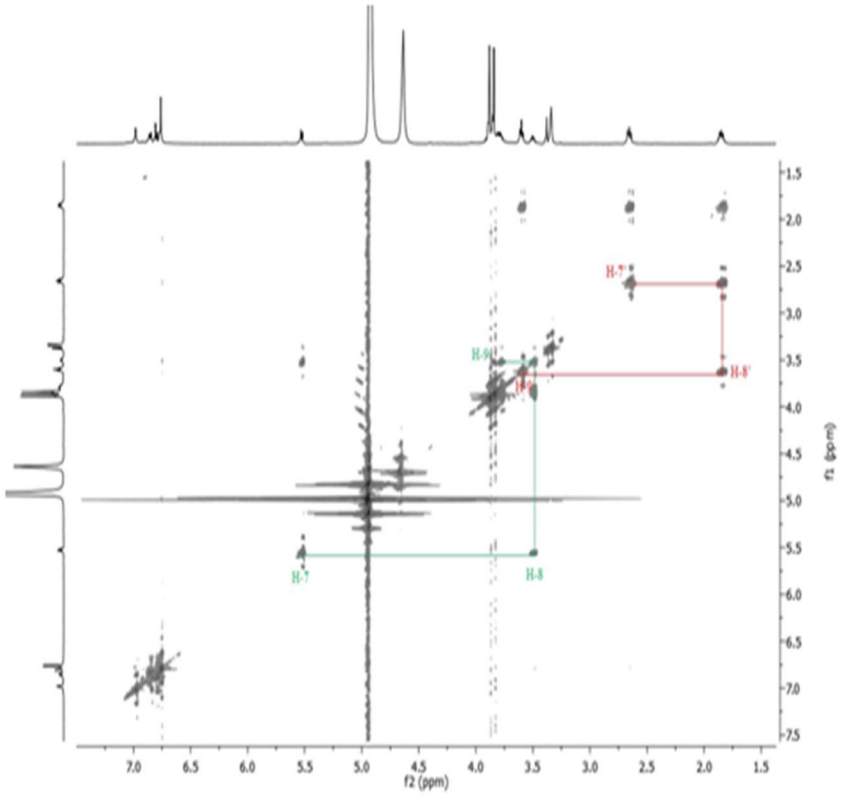

Figure S.5. *2D-DQF COSY spectrum of compound*

Table S.2. ^{1}H and ^{13}C NMR data of compound **21** (Chestanin) from CSB-M in CD_3OD[a]

	Position[a]	δ_C	δ_H (J in Hz)[b]
	1A	112.2	-
	2A	107.9	6.70 (1H, d, 1.8)
	3A	148.5	-
	4A	141.1	-
	5A	146.6	-
	6A	111.7	7.18 (1H, d, 1.8)
	7A	167.5	-
	1B	115.4	-
	2B	109.5	7.09 (1H, s)
	3B	143.9	-
	4B	140.7	-
	5B	137.7	-
	6B	140.8	-
	7B	166.8	-
Glc[c]	**1'**	107.4	4.61 (2H, d, 7.6)
	2'	74.9	3.50 (2H, t, 8.8)
	3'	78.2	3.45 (2H, m)
	4'	70.6	3.45 (2H, m)
	5'	77.4	3.40 (2H, m)
	6'	61. 9	3.77 (2H, dd, 11.8, 4.6)
Tree hydroxy benzyl alcohol A	**1**	135.1	-
	2, 6	107.8	6.27 (2H, s)
	3	151.4	-
	4	134.3	-
	5	151.4	-
	7	66.9	4.94 (2H, s)
Tree hydroxy benzyl alcohol B	**1**	135.7	-
	2, 6	108.5	6.43 (2H, s)
	3	151.2	-
	4	134.4	-
	5	151.2	-
	7	67.2	5.07 (2H, s)

[a]assignments confirmed by 2D-DQF-COSY, HSQC, HMBC experiments;
[b]1H-1H coupling constants measured in Hz using 2D-DQF-COSY spectra;
[c] β-D-glucopyranoside

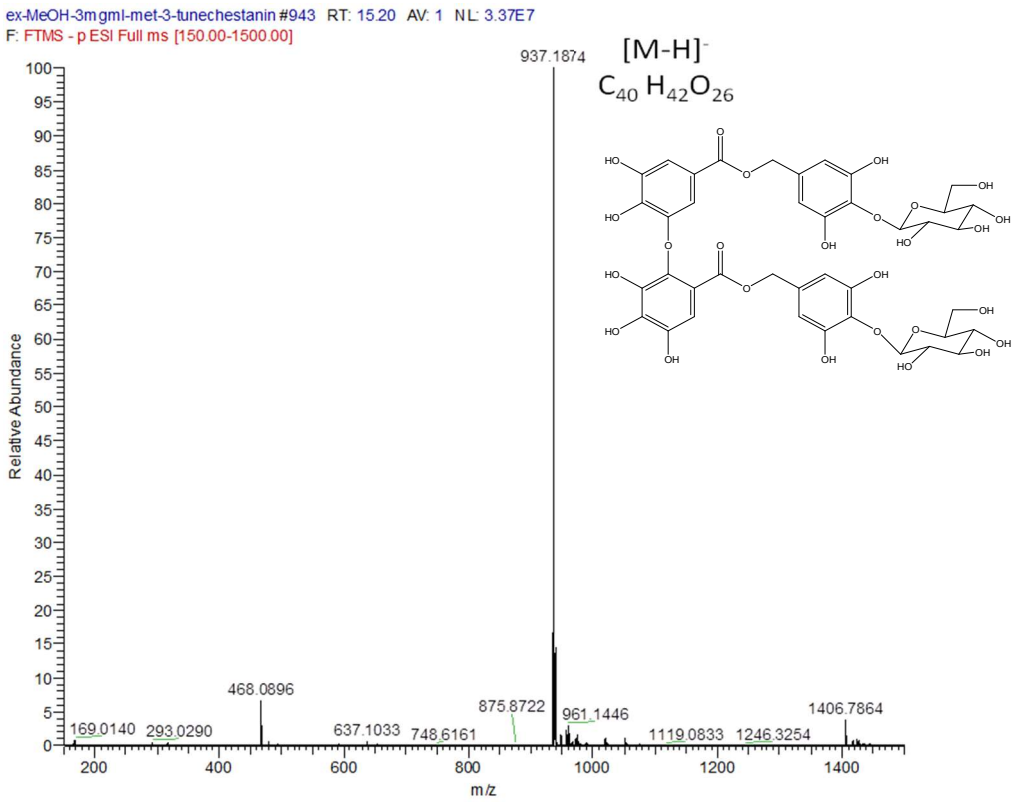

Figure S.6. *HRESIMS spectrum of compound* ***21***

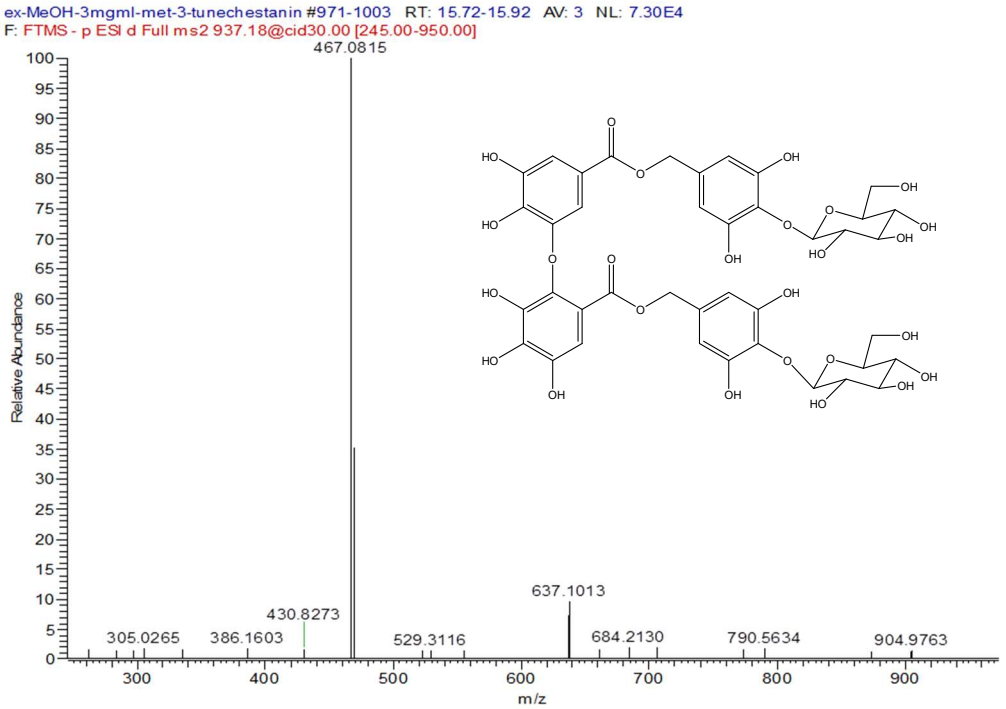

Figure S.7. *MS/MS spectrum of compound **21***

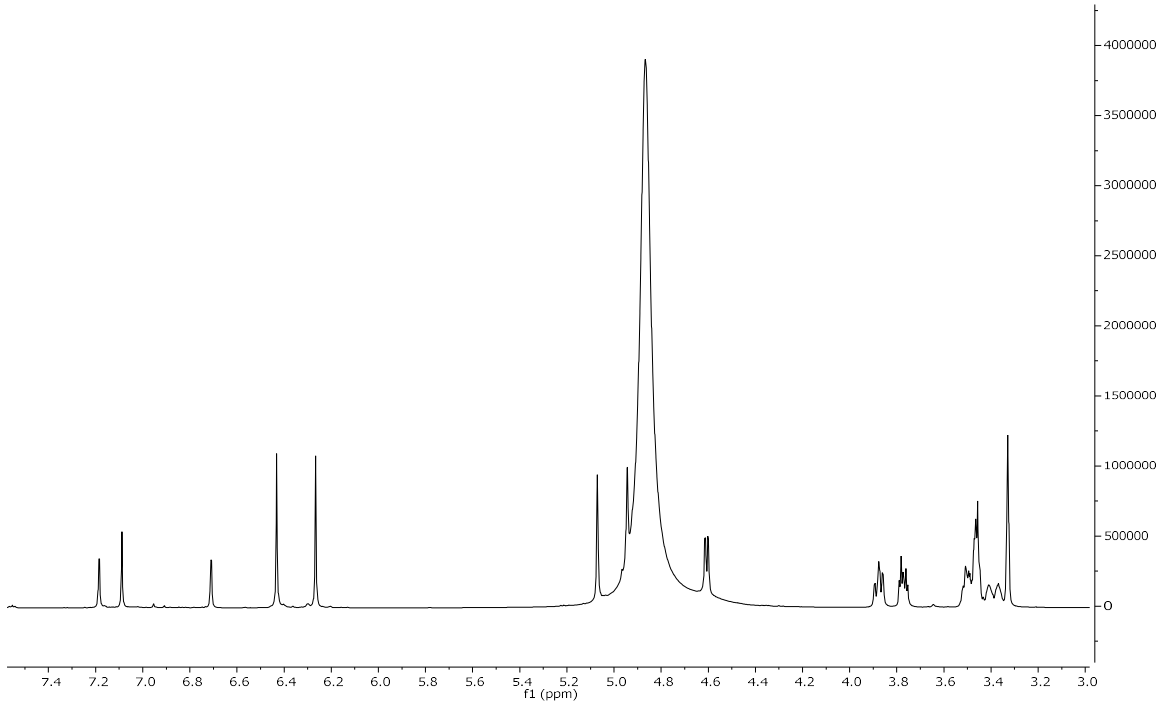

Figure S.8. *^{1}H NMR spectrum of compound **21***

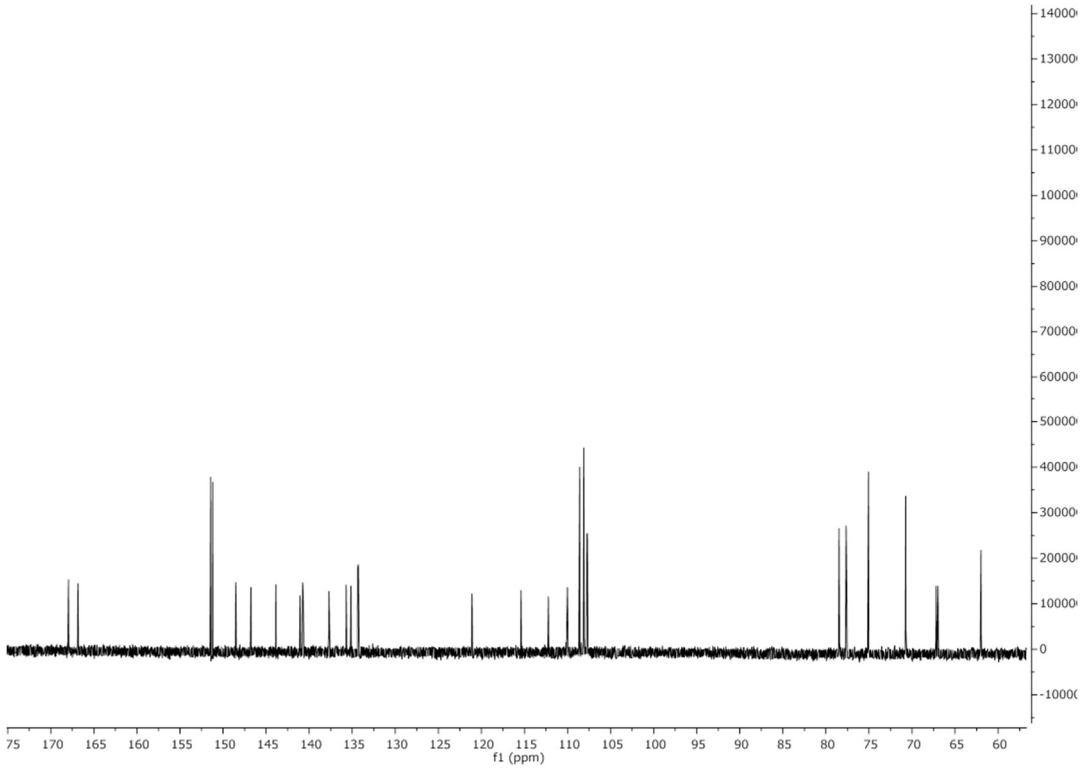

Figure S.9. *^{13}C NMR spectrum of compound **21***

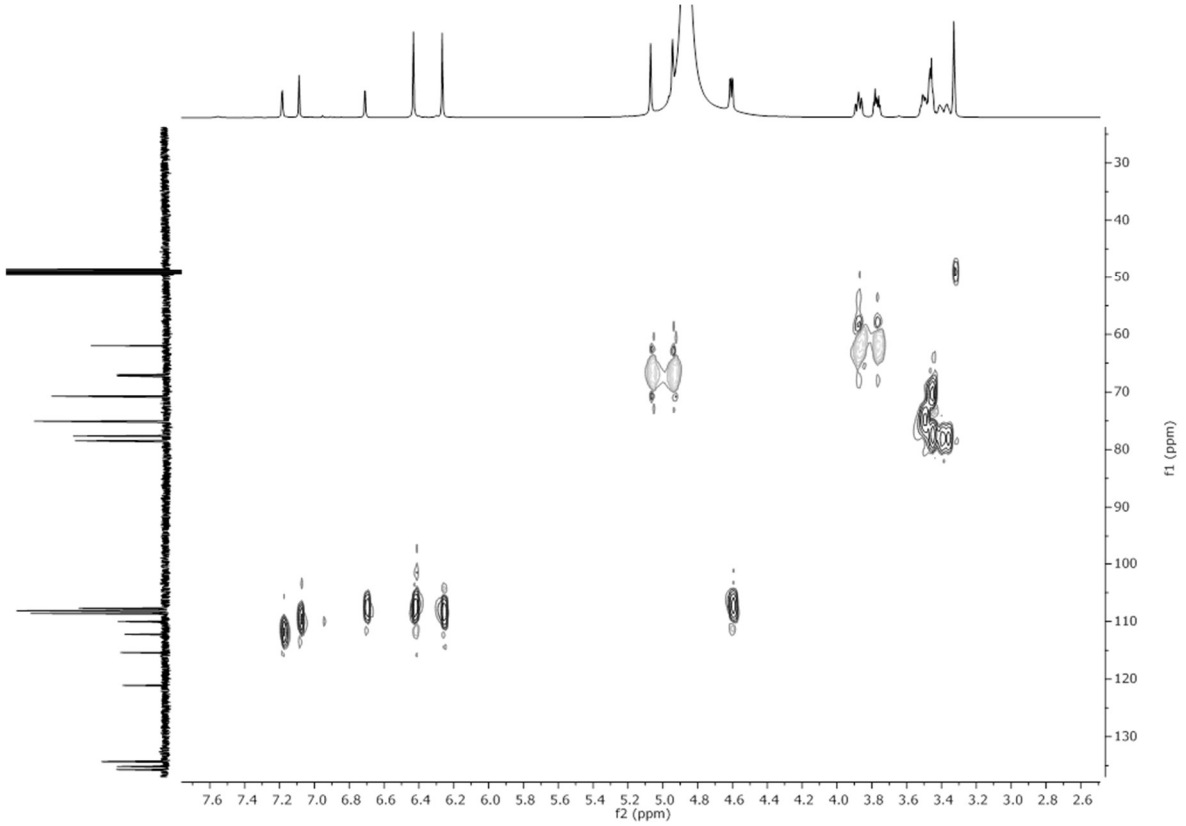

Figure S.10. *HSQC spectrum of compound **21***

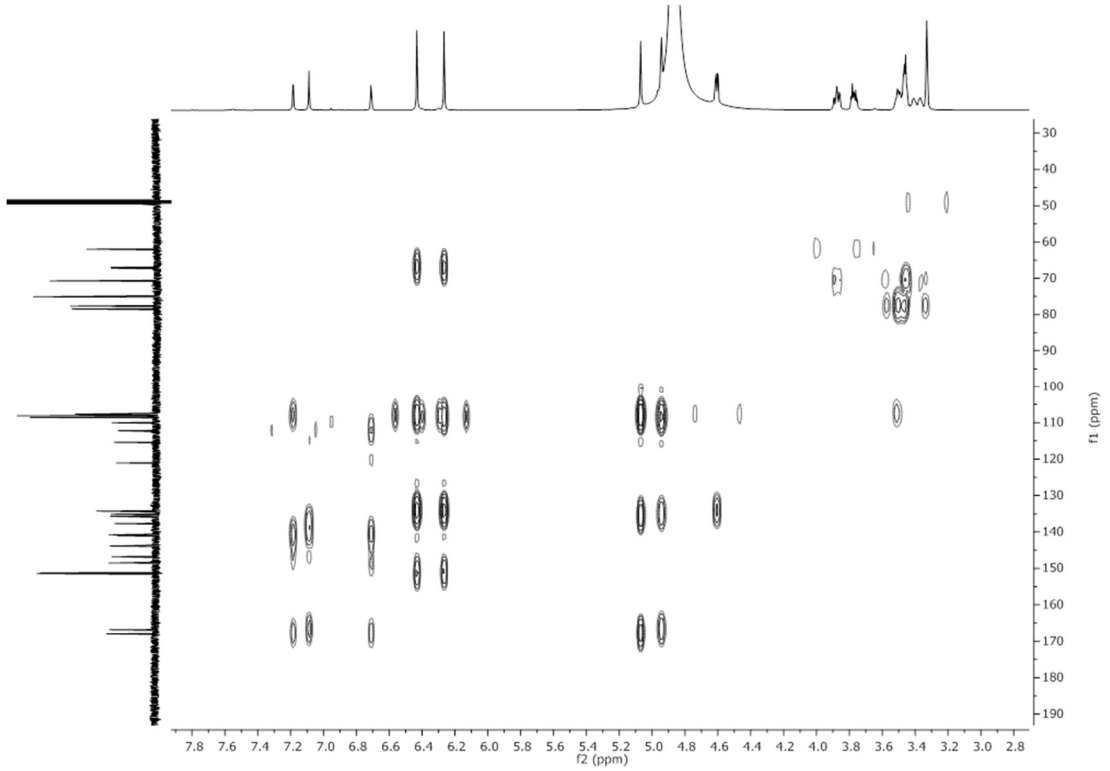

Figure S.11. *HMBC spectrum of compound **21***

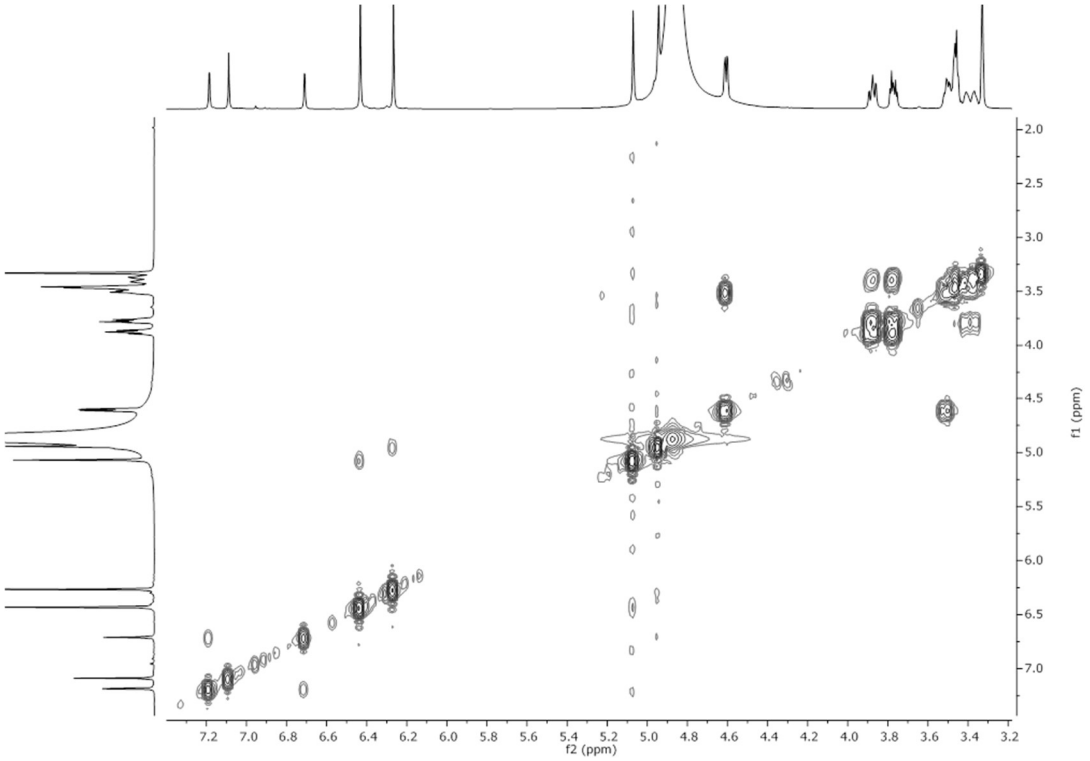

Figure S.12. *DQF-COSY spectrum of compound* ***21***

REFERENCES

Kerbab, K., Mekhelfi, T., Zaiter, L., Benayache, S., Benayache, F., Picerno, P., Mencherini, T., Sansone, F. & Rastrelli, L. (2015). Chemical composition and antioxidant activity of a polar extract of *Thymelaea microphylla* Coss. et Dur. Natural product research, 29(7), 671-675.

ACKNOWLEDGEMENT

Non sono molto brava con le parole a descrivere la gratitudine per tutte quelle persone che mi hanno aiutato in questo percorso, figuriamoci in inglese. Quindi ci proverò almeno in italiano.

Questo grande traguardo sembra essere davvero arrivato. Non sembra quasi vero; dopo tante avventure e vicissitudini, è finalmente giunto alla fine. Scorrono nella mente questi 3 anni e rivedo ogni singolo giorno. Tutti i sacrifici fatti, mesi ad aspettare un risultato che sembrava non arrivare mai, esperimenti su esperimenti per rincorrere una soluzione, le pagine della tesi in bianco che non pensavo di riuscire a terminare. Ma rivivi anche tutti i momenti di gioia condivisi con le persone che sono diventate una seconda famiglia per me, che hanno contribuito al raggiungimento di questo traguardo e che non posso fare a meno di ringraziare.

Vorrei ringraziare la prof.ssa Rita Patrizia Aquino, la quale mi ha dato la possibilità di crescere professionalmente e umanamente nel suo gruppo di ricerca, per la sua professionalità e soprattutto per quei suggerimenti che come per magia, puntualmente, facevano quadrare ogni cosa, idee, discorsi e slide.

Un ringraziamento di cuore va a due persone speciali, la dott.ssa Mencherini e dott.ssa Sansone, per me ormai diventate Terry e Francy. Sono una parte della mia famiglia. Abbiamo condiviso non solo il lavoro, ma anche momenti di vita felici e momenti difficili. Mi hanno sempre sostenuta in questi anni, hanno sempre creduto in me e mi hanno spinto a non mollare. Mi hanno insegnato che con lo studio e l'umiltà si può affrontare qualunque difficoltà e che si può dare il massimo, anche se qualcuno prova a minimizzare quello che fai. Tanti obiettivi si raggiungono solo se alle spalle hai persone che ti guidano con il cuore, hanno la passione e la curiosità verso il proprio lavoro e sanno come riprenderti quando perdi la strada. Che dire, non sarebbe stato lo stesso persorso senza di voi.

Ringrazio tutto il gruppo di ricerca dei laboratori 12 e 13, prof. Del Gaudio (che mi ha sopportato per 46 SEM, nonostante due filamenti rotti e un computer che sembrava morto per sempre), la prof.ssa Paola Russo, la dott.ssa Patrizia Picerno, la dott.ssa Giulia Auriemma, e tutti i tesisti che hanno condiviso con me la quotidianità, regalandomi tante risate. Come dimenticare tutte le mie tesiste, Roberta, Laura, Mariangela, Luana, Teresa, Rossella e il trio della Gioa, Rita, Francesca e Antonella (un trio pericolosissimo ma che riesce a strapparti un sorriso anche nelle giornate più negative).

Ringrazio Giulio, Marilena e Chiara, che mi hanno sopportato e supportato con una chiacchiera, un aiuto con il computer quando non voleva collaborare, con una parola di conforto quando mi hanno vista in difficoltà e per i tanti momenti belli passati insieme.

Ringrazio il dot. Catello Pane, che mi ha seguito nella parte degli esperimenti condotti presso il CREA-OF, Centro di Ricerca Orticoltura e Florovivaismo di Pontecagnano. Una persona disponibile e generosa, che mi ha lasciato pieno spazio nel suo laboratorio, che mi ha fatto sentire parte del suo gruppo e per le belle parole che ogni volta mi diceva per incoraggiarmi ad avere fiducia, che tutto si sarebbe risolto.

E poi c'è Rosalia, conosciuta proprio grazie al dottorato. Una persona dolcissima e dal grande cuore, con la quale ho condiviso non solo questo percorso. Ci siamo sostenute a vicenda nelle difficoltà, abbiamo riso tanto e condiviso ansie, preoccupazioni, ma anche tanti momenti belli che hanno arricchito la nostra amicizia. Quante serate passate insieme in laboratorio nella speranza di riuscire a finire uno degli obiettivi del giorno. E quante risate ci siamo fatte nell'attesa di questo grande giorno.

Un grazie va anche ad Ilaria e Anna Maria, l'altro trio ora diventato un quartetto, con il piccolo Gabriele. Ci siamo trovate fin da subito e con il tempo abbiamo

costruito una bella amicizia che ci ha supportato nei momenti di difficoltà, perché laddove una era pessimista e sfiduciata, l'altra (direi quasi sempre Ilaria) interveniva per sdrammatizzare e far tornare il sereno.

Ringrazio la prof.ssa Carmen Freire che mi ha accettata subito per iniziare il mio periodo di ricerca presso il dipartimento di Chimica di Aveiro, e per le meravigliose parole spese per me prima di ritornare in Italia. Un'avventura che mi ha cambiato completamente, umanamente e professionalmente. Un grazie va soprattutto Carla e Nuno, che mi hanno seguita negli esperimenti e mi hanno sostenuta nei momenti di difficoltà, regalandomi anche un semplice sorriso o dicendomi, non ti preoccupare andrà tutto bene. E poi ci sono Bruno G., Bruno V., Guillaume, Tiago, Filipa, Daniela e Francesca che mi hanno fatta sentire sempre ben voluta, mai a disagio, nonostante il mio inglese, e che mi hanno reso parte integrante del loro gruppo di ricerca. E infine ringrazio la prof.ssa Adelaide Almeida e Cristina che mi hanno seguito negli esperimenti riguardanti la parte microbiologica.

Un ringraziamento va anche a Giorgia, Marco e Serena, tre ragazzi che sono stati il mio punto di riferimento durante il mio periodo ad Aveiro, che mi hanno fatto riscoprire la spensieratezza e la leggerezza nonostante la differenza generazionale. Ma soprattutto, senze che io chiedessi, non mi hanno mai lasciata sola durante le mie lunghe giornate in laboratorio.

Non per ultimo un grazie di cuore va a tutta la mia famiglia, che ha sempre gioito dei miei successi, in particolar modo a mio padre e mia madre che, nonostante i tanti momenti difficili, mi hanno sempre incoraggiata a perseguire i miei obiettivi, anche quando sembrava tutto vano, perché, mi dicevano sempre che prima o poi i sacrifici vengono ricompensati.

E infine un grazie speciale va a Roberto. Sono stati tre anni complessi; so che non è stato semplice questo periodo nemmeno per te. Le nostre scelte ci hanno tenuto a distanza per tutto il percorso, ma nonostante questo siamo stati l'uno il supporto

dell'altro. Nonostante i momenti difficili e il fatto che molto spesso ti sei sentito messo da parte perché la mia priorità fosse raggiungere i risultati che inseguivo, non me lo hai mai fatto pesare, anzi mi hai sempre spinto a credere in me e nelle mie capacità. Tanti traguardi si possono raggiungere solo se la persona che hai accanto crede in te e soprattutto nei tuoi sogni e nelle tue ambizioni, sopportando e supportando sempre e comunque le tue scelte.

Alla fine, quello che resta, non sono solo le conoscenze acquisite, ma soprattutto tutte quelle persone che hai incontrato sul tuo cammino e che hanno arricchito la tua vita, e che resteranno sempre la parte più bella di questa avventura.

Spero di non aver dimenticato nessuno, ad ogni modo grazie di cuore a tutti.

Tiziana